Title
Representations of eye and image velocity in motion sensitive cortex

Author
Churchland, Anne Kathryn

Publication Date
2003

Peer reviewed|Thesis/dissertation

Representations of eye and image velocity in motion sensitive cortex

by

Anne Kathryn Churchland

DISSERTATION

Submitted in partial satisfaction of the requirements for the degree of

DOCTOR OF PHILOSOPHY

in

Neuroscience

in the

GRADUATE DIVISION

of the

UNIVERSITY OF CALIFORNIA, SAN FRANCISCO

Dedication

To Michael, who was always ready with a snowboard, a java script, a climbing harness and a warm smile, just in case I needed something.

I would first like to
Steven Lisberger. Steve e
my ability to see them thro
tasched here in part to th
pecially Mark Churchilan
colleagues from other area
knowledge and encouragem
simulation experiments.

The technical supp
Stefanie Tokiyama, a cowo
a skilled hand to help with
Laszlo Bocskai, Barbara S
that was necessary for my

The support of my
of graduate work in stride.
recreational coordinator. N
Mark and Clarissa Wattes
with her dedication to sp
experience a lot more enjo
Miller, Alex Baker, Cathy
much needed comic relief

Acknowledgements

I would first like to acknowledge the contributions of my thesis advisor, Dr. Steven Lisberger. Steve encouraged me to take on challenging projects and had faith in my ability to see them through. In addition, I owe the success of the experiments described here in part to the collaborative spirit of my colleagues in the Lisberger lab, in particular Mark Churchland, Justin Gardner, I-han Chou and Nicholas Priebe. Help of colleagues from other universities was also essential. Most importantly, technical knowledge and encouragement from Martin Paré were a critical contribution to stimulation experiments.

The technical support of other colleagues in the lab was equally appreciated. Stefanie Tokiyama, a coworker for my entire tenure in the lab, was always willing to lend a skilled hand to help with monkey training and surgery. Liz Montgomery, Ken McGary, Laszlo Bocskai, Barbara St. Amant and Karen Macleod also provided technical support that was necessary for my being able to successfully conduct experiments.

The support of my family and friends allowed me to take the challenging aspects of graduate work in stride. My husband, Michael Brodesky, was my cheerleader and recreational coordinator. My other family members, Paul and Patricia Churchland, and Mark and Clarissa Waites provided encouragement from the beginning. Robin LeWinter, with her dedication to spin class, craft design and reality television made the whole experience a lot more entertaining. Other friends, including Nora El Samahy, Jim Muller, Alex Baker, Cathy Garabedian Jennifer Grady and Tiffany Hoover also provided much needed comic relief.

In order to success
make accurate computation
the ongoing velocity of the
middle temporal area (MT
been examined in some de
later cortical areas have be
some parts of cortex, inclu
sensitive to the direction of
been studied.

The thesis will beg
neurons sensitive to pursu
chapter 2, I will describe th
image velocities. Chapter 3
might be combined to gene
4 will explore how visual r
is generated using appare
these stimuli suggests that
decode responses from are
ask whether the MST neur
frontal eye fields are distin

Abstract

In order to successfully pursue a moving target, the oculomotor system must make accurate computations about both the velocity of image motion on the retina and the ongoing velocity of the eye. In sensory areas, such as primary visual cortex and the middle temporal area (MT), the responses of neurons to different image velocities have been examined in some detail. However, the responses of neurons to image velocities in later cortical areas have been comparatively less studied. Further, although neurons in some parts of cortex, including the medial superior temporal area (MST) are known to be sensitive to the direction of pursuit, their responses to different pursuit velocities have not been studied.

The thesis will begin with a series of behavioral experiments suggesting that the neurons sensitive to pursuit direction are likely also sensitive to pursuit velocity. In chapter 2, I will describe the responses of MST neurons during different pursuit and image velocities. Chapter 3 will detail how the responses of eye velocity tuned neurons might be combined to generate an accurate population estimate of eye velocity. Chapter 4 will explore how visual responses in MST change when the illusion of smooth motion is generated using apparent motion stimuli. The surprising response of MST neurons to these stimuli suggests that the neurons may be using a center-of-mass computation to decode responses from area MT. In the final chapter, I will use antidromic stimulation to ask whether the MST neurons projecting to the smooth eye movement region of the frontal eye fields are distinct from the general population.

Table of contents

List of Tables and Figures

Chapter 1

Chapter 2

Chapter 3

Chapter 4

Chapter 5

Chapter 3

Chapter 4

Chapter 5

General Introduction

Determining the speed of moving stimuli in the visual world is a critical problem for the nervous system. Successfully computing the speed of visual inputs enables a host of behaviors. For example, an accurate estimate of the speed of a moving target is critical for a predator trying to acquire his prey. In addition, comparing the speed inputs from different parts of the visual field can reveal their locations in depth. Lastly, identifying different speeds at different radial positions in the visual field is necessary in computing direction of heading.

The abundance of cortical circuitry dedicated to processing visual speed is testimony to the importance of these behaviors. Neurons in the middle temporal area (MT) respond preferentially not only to the direction of a moving stimulus, but also to its speed (Maunsell and Van Essen 1983). Neurons in the medial superior temporal area (MST) are likewise sensitive to both the direction and speed of moving simuli (Komatsu and Wurtz 1989; Orban et al. 1995).

Importantly, however, interpreting the visual world requires not only processing visual signals but also understanding them in the context of movements. For example, motion on the retina can result from movement of an object in the visual word, or from the movement of the observer. Conversely, an object might appear still on the retina because it is truly stationary in the world, or because the object's speed is matched by the speed of an observer's eyes, eliminating any image motion. That we seldom confuse our

own motion with the motion of objects argues that cortical and subcortical circuitry can correctly interpret visual signals in the face of movements.

Smooth pursuit eye movements provide an ideal system in which to investigate how visual signals are processed in the context of movements. Smooth pursuit eye movements act to eliminate image velocity on the retina by matching eye velocity to target velocity (for review, see Keller and Heinen 1991; Lisberger et al. 1987). Importantly, the pursuit system aims to bring small targets of interest onto the fovea, changing dramatically the pattern of visual inputs to the brain. For example, consider an observer watching a target of interest move across a patterned background. Once the subject begins to accurately pursue the target, motion from the target on the retina is mostly eliminated. This same movement of the eyes will add motion signals to the stationary patterned background surrounding the target. From the point of view of the retina and early visual areas, the moving target will appear stationary while the stationary background appears to move. The motion signals from the background can be quite complex, particularly if the movement of the eyes is added to movement of the observer through space: in this case, pursuit can further distort the complex optic flow fields caused by self motion (Royden et al. 1992; Royden et al. 1994).

Without clear neural estimates of both eye and image velocity, subjects would be unable to accurately indicate direction of heading during pursuit. Further, even pursuing a single target on a dark background would be difficult because the successful initiation of pursuit would eliminate the visual motion inputs that engage pursuit. In chapter 1,

behavioral evidence for

present an examination

pursuit system depends

made in monkeys, the da

humans reveals that resp

ongoing pursuit scale wi

These experiment

velocity. Separate experi

gain in the cortex (Tanaka

estimate had not been exp

in motion sensitive neuro

responses has never been

eye velocity responses is

of pursuit speeds from a

isual motion inputs ar

neurons in MST to differe

exhibited responses that w

velocity signal in MST wa

by chapter 1, we measured

an estimate of the resoluti

revealed that the responses

behavioral evidence for a neural estimate of eye velocity will be explored. We will present an examination of the behavioral observation that the visuomotor gain of the pursuit system depends on the animal's behavioral state. The original observation was made in monkeys; the data presented here extend the finding to humans. Data from humans reveals that responses to perturbations of target velocity presented during ongoing pursuit scale with ongoing eye velocity.

These experiments confirm that the pursuit system has an estimate of ongoing eye velocity. Separate experiments have indicated that the eye velocity estimate modulates gain in the cortex (Tanaka and Lisberger 2002), but the neural locus of the eye velocity estimate had not been explored. Although the existence of speed-tuned *visual* responses in motion sensitive neurons is well-documented, the existence of speed-tuned *eye velocity* responses has never been clearly shown. Demonstrating that neurons exhibit speed tuned eye velocity responses is difficult because the experimenter has to not only elicit a variety of pursuit speeds from a subject, she must also ensure that responses are measured when no visual motion inputs are present. In chapter 2, we explore in detail the responses of neurons in MST to different pursuit speeds under these conditions. Many neurons exhibited responses that were clearly speed-tuned. To determine whether the eye velocity signal in MST was a could serve as the neural estimate of eye velocity suggested by chapter 1, we measured its resolution using ideal observer analysis, and compared it to an estimate of the resolution suggested by the behavior. The ideal observer analysis revealed that the responses of some neurons have sufficient resolution to provide the

pursuit system with a h

not.

In chapter 3, d

improve the resolutio

Each of the pooling s

neurons might be sele

velocity. Very little is

different areas, so we

strength of the analysis

according to a number

lower bound for the res

One interesting

responses in MST is tha

MST neurons simply fi

of these MST neurons.

This monotonically inc

where most responses f

However, bandpass resp

monotonically increases

likewise increase monot

pursuit system with a high resolution eye velocity signal, but the average neuron does not.

In chapter 3, different strategies were used to pool MST neurons in an attempt to improve the resolution with which the population was able to represent eye velocity. Each of the pooling strategies used took advantage of different assumptions about how neurons might be selected to play a role in generating the population estimate of eye velocity. Very little is known about the projection of different neurons in MST to different areas, so we had no way of knowing which assumptions were correct. The strength of the analysis is that by estimating the resolution of the eye velocity signal according to a number of different assumptions, we were able to generate an upper and lower bound for the resolution of the population response.

One interesting aspect of the speed tuning for both extraretinal and visual responses in MST is that they are frequently monotonically increasing. That is, many MST neurons simply fire progressively more as stimulus speed increases. The responses of these MST neurons, at least over a range, increase in parallel with stimulus speed. This monotonically increasing response is quite different from responses in area MT where most responses first increase in parallel with stimulus speed and then decrease. However, bandpass responses in MT can be combined so that the population response monotonically increases in parallel with stimulus speed. Because MST responses likewise increase monotonically with stimulus speed, one possibility is that their

distinct coding strate

mere existence of su

reflects decoded resp

In chapter 4, indepen

in MST reflect decod

One difficulty

that it is hard to deter

projects to a host of c

rather different behavi

projects to the smooth

be distinct from the pop

antidromic stimulation

Because the projection f

locating such neurons pr

the projection from MST

Boussaoud D, Ungerleide

connections of the media

areas in the macaque. J C

Keller EL and Heinen SJ

mechanisms and pathway

Komatsu H and Wurtz RH

cortical areas MT and MS

distinct coding strategy reflects the population response from area MT. However, the mere existence of such neurons is, by itself, weak evidence that speed tuning in MST reflects decoded responses from earlier visual areas like MT that have bandpass tuning. In chapter 4, independent evidence from apparent motion further suggests that responses in MST reflect decoded responses from area MT.

One difficulty in interpreting single unit responses from MST arises from the fact that it is hard to determine for which behavior a neuron is actually important. MST projects to a host of cortical and subcortical areas, many of which are likely to subserve rather different behaviors (Boussaoud et al. 1990). The population of neurons that projects to the smooth eye movement region of the frontal eye fields (FEF_{SEM}) might well be distinct from the population in general. Chapter 5 describes experiments using antidromic stimulation to identify those MST neurons that project to the FEF_{SEM}. Because the projection from MST to the FEF_{SEM}, is small (Tian and Lynch 1996), locating such neurons proved difficult. A small amount of data regarding the nature of the projection from MST to the FEF_{SEM} is provided.

Boussaoud D, Ungerleider LG, and Desimone R. Pathways for motion analysis: cortical connections of the medial superior temporal and fundus of the superior temporal visual areas in the macaque. *J Comp Neurol* 296: 462-495, 1990.

Keller EL and Heinen SJ. Generation of smooth-pursuit eye movements: neuronal mechanisms and pathways. *Neurosci Res* 11: 79-107, 1991.

Komatsu H and Wurtz RH. Modulation of pursuit eye movements by stimulation of cortical areas MT and MST. *J Neurophysiol* 62: 31-47, 1989.

Lisberger SG, Morris EJ, and Tychsen L. Visual motion processing and sensory-motor integration for smooth pursuit eye movements. *Annu Rev Neurosci* 10: 97-129, 1987.

Maunsell JH and Van Essen DC. Functional properties of neurons in middle temporal visual area of the macaque monkey. I. Selectivity for stimulus direction, speed, and orientation. *J Neurophysiol* 49: 1127-1147, 1983.

Orban GA, Lagae L, Raiguel S, Xiao D, and Maes H. The speed tuning of medial superior temporal (MST) cell responses to optic-flow components. *Perception* 24: 269-285, 1995.

Royden CS, Banks MS, and Crowell JA. The perception of heading during eye movements. *Nature* 360: 583-585, 1992.

Royden CS, Crowell JA, and Banks MS. Estimating heading during eye movements. *Vision Res* 34: 3197-3214, 1994.

Tanaka M and Lisberger SG. Enhancement of multiple components of pursuit eye movement by microstimulation in the arcuate frontal pursuit area in monkeys. *J Neurophysiol* 87: 802-818, 2002.

Tian JR and Lynch JC. Corticocortical input to the smooth and saccadic eye movement subregions of the frontal eye field in Cebus monkeys. *J Neurophysiol* 76: 2754-2771, 1996.

Chapter 1

The text of this cha

Chapter 1: Gain control in human smooth pursuit eye movements

The text of this chapter is a re-print of the material as it appears in the Journal of Neurophysiology 87(6), 2002.

Abstract

In previous experiments, on-line modulation of the gain of visual-motor transmission for pursuit eye movements was demonstrated in monkeys by showing that the response to a brief perturbation of target motion was strongly enhanced during pursuit relative to during fixation. This first chapter elaborates the properties of on-line gain control by recording the smooth pursuit eye movements of human subjects during tracking of a spot target. For small perturbations that consisted of a single sine wave at 5 Hz, $\pm$10°/s, the response to the perturbation was significantly larger during pursuit at 15°/s than during fixation. Enhancement persisted but was smaller for perturbations that consisted of a single sine wave at 5 Hz, $\pm$5°/s during pursuit at 10°/s. Thus, human pursuit, like monkey pursuit, is modulated by on-line gain control. For larger perturbations consisting of a single sine wave at 2.8 Hz, $\pm$19/s, the degree of enhancement depended strongly on the orientation of the perturbation. Enhancement was present when "peak-first" perturbations caused the target speed to increase first, and was attenuated when "trough-first" perturbations caused target speed to decrease first. This effect was most profound when the perturbation was 2.8 Hz, $\pm$19°/s, but was also present when the amplitude of the trough-first perturbation was decreased to 5°/s. For trough-first perturbations, the eye velocity evoked by the later peak of the perturbation was inversely related to that evoked by the trough of the perturbation. We interpret the effect of perturbation orientation on the size of the response it evokes as evidence that trough-first perturbations cause a decrease in the on-line gain of visual-motor transmission for

pursuit. Our observation argues that gain control is continuously updated on a timescale as short as 100ms as behavioral conditions change. Finally, when perturbations were presented as a sequence of 3 large, trough-first sine waves starting at the onset of target motion at 10°/s, repeating the conditions used in prior studies, we were able to replicate the prior data on humans that the response to the perturbations was, on average, only slightly larger during pursuit than during fixation. We conclude that online gain control modulates human pursuit, and is updated on a sufficiently short timescale that it is probed most reliably with small, brief perturbations.

Introduction

Smooth pursuit eye movements allow primates to stabilize the images from moving objects on the retina. Pursuit is a negative feedback control system, so that its input, image motion across the retina, causes smooth eye acceleration that eliminates image motion by driving eye velocity to match target velocity. Information about the speed and direction of image motion is provided to pursuit by neurons in two extrastriate visual areas: the middle temporal area (MT)(Maunsell and Van Essen 1983; Newsome and Pare 1988) and the medial superior temporal area (MST)(Komatsu and Wurtz 1989). Once a target has been selected for pursuit, these cortical areas send a motor command through a variety of pathways to the cerebellum and then to the brainstem (for review, see (Keller and Heinen 1991; Lisberger et al. 1987).

The negative-feedback configuration of the pursuit system has led to the view that pursuit is a visual-motor reflex. However, considerable evidence now indicates that visual-motor processing for pursuit is subject to modulation by a mechanism that we call "on-line gain control". Evidence for online gain control first arose quite long ago when Robinson (Robinson 1965) observed that eye velocity tends to undergo spontaneous oscillations only during ongoing pursuit but not during fixation. Robinson (1965) proposed that a moving target engages neural pathways not normally engaged during fixation. Further evidence that the gain of visual-motor processing might differ during pursuit and fixation came from the observation that the dynamics of the eye velocity response to a given image motion depended on whether the image motion was used to start or stop pursuit (Krauzlis and Lisberger 1994; Luebke and Robinson 1988). The results of Robinson (1965) provide an *a posteriori* rationale for the existence of a gain

control. Some degree of oscillation is tolerable when a high gain of visual-motor transmission allows pursuit to accomplish its major goal of reducing image velocity from 30 to about 2°/s. The low gain during fixation obviates the same oscillations, which would pose a problem for visual stability and high-acuity vision.

The most direct evidence for on-line control of the gain of pursuit came from an experiment in our laboratory showing that the eye velocity evoked by a brief perturbation of target velocity was much larger when the perturbation was presented during ongoing pursuit versus during fixation (Schwartz and Lisberger 1994). The gain of the response to the perturbations was related to eye velocity, so that the perturbations presented during 20°/s tracking elicited larger responses than did the same perturbations presented during 10°/s tracking. This finding suggests a distinction between the gain of pursuit, which was nearly one for both 10°/s and 20°/s pursuit, and the feedforward gain of the pursuit pathways, which was clearly different at the two velocities. The former gain is measured as steady-state eye velocity divided by target velocity and reflects the overall performance of a complex feedback system with many internal parameters, while latter gain is probed by our perturbations and is an internal parameter in pursuit. We refer to the latter gain when describing "on-line gain control".

The existence of online gain control has not only been observed in primates, but its neural basis has begun to be understood. Both behavioral and neural evidence suggest that online gain control is modulated cortically. The first behavioral observation is that perturbation responses are large during VOR cancellation when the head and eyes move in tandem to track a moving target (Churchland & Lisberger, 1998). Under these conditions, the eyes are not moving in the sockets. This observation refuted the

possibility that enhanced responses seen during pursuit are due to a reduction in the amount of inertia to be overcome during ongoing pursuit relative to during fixation. Further evidence against this possibility comes from the observation that responses to perturbations are small during the VOR when the eyes are clearly moving in the socket at high velocity (Carey and Lisberger 2002). Neural evidence that the online gain is modulated cortically comes from stimulation of the frontal eye fields (Tanaka and Lisberger 2002). Small amounts of current injected during pursuit have a larger effect on the resulting smooth eye movement that the same amount of current injected during fixation.

However, the existence of on-line gain control as a general feature of primate visual-motor processing has been called into question. One group measured human eye movements and compared responses to perturbations presented during fixation or pursuit. They report that responses to perturbations presented in either condition were equal, suggesting that the gain control seen in monkeys might require extensive practice or be specific to non-human primates (Das et al. 1998; Das et al. 1995).

The goal of the present paper was to evaluate on-line gain control in human pursuit using the same experimental approaches as had been used on monkeys and humans. Eye velocity responses to perturbations presented during either fixation or pursuit were compared. Human subjects, like monkeys, showed larger responses to brief perturbations of target motion presented during pursuit. Moreover, some of the experiments reported here seem to explain why human studies have not replicated the results from monkeys: instead of merely probing it, the perturbations used by Das et al. (1995, 1998) may also have altered the gain of visual-motor transmission.

Methods

Subjects

The participants in this study were scientists and students from the Keck Center for Integrative Neuroscience at UCSF. A total of 10 subjects were tested. The 5 subjects in Group 1 were tested on only two conditions to illustrate the basic phenomenon of on-line gain control. A single subject from group 1 as well as 5 additional subjects were recruited for Group 2. Different subjects had to be recruited because most subjects were only willing to participate in one testing session. Most subjects in group 2 were tested both on conditions similar to those used for Group 1, in addition to a number of other conditions designed to probe on-line gain control in more detail. One subject, who is an author, was tested in both groups, but was not tested as extensively as the other subjects in group 2 since she failed to show the enhancement characteristic of all other subjects. All subjects gave their informed consent at the beginning of each experiment. Seven of the subjects were completely naIve, two had some previous pursuit experience but were naïve to the specific hypothesis being tested, and one is an author. All subjects had normal or corrected vision. Experimental procedures were approved by the Human Subjects Committee at UCSF.

Eye Movement Recording

Two-dimensional movements of the right eye were measured using the Fourward Technologies Dual Purkinje Image Tracker (Generation 6.1). The subjects' heads were stabilized using a chin rest and a head strap that subjects adjusted to be snug, but comfortable. The tracker's automatic moveable optical stage (auto stage) and focus servo

were both disabled to avoid introducing head position artifacts into the eye position signal.

Visual Stimuli

Visual stimuli were projected onto the back of a tangent screen that was 40 cm from the subject and subtended a visual angle of 32° by 26°. The image from a red LED provided a circular, 0.1° stationary fixation target. Circular 0.5° pursuit targets were created by reflecting the beam from a fiber-optic light source off orthogonally-placed x-y pairs of mirror galvanometers. The galvanometers were driven by the digital-to-analog outputs from a Pentium PC computer. During the experiment, the experimental room was quite dark, as the tracker works best when the pupil is dilated.

Experiments were presented as a series of trials of duration 2.5-3 seconds. Each trial began with the presentation of a stationary fixation point in the center of the tangent screen. In experiments that measured responses during fixation, a second target appeared in the center of the screen, replacing the red fixation target. In experiments that measured responses during pursuit, the second target appeared 5° to the left or right of the fixation target after a random interval of 800 to 1000 ms (Rashbass 1961). The eccentric pursuit target remained stationary for 300 ms. The red fixation target was then extinguished and the eccentric target began moving at 10 or 15°/s toward the position of fixation. Most experiments also included separate trials (not included in subsequent analyses) in which the pursuit target moved away from the position of fixation so that the subject could not correctly anticipate the direction of target motion. The target velocities were selected because they were slow enough to ensure that an average subject could successfully acquire the target and pursue it with minimal residual image motion. It is important to

minimize image motion at the time of the perturbation because the presence of image motion can reduce the responses to perturbations (Churchland and Lisberger 2001). In addition, the target velocities chosen are identical to those reported in other papers, allowing a direct comparison of findings.

In some trials (see below) the ongoing target velocity was perturbed briefly. Perturbations of target velocity were created by adding at least one full cycle of a 2.8 or 5 Hz sine wave to the preexisting command for target position. Target velocity was in one direction for the first half of the cycle (the first component) and in the opposite direction for the second half of the cycle (the second component). As a result, there was no net change in target trajectory. Perturbations were always along the axis of target motion in one of two orientations. Perturbations that began with an increase in target speed are referred to as "peak-first" because the peak of those perturbations occurred in the first component of the perturbation and the trough occurred in the second component. Perturbations that began with a decrease in target speed are referred to as "trough-first" since the trough of those perturbations occurred in the first component and the peak occurred in the second component. Perturbations were superimposed upon constant target velocities of 10 or 15°/s, modulating that target velocity by ± 5 to ± 19°/s depending on the perturbation. The larger, ± 19°/s perturbation was chosen to allow a direct comparison to other published data. In each experiment, trials with and without perturbations were randomly interleaved. Trials without perturbations ensured that subjects could not predict whether a given trial would contain a perturbation and provided control traces against which the responses to perturbations could be compared.

Perturbations were presented either during fixation ("fixation perturbations") or during pursuit ("pursuit perturbations"). Pursuit perturbations began either at the time of or at least 500 ms after the onset of ramp target motion. Perturbations were presented late enough in the trial to ensure that the subjects had successfully acquired the target and were experiencing minimal residual image motion. Responses to perturbations that began 550 ms after the onset of target motion were analyzed, but each experimental block also included trials (not included in subsequent analyses) in which perturbations occurred earlier or later so that the occurrence of the perturbation could not be predicted. Pursuit perturbations presented at the onset of ramp motion consisted of multiple perturbations at the same frequency. Fixation perturbations began at the same times relative to the onset of trials as they would have if the target had been moving.

Data acquisition and analysis

Data were digitized during the experiment at a sampling rate of 1000 samples/s for each channel. Channels were selected from horizontal eye velocity, eye position, and target position. The eye position signal was low-pass filtered with a cutoff at 330 Hz and voltages proportional to eye velocity were obtained by differentiating the eye position signals with an analog circuit (DC to 25 Hz, -3 dB). Signals related to target velocity were obtained during data analysis by digital differentiation of the target position samples with a bandpass of 50 Hz.

Data analysis was performed after the experiment by aligning trials to the onset of target motion and averaging responses to identical stimuli on a UNIX workstation. The digitized data from each trial were displayed on the computer screen to ensure that they were not contaminated with large saccades, particularly during the presentation of the

perturbation. Occasionally, small, corrective saccades were removed using a keystroke-controlled cursor to mark the beginning and end of each small deflection in eye velocity. The computer replaced each deflection with a straight line that connected the eye velocity traces before and after the saccade. Trials were sorted according to stimulus condition and responses to identical stimuli were aligned on the onset of target motion and averaged together. At least 15 responses were used for each average. Averaged traces were then passed through a 25 Hz digital filter to reduce noise. Superposition of the filtered and unfiltered traces confirmed that this step did not change the responses (there was no ringing, for example), but only reduced the noise to facilitate quantitative analysis.

Averaged responses to perturbations presented during fixation reflect only the response to the perturbation since there is no ongoing pursuit. However, averages of the eye velocity evoked by perturbations presented during pursuit reflect both the response due to the perturbation and the ongoing pursuit eye velocity. To compare responses to pursuit-perturbations and fixation-perturbations, it was necessary to eliminate the component of the response to pursuit-perturbations that was due to ongoing pursuit and thus "isolate" the response to the perturbation. The isolation was achieved by computing the difference between the eye velocity averages for trials that did and did not contain a perturbation at each time point in the averages (Fig. 1A). This conservative approach ensured that any modulation of the ongoing pursuit response could not contribute to (and potentially enhance) the perturbation response that was measured.

Once the responses to perturbations were isolated, their amplitude was quantified in one of two ways. 1) In most cases, amplitude was estimated by measuring half the

peak-to-trough eye velocity in an interval that started 120 ms after the perturbation and had the same duration as the perturbation. When multiple perturbations were presented in sequence, half the peak-to-trough eye velocity was computed for each cycle of the perturbation and then these were averaged. This method of estimating amplitudes was selected because it is most similar to those used in other papers with which we would like to compare results (i.e. Das et al. 1995, 1998; Schwartz & Lisberger 1994). 2) For some experiments, especially those with consistently asymmetric responses to perturbations, we measured the amplitudes of the responses to the first and second components separately. For large fixation perturbations, the amplitude of the each component was estimated as the maximal deviation from zero eye velocity during the first or second half of the response. For large pursuit perturbations, the same analysis was performed on the responses to the perturbation that remained after the response to unperturbed target motion had been subtracted. It is worth noting that the response to the first component of the response is essentially the response to a unidirectional perturbation.

To determine the statistical significance of the population differences between responses to fixation and pursuit perturbations, responses to leftwards and rightwards perturbations were analyzed separately. Statistical tests performed on pooled leftwards and rightwards data would be invalid since leftward and rightward responses in a given subject are not independent. The statistical significance of individual responses is not reported since the variance that is required for a t-test needs to be scaled at least once for every condition. Both our method of "isolating" responses to perturbations, and our method of estimating response amplitude include computations that change the variance

nonlinearly. Fortunately, sufficiently many subjects were tested to enable statistical testing on group data, rather than individual responses.

Results

The traces in Figure 1A show the results of averaging 15 trials to illustrate how stimuli were presented and to demonstrate that the perturbations evoked clear, bi-directional changes in eye velocity. The basic approach in our data analysis (see Methods for details) was to isolate the response to the perturbations by comparing the responses to trials that were identical except for the presence or absence of perturbations (Fig. 1A, 2nd trace). In this example, the modulation of eye velocity evoked by the perturbation during pursuit (Fig. 1A, 3rd trace) was clearly larger than that evoked by the same perturbation during fixation (Fig. 1A, bottom trace).

Perturbations of target motion during fixation and pursuit

Two groups of subjects were used to test the hypothesis that responses to pursuit-perturbations are larger than responses to fixation-perturbations. The five subjects in Group 1 were tested with perturbations that consisted of single sine waves at 5 Hz, ±10°/s presented during 15°/s pursuit. Perturbations were always in the peak-first orientation: the speed was increased during the first component and decreased during the second component. The black squares in Figure 1B show that for individual subjects, the response to pursuit-perturbations is always larger than the response to fixation-perturbations: all black squares lie above the dashed line. Average responses to fixation perturbations (open bars) and pursuit perturbations (black bars) are shown in the left side of the inset to Figure 1B. A two-tailed paired t-test for the equality of two sample means

revealed that pursuit-perturbations yielded larger responses than fixation perturbations for both directions (Left: $p<.01$; Right: $p< .01$).

The six subjects in Group 2 (one of whom was also in Group 1) were tested with smaller 5 Hz perturbations (±5°/s) and during slower pursuit (10°/s). As illustrated by the gray symbols in Figure 1B and the right half of the inset, the responses to pursuit perturbations were larger than those to fixation perturbations in all except one case when they were nearly equal. As summarized in the right half of the inset in Fig. 1B, a two-tailed paired t-test for the equality of two sample means revealed that pursuit perturbations yielded larger responses than fixation perturbations for both directions (Left: $p<.005$; Right: $p< .02$). Responses from Group 1 and Group 2 cannot be compared directly since the stimuli differed in two ways. The use of smaller amplitude perturbations during slower pursuit may have contributed to the smaller amount of gain enhancement for pursuit perturbations in Group 2 (Schwartz & Lisberger 1994).

Figure 1C uses the same format to present the same data subjected to a slightly different analysis. Here, the amplitude of only the first component of the response to the peak-first perturbations is reported. Because the response to the first component is over before the first visual information arrives about the second component, this analysis is equivalent to performing separate experiments with unidirectional perturbations. The enhancement of the response to pursuit perturbations is still evident, although the differences between responses to pursuit and fixation perturbations are smaller. Statistical analysis with paired t-tests showed that the difference between pursuit and fixation was significant in three cases (Group 1: Left: $p<.02$, Right: $p<.03$; Group 2: Left: $p<.05$) and just barely missed significance in the fourth case (Group 2: Right: $p<.055$). Taken

together, the data in Figure 1 show that an enhanced response to perturbations is seen during 10°/s and 15°/s pursuit in humans. The data so far are in agreement with the results of the same experiments on monkeys.

The subjects used in the rest of our experiments are the subjects from Group 2, excluding one subject who did not show enhanced responses to perturbations presented during pursuit. Exclusion of this subject (who was an author) was justified because the experiments described below were designed to test whether subjects who demonstrated enhanced responses to small, brief perturbations also showed enhancement in other conditions.

Response depends on orientation of perturbation

To examine the possibility that perturbations need to be small and brief to elicit enhanced responses during pursuit, we tested five subjects with perturbations that consisted of a single sine wave at 2.8 Hz, ±19°/s superimposed on target velocity at 10°/s, with perturbations in the peak-first orientation. Data were analyzed by measuring half the peak-to-trough eye velocity for the entire response to the perturbation. For peak-first perturbations, the black squares in Figure 2 indicate that for all subjects tested, responses to pursuit perturbations were larger than responses to fixation perturbations, even when perturbations were large and low-frequency. The black bars in the left half of the inset show the average responses across all subjects and indicate that responses during pursuit were significantly larger than responses during fixation for both directions when assessed by a two-tailed, paired t-test (Left: $p<.03$; Right: $p<.005$).

For trough-first perturbations of 2.8 Hz, ±19°/s, the difference between responses to pursuit perturbations and fixation perturbations was less convincing and did not reach

statistical significance. Almost all of the gray squares in Figure 2 plot near the line of slope one (dashed line) indicating that fixation perturbations and pursuit perturbations yielded similar responses. The similarity of the responses can also be seen in the across-subjects averages that appear in the right half of the inset of Figure 2 (gray bars). Statistical analysis did not reveal a significant difference between responses to pursuit perturbations and fixation perturbations with a two-tailed paired t-test (Left: $p<.16$, Right, $p<.4$). In addition, the responses to the trough-first pursuit-perturbations were significantly less than responses to the peak-first pursuit-perturbations as assessed by a two-tailed paired t-test (Left: $p<.05$; Right: $p<.01$).

Averaged responses to peak-first and trough-first perturbations of 2.8 Hz, $\pm$19°/s are aligned in Figure 3 to illustrate why the responses to perturbations in the trough-first orientation were so small. The target velocity traces in Figure 3A show target motion for peak-first (dashed trace) and trough-first (bold, continuous trace) perturbations relative to a control trace consisting of unperturbed target motion (fine, continuous trace). The peak-first perturbations should drive eye velocity first above and then below the response to unperturbed target motion, while trough-first perturbations should drive eye velocity first below and then above the response to unperturbed target motion. The eye velocity traces in Figure 3A show that only the response to the peak-first perturbation fulfilled this prediction: the first component of eye velocity evoked by the peak-first perturbation (dashed trace) rose above the trace indicating the response to unperturbed target motion and the second component (thick trace) of the response dipped below the trace indicating the response to unperturbed target motion. The response to trough-first perturbations was very different: although the first component of the response dipped below the control

trace, as it should, the second component never rose above the control trace. Note that the same target velocity was present at arrows I and II, but the magnitude of the eye velocity responses is very different. Importantly, the eye velocity trajectory preceding point I is very different from the eye velocity preceding point II: the latter occurs after eye velocity drops almost to zero, so that the eyes are almost stationary, as for fixation perturbations. The effect of reducing eye velocity to near zero also appears after the second component of the response to the peak-first perturbations in Figure 3A, where average eye velocity (dashed trace) never reached that achieved in control trials (thin continuous trace). If the strength of online gain control were updated about eye velocity on a short timescale, then the near-zero eye velocity in response to the trough of a large perturbation should reduce the on-line gain of pursuit, yielding data like those shown in Figure 3A.

If the very different responses at points I and II are indeed due to the near-zero eye velocity that precedes point II, then using perturbations that do not drive eye velocity so close to zero should make the responses at points I and II more similar. This hypothesis was tested by presenting a smaller trough-first perturbation. The smaller perturbation should elicit a smaller decrease of eye velocity in the first component, maintain eye velocity well above zero, keep online gain high, and result in an improved response to the second component. The responses to a 2.8 Hz, ± 5°/s perturbation confirmed this prediction (Figure 3B). Now, the perturbations caused eye velocity to oscillated around the control trace for *both* peak-first and trough-first perturbations. The responses at points I and II, which again are driven by identical target velocities, are much more similar than they were in Figure 3A. The data in Figure 3 are consistent with

the hypothesis that a large decrease in ongoing eye velocity reduces the on-line gain of pursuit and, in the case of the trough-first perturbation, the response to the second component.

Figure 3 predicts that, at least for trough-first perturbations, the amplitude of the first and second components of the response should be inversely related. To test this, we presented a range of trough-first perturbations of different amplitudes ($\pm$5 to $\pm$19°/s) and frequencies (2.8 to 5 Hz) to elicit a range of responses to the first component of the perturbation. Plotting the amplitude of the response to the second component as a function of that to the first component verified that the magnitudes of the responses to the first and second components were inversely related in each subject (Fig. 4). To obtain the numbers plotted in Figure 4, we measured the responses to each component separately as the value of the peak and trough of each response relative to the control trace. Each response was given a positive sign if it caused eye velocity to deviate in the direction of that component of the perturbation. Thus, negative values of the amplitude of the second component indicate that the "peak" of the response to the perturbation was less than the response to unperturbed target motion (as in Fig 3A).

The data in Figures 3 and 4 are consistent with the hypothesis that large decreases in target velocity change the strength of online gain control, affecting subsequent responses. However, an alternative explanation exists: perhaps the low velocity preceding point II does not change online gain control, but simply provides a very low starting point to which a major change in eye velocity must be added. That is, perhaps the oculomotor system is poor at making large, rapid changes in smooth eye velocity. While we cannot rule out this possibility, we think it unlikely. Consider point I: although the velocity at

this point is the highest of all three traces, the eye velocity 150 ms later is almost at the lowest point of all three traces. This suggests that the system is well equipped to make the large, rapid velocity changes that are required by trough-first perturbations. Moreover, pursuit initiation provides a second example of a large, rapid change in eye velocity, this time in the same direction as required by the second half of the responses to a trough-first perturbation.

Replication of conditions that did not produce enhancement of responses to perturbations in prior studies.

When Das et al. (1995, 1998) examined on-line gain control in human pursuit, they used conditions that differed in several ways from the successful conditions shown in Figure 1. They began perturbations at the onset of target motion, used perturbations that consisted of multiple cycles of sine waves in the trough-first configuration, and took target velocity to or below zero on each cycle. To understand the apparent difference between their data and ours, we repeated their experimental conditions with our subjects, who showed enhanced responses to perturbations in other conditions. As shown in Figure 5A, target velocity consisted of a 10°/s step of target velocity summed with several cycles of sinusoidal target velocity at 2.8 Hz, $\pm$19°/s (solid trace). Responses were analyzed as before, by subtracting the response to 10°/s target motion alone (dashed traces) from the response to the combined target (solid traces), yielding a difference eye velocity during pursuit for comparison with the response to the sine waves presented alone during fixation (bottom trace in Fig. 5A). In agreement with the data of Das et al. (1995, 1998), we did not observe a striking difference in the size of the response to pursuit perturbations versus fixation perturbations. Figure 5B reports the average of half the

peak-to-trough value of all three cycles in the sine wave. A number of subjects showed enhanced responses to pursuit perturbations, evidenced by points that lie above the line of slope one, while two showed the opposite effect: larger responses to fixation perturbations. The inset in Figure 5B shows averaged responses for pursuit and fixation in each direction: for neither rightward nor leftward pursuit were responses to pursuit perturbations significantly larger than those to fixation perturbations (left: $p<.07$, right: $p<.2$).

To better understand the large inter-subject variability, we analyzed individual subjects' responses to each of the 3 sinusoidal cycles of target velocity that comprised the perturbations. The example traces shown in Figure 5A suggest that the size of the response to pursuit perturbations increases over the course of the trial, even though target velocity is the same for all 3 cycles. Analysis of each subject's responses to each of the 3 sinusoidal cycles of target velocity that comprised the perturbations confirms that the response to pursuit perturbations grew as a function of cycle number for almost every subject tested (Fig. 5C, small symbols connected by thin black lines), and for the mean across subjects (Fig. 5C, large symbols connected by bold black lines). For fixation perturbations, the same general trend was present (Fig. 5C, gray lines) albeit to a slightly lesser degree (significance levels given in the figure legend).

Finally, the inset in Figure 5C shows data from one subject who showed similarly large responses to both pursuit perturbations (large black squares) and fixation perturbations (large gray squares). The similarity was present in the responses to perturbations during both rightward and leftward pursuit (two trios of small black symbols connected by fine black lines). Note that the data for the two directions of

fixation perturbations are obscured by the averages. The absence of enhancement for this subject was specific to the stimulus presentation used in Figure 5. In the experiments with perturbations that consisted of single cycles of a 5 Hz sine wave, this subject exhibited small responses to fixation perturbations and normal enhancement of the responses to pursuit perturbations. We suspect that the 3 cycles of the sine wave perturbation provided a convincing enough target motion so that this subject was able to modulate the on-line gain of pursuit during fixation to the level that he, and most subjects, modulated the gain during pursuit.

Discussion

Lisberger and Schwartz (1994) showed that, in monkeys, perturbations of target velocity presented during pursuit elicit larger responses than those presented during fixation. They interpreted the enhancement as the result of the on-line gain control that had been postulated earlier by a number of investigators (Luebke and Robinson 1988; Robinson 1965). However, the existence of gain control in monkey pursuit did not necessarily imply it would be a general feature of primate smooth pursuit. Human and monkey pursuit systems seem to be similar in most regards (Lisberger et al. 1981; Lisberger and Westbrook 1985; Tychsen and Lisberger 1986), but species differences cannot be ruled out *a priori*. In addition, the monkeys tested by Lisberger and Schwartz (1994) had extensive pursuit experience. Their repeated exposure to moving targets might have made their enhanced responses atypical of untrained subjects. The data presented here argue strongly that the observed enhancement during pursuit a) is not limited to non-human primates and b) occurs in untrained subjects.

Our data present a consistent picture of on-line gain control in human and monkey pursuit, a picture that is in reasonable agreement with both sets of seemingly conflicting data in the literature. In the experiments designed to mimic those conducted by Schwartz and Lisberger (1994) on monkeys, the same results were obtained: responses to perturbations of target velocity were enhanced during pursuit versus during fixation. The gain of responses to pursuit perturbations were somewhat lower in humans (0.16 - 0.56) than in the monkeys (0.39 - 0.8) studied by Schwartz and Lisberger (1994). However, the gains were also lower for most humans than monkeys for fixation perturbations (0.06 to 0.37 for humans; 0.19 to 0.25 for monkeys) so that the amount of enhancement was about the same in both species. Note that enhancement during pursuit was observed even when the most conservative amplitude estimate (the peak of the response) was used. Although the enhancement was smaller when this measurement was used, indicating that both the increase and the decrease in eye velocity contributed to the enhancement, it was still significant in three groups of data and almost reached significance in the fourth. In the experiments we designed to mimic those conducted on humans by Das et al. (1995, 1998), we obtained a similar result to theirs: relatively little enhancement of the responses to perturbations during pursuit versus fixation. Our ability to reproduce in a single group of human subjects the basic features of prior data on on-line gain control for both monkey and human pursuit argues strongly that the modulation of the gain of visual-motor transmission for pursuit as a function of behavioral state is a general property of primate pursuit systems.

Our analysis indicates that the Das et al. (1995, 1998) experiments probably found similar responses to perturbations during pursuit and fixation because of several factors

that combined to defeat on-line gain control. First, large perturbations up to ±18.6°/s were used, causing target velocity to decline to or below zero during the perturbations, possibly reducing the very gain of visual-motor transmission that was being probed. Second, the perturbations were presented in the trough-first orientation, which our data show is a poor orientation for demonstrating larger responses during pursuit than during fixation since it starts by driving eye velocity close to zero. Third, their smaller subject pool may have included mainly subjects who were able to increase the on-line gain of pursuit during fixation when the perturbation has a frequency close to the normal tracking range. A 2.8 Hz stimulus, for example, which was used in both studies, enhanced responses to fixation perturbations in one of our subject's who normally only showed enhancement during pursuit. In future studies, it will be important to use perturbations that are suitable for probing the gain of visual-motor transmission without altering it.

The responses reported here to the conditions used by Das et al. (1995, 1998) remain puzzling in several ways. First, although we found, as they did, that pursuit and fixation responses were of similar size, the magnitudes reported here are somewhat lower than those reported in Das et al (1995, 1998). Second, the responses in our subjects were very heterogeneous: some showed larger responses to pursuit perturbations, suggesting a possible enhancement, while one subject showed larger responses to fixation perturbations. Perhaps the use of 3 cycles of a relatively low-frequency sine wave may explain why one subject exhibited responses during fixation that were close to pursuit. One cycle of a perturbation may not allow human subjects to engage predictive mechanisms (Barnes and Asselman 1991a, b), whereas 3 cycles might allow them to enhance their pursuit even when the sine waves are delivered during fixation. The

capacity to take advantage of predictions could vary among subjects. In this regard, it is worth noting that our subject with unusually large responses to the 3-cycle fixation perturbations was also the subject with the most pursuit experience, and was in this respect most like the subjects of Das et al. (1995, 1998). Note that an enhanced response to repetitive pursuit perturbations might not exclusively reflect a subject's ability to predict target motion. If the repetitive perturbations do not bring eye velocity close to zero (as in (Goldreich et al. 1992), either on-line gain control or predictions (or both) might contribute to enhanced responses.

In our experiments, perturbations were meant as probes to read out the instantaneous gain of visual-motor transmission for pursuit. Our finding that the amount of on-line gain control that can be demonstrated depends on the amplitude and frequency of the perturbations emphasizes the importance of choosing a perturbation that can probe the state of the system without altering it. Small, brief perturbations (like the ones we use in Figure 1) can probe on-line gain control without changing it because the changes in eye velocity evoked by the perturbation are small. On the other hand, when perturbations require a large decrease in eye velocity, they have the unfortunate side-effect of decreasing the on-line gain of pursuit, providing data that are challenging to interpret. However, the need for careful choice of perturbations should not be taken as evidence that on-line gain control is present only in restricted conditions. In fact, the opposite appears to be true: a careful choice of perturbations is necessary because online gain control may modulate pursuit so continuously that an ill-chosen perturbation can reduce the same online gain it was designed to measure. If a suitable perturbation was chosen,

our data showed that on-line gain control was evident when pursuit was underway in all the subjects we tested.

A more thorough exploration of the time course of online gain control would be particularly interesting since the data here imply that the gain of transmission in visual-motor pathways may be dynamically updated on a rather short time scale. Schwartz and Lisberger (1994) demonstrated that behavioral conditions can affect pursuit gain and showed that the gain of the response to perturbations grew with eye or target velocity at the time of the perturbation. Their data argued that that on-line gain varies continuously rather than as a bimodal switch. Our finding of a difference in the degree of enhancement for trough-first and peak-first perturbations implies that the gain is variable over a time course that may be as short as 100 ms. This interpretation is supported by the inverse relationship between the eye velocity in the first and second components of the responses to trough-first perturbations. The linearity of the relationship, in the face of different amplitude perturbations, argues that the effect of the perturbation on the on-line gain of pursuit can be, under inopportune circumstances, a predominant factor determining the size of the response.

The data reported here, in combination with previous observations (Schwartz and Lisberger 1994) that online gain control depends on eye velocity, imply that the pursuit system is informed about eye velocity. That perturbation responses during 5°/s and 10°/s pursuit are different argue that this eye velocity signal is sufficiently precise to differentiate eye velocities separated by only 5°/s. The experiments here were not designed to reveal the resolution of the eye velocity signal in detail, and human subjects may not be best suited to such an experiment since they frequently become annoyed

when asked to perform too many trials. Identifying the resolution of the eye velocity signal, and locating a neural signal with the appropriate resolution to furnish such a signal would provide a more complete picture of online gain control in pursuit. We will return to this point in chapter 2.

In summary, we have presented evidence that humans, like monkeys, show enhanced responses to perturbations of target velocity presented during pursuit. Our data show that the pursuit systems of both humans and monkeys are modulated by a variable gain control that is, in turn, modulated by behavioral state. Our analysis also suggests that the variable gain control may be continuously updated, even on a scale of milliseconds, as behavioral conditions change.

Acknowledgements

We gratefully acknowledge the support from the Howard Hughes Medical Institute and the National Science Foundation (AKC). We are also indebted to Scott Ruffner for his help in developing the software for stimulus presentation and data acquisition.

References

Barnes GR and Asselman PT. The assessment of predictive effects in smooth eye movement control. *Acta Otolaryngol Suppl* 481: 343-347, 1991a.

Barnes GR and Asselman PT. The mechanism of prediction in human smooth pursuit eye movements. *J Physiol* 439: 439-461, 1991b.

Carey MR and Lisberger SG. Behavioral analysis of gain control for smooth pursuit eye movements. *Ann N Y Acad Sci* 978: 507, 2002.

Churchland MM and Lisberger SG. Experimental and computational analysis of monkey smooth pursuit eye movements. *J Neurophysiol* 86: 741-759, 2001.

Das VE, DiScenna AO, Feltz A, Yaniglos S, and Leigh RJ. Tests of a linear model of visual-vestibular interaction using the technique of parameter estimation. *Biol Cybern* 78: 183-195, 1998.

Das VE, Leigh RJ, Thomas CW, Averbuch-Heller L, Zivotofsky AZ, Discenna AO, and Dell'Osso LF. Modulation of high-frequency vestibuloocular reflex during visual tracking in humans. *J Neurophysiol* 74: 624-632, 1995.

Goldreich D, Krauzlis RJ, and Lisberger SG. Effect of changing feedback delay on spontaneous oscillations in smooth pursuit eye movements of monkeys. *J Neurophysiol* 67: 625-638, 1992.

Keller EL and Heinen SJ. Generation of smooth-pursuit eye movements: neuronal mechanisms and pathways. *Neurosci Res* 11: 79-107, 1991.

Komatsu H and Wurtz RH. Modulation of pursuit eye movements by stimulation of cortical areas MT and MST. *J Neurophysiol* 62: 31-47, 1989.

Krauzlis RJ and Lisberger SG. A model of visually-guided smooth pursuit eye movements based on behavioral observations. *J Comput Neurosci* 1: 265-283, 1994.

Lisberger SG, Evinger C, Johanson GW, and Fuchs AF. Relationship between eye acceleration and retinal image velocity during foveal smooth pursuit in man and monkey. *J Neurophysiol* 46: 229-249, 1981.

Lisberger SG, Morris EJ, and Tychsen L. Visual motion processing and sensory-motor integration for smooth pursuit eye movements. *Annu Rev Neurosci* 10: 97-129, 1987.

Lisberger SG and Westbrook LE. Properties of visual inputs that initiate horizontal smooth pursuit eye movements in monkeys. *J Neurosci* 5: 1662-1673, 1985.

Luebke AE and Robinson DA. Transition dynamics between pursuit and fixation suggest different systems. *Vision Res* 28: 941-946, 1988.

Maunsell JH and Van Essen DC. Functional properties of neurons in middle temporal visual area of the macaque monkey. I. Selectivity for stimulus direction, speed, and orientation. *J Neurophysiol* 49: 1127-1147, 1983.

Newsome WT and Pare EB. A selective impairment of motion perception following lesions of the middle temporal visual area (MT). *J Neurosci* 8: 2201-2211, 1988.

Rashbass C. The relationship between saccadic and smooth tracking eye movements. *Journal of Physiology (London)* 159: 326-338, 1961.

Robinson DA. The mechanics of human smooth pursuit eye movement. *J Physiol* 180: 569-591, 1965.

Schwartz JD and Lisberger SG. Initial tracking conditions modulate the gain of visuo-motor transmission for smooth pursuit eye movements in monkeys. *Vis Neurosci* 11: 411-424, 1994.

Tanaka M and Lisberger SG. Enhancement of multiple components of pursuit eye movement by microstimulation in the arcuate frontal pursuit area in monkeys. *J Neurophysiol* 87: 802-818, 2002.

Tychsen L and Lisberger SG. Visual motion processing for the initiation of smooth-pursuit eye movements in humans. *J Neurophysiol* 56: 953-968, 1986.

Figure Legends

Figure 1. Enhancement of the response to brief perturbations of target motion during ongoing pursuit. A: Eye and target velocity traces to illustrate how stimuli were presented and measured. The traces labeled "Target velocity" show examples of two trajectories of target motion. The dashed trace describes the trajectory of a rightwards pursuit target moving at 10°/s. The continuous trace describes the trajectory of a rightwards target with a 5 Hz, ±5°/s perturbation. The traces labeled "Eye velocity" show averaged responses to the two target motions. The trace labeled "Difference eye velocity during pursuit" shows the difference between the responses to target motion with and without the perturbation at each millisecond. The trace labeled "Difference eye velocity during fixation" shows the response to a 5 Hz, ±5°/s fixation perturbation. In all cases, upward deflections of the traces indicate rightwards motion. B, C. Comparison of responses under the two conditions: each symbol plots data for one subject and shows responses to 5 Hz pursuit perturbations as a function of the response to the same fixation perturbations. Black squares indicate subjects from Group 1: ±10°/s perturbations presented during 15 deg/s pursuit; gray squares indicate subjects from Group 2: ±5°/s perturbations presented during 10 deg/s pursuit. The dashed line has a slope of one and would be obtained if the responses were the same under the two conditions. Data from the subject whose traces are shown in Figure 1A is indicated by the arrow. Inset: Averaged responses to rightward or leftward fixation perturbations (open bars) or pursuit perturbations (filled bars) for all subjects. Black and gray bars indicate responses from Group 1and 2, respectively. "R" and "L" in x-axis labels indicate the direction of pursuit and of the first component of the perturbation. Significance at $p<0.05$ is represented by (*); significance at $p<0.005$ is

represented by (**). Error bars indicate standard deviations. The graphs and B and C were derived from the same data but represent different measures of the response to the perturbation: half of peak-to-trough excursion of average eye velocity in B and peak excursion in C.

Figure 1

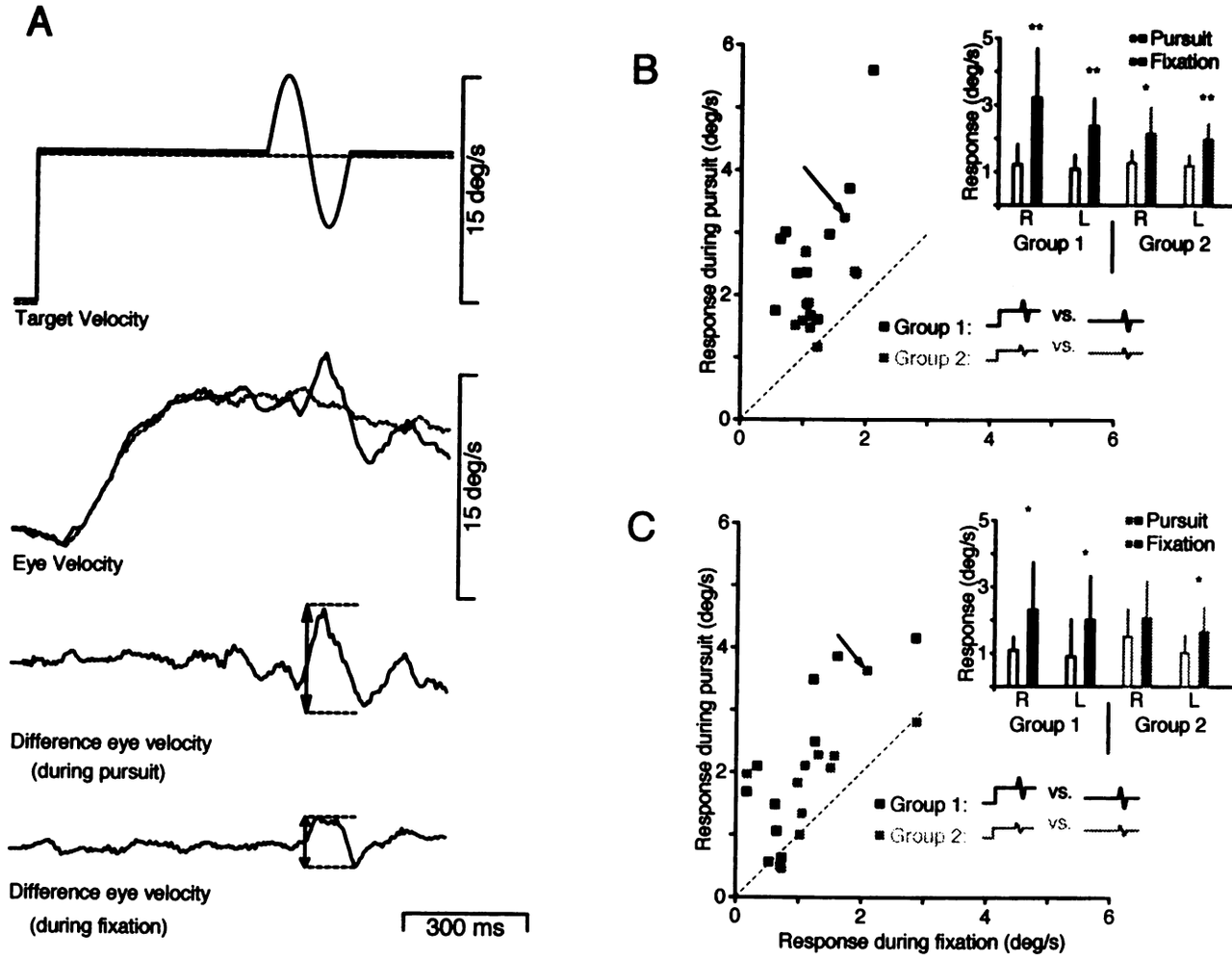
A
15 deg/s
Target Velocity
15 deg/s
Eye Velocity
Difference eye velocity
(during pursuit)
Difference eye velocity
(during fixation)
300 ms
B
Response during pursuit (deg/s)
Response (deg/s)
Pursuit
Fixation
R
L
R
L
Group 1
Group 2
Group 1:
vs.
Group 2:
vs.
C
Response during pursuit (deg/s)
Response during fixation (deg/s)
Response (deg/s)
Pursuit
Fixation
Group 1
Group 2
Group 1:
vs.
Group 2:
vs.

Figure 2. Enhancement of the response to a pursuit perturbation can depend on perturbation orientation. Each point plots data from one subject for 2.8Hz, ±19°/s perturbations, showing the response during pursuit as a function of that during fixation. Gray and black squares indicate responses to perturbations in the trough-first and peak-first orientation, respectively. The dashed line has a slope of one and would be obtained if the responses were the same under the two conditions. Inset: Averaged responses to rightward or leftward perturbations presented during fixation (open bars) or pursuit (filled bars) for all subjects. Gray and black bars indicate responses to trough-first and peak-first perturbations. "R" and "L" in the x-axis labels indicate the direction of the first phase of the perturbation. Note that the responses during fixation are the same in A and B. Significance at $p<0.05$ is represented by (*); significance at $p<0.005$ is represented by (**). Error bars indicate standard deviations.

Figure 2

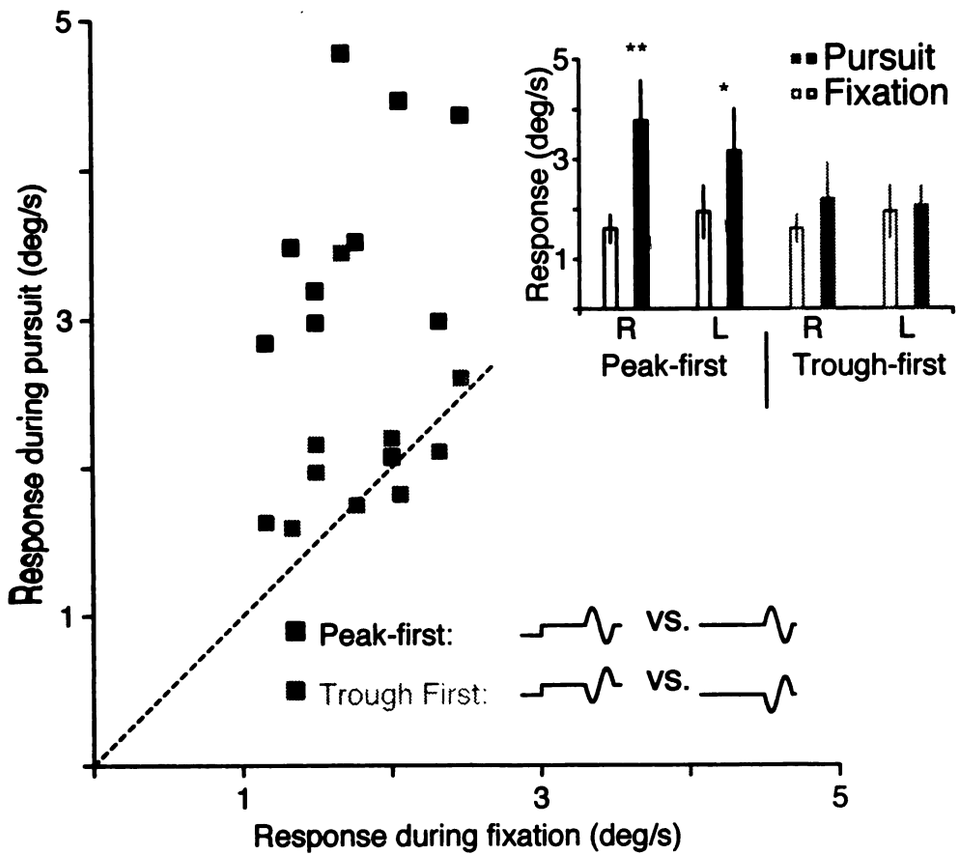
Response during pursuit (deg/s)
5
3
1
Response during fixation (deg/s)
1
3
5
Peak-first:
vs.
Trough First:
vs.
Response (deg/s)
5
3
1
**
*
Pursuit
Fixation
R
L
R
L
Peak-first
Trough-first

Figure 3. Average traces explaining why responses to large, but not small perturbations might depend strongly on the orientation of the perturbation. A. Target velocity and average eye velocity in response to perturbations of 2.8 Hz, ±19°/s presented during ongoing pursuit at 10°/s. B. Target velocity and average eye velocity in response to perturbations of 2.8 Hz, ±5°/s presented during ongoing pursuit at 10°/s. In both panels, dashed traces indicate trials where perturbations were presented in the peak-first orientation, bold continuous traces indicate trials where the perturbation was presented in the trough-first orientation, and fine continuous traces indicate the control condition where no perturbation was presented. Points I and II indicate times when the response was driven by the same target velocity, but after different histories.

Figure 3

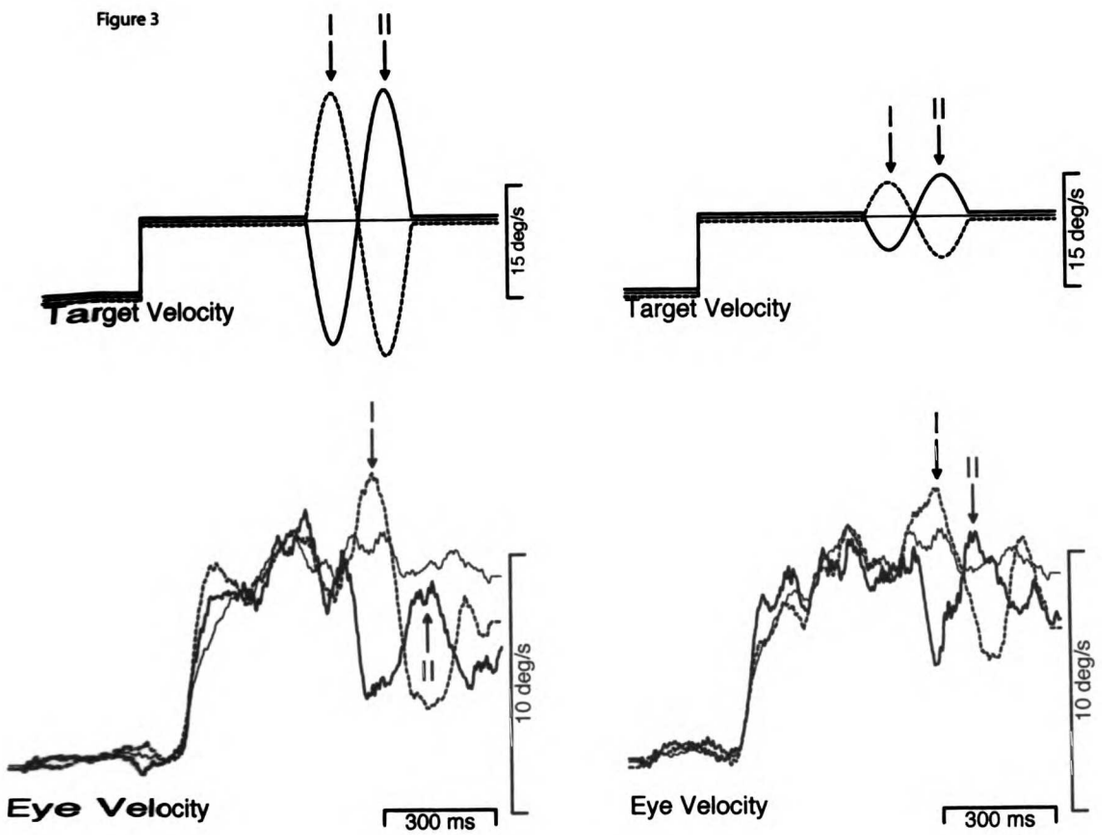
I
II
15 deg/s
Target Velocity
I
II
15 deg/s
Target Velocity
I
II
10 deg/s
Eye Velocity
300 ms
I
II
10 deg/s
Eye Velocity
300 ms

Figure 4. Inverse relationship between the amplitude of the responses to the first and second components of trough-first perturbations. Each graph shows data from a different subject. Different symbols show responses to perturbations of 3 sizes (±5, ±10 and ±18.6°/s) and 2 frequencies (5 and 2.8 Hz), as defined in the key.

Figure 4

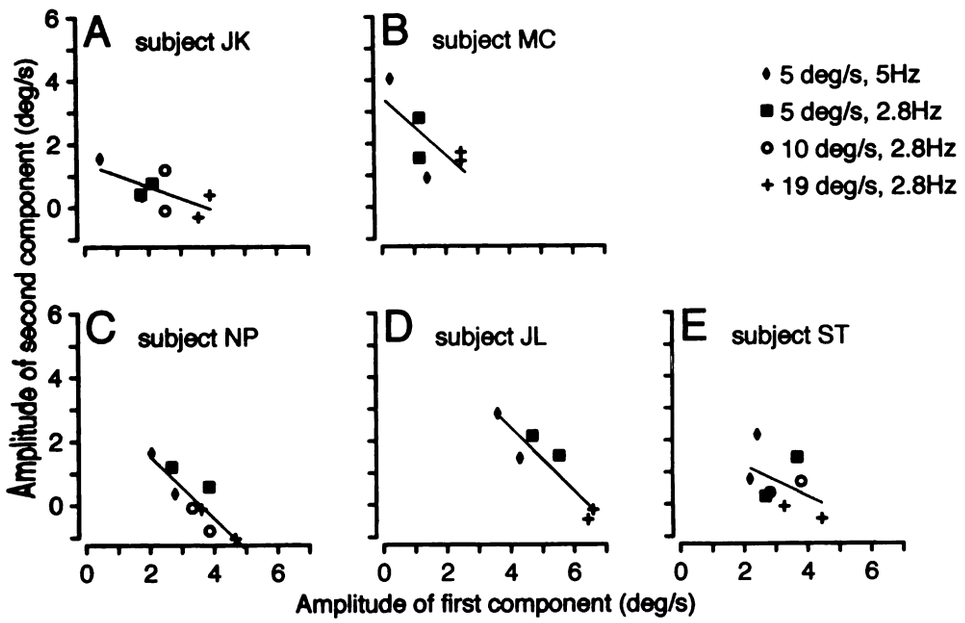
A subject JK
B subject MC
C subject NP
D subject JL
E subject ST
5 deg/s, 5Hz
5 deg/s, 2.8Hz
10 deg/s, 2.8Hz
19 deg/s, 2.8Hz
Amplitude of second component (deg/s)
Amplitude of first component (deg/s)
0
2
4
6

Figure 5. Weak or absent enhancement of the response to continuous, sinusoidal perturbations imposed starting from the onset of ramp target motion. A. Target and eye velocity traces. Solid and dashed traces represent data from trials with and without perturbations, respectively. From top to bottom, the traces are target velocity, average eye velocity, the time course of the difference between average eye velocity in trials with and without perturbations, and average eye velocity for perturbations presented during fixation. B. Comparison of responses under the two conditions: each symbol plots data for one subject and shows responses to pursuit perturbations tracking as a function of the response to the same fixation perturbations. The dashed line has a slope of one and would obtain if the responses were the same under the two conditions. Inset: Black and white bars indicate the average peak-to-trough amplitude of the response to three perturbations presented during pursuit and fixation, respectively. "R" and "L" in the x-axis labels indicate the direction of either ongoing pursuit, if perturbations were presented during ongoing pursuit, or the first phase of the perturbation, if perturbations were presented during fixation. C. Sequential development of the response to perturbations as a function of the number of the perturbation in the sequence. Each symbol plots the response to one of the perturbations and the connected symbols show the response to the 3 perturbations for a given subject and direction of pursuit. Black lines and symbols indicate responses to pursuit perturbations and gray lines indicate responses to fixation perturbations. Thin lines and small symbols represent individual responses; thick lines and large symbols plot the average response. Responses to both the second and third pursuit perturbations were significantly larger than responses to the first pursuit

perturbation (one-tailed t-test: 1st vs 2nd : Left: p<.05, Right p<.04; 2nd vs 3rd : Left: p<.02, Right: p<.04). Responses to both the second and third fixation perturbations were larger than responses to the first pursuit perturbation, but this difference did not reach significance in every case (one-tailed t-test: 1st vs 2nd : Left: p<.08, Right p<.03; 2nd vs 3rd : Left: p<.06, Right p<.05). Inset: The same plot for one subject who did not show enhancement of the response to the 3 sine wave perturbation during pursuit. This subject's data are also included in the main graph.

Figure 5

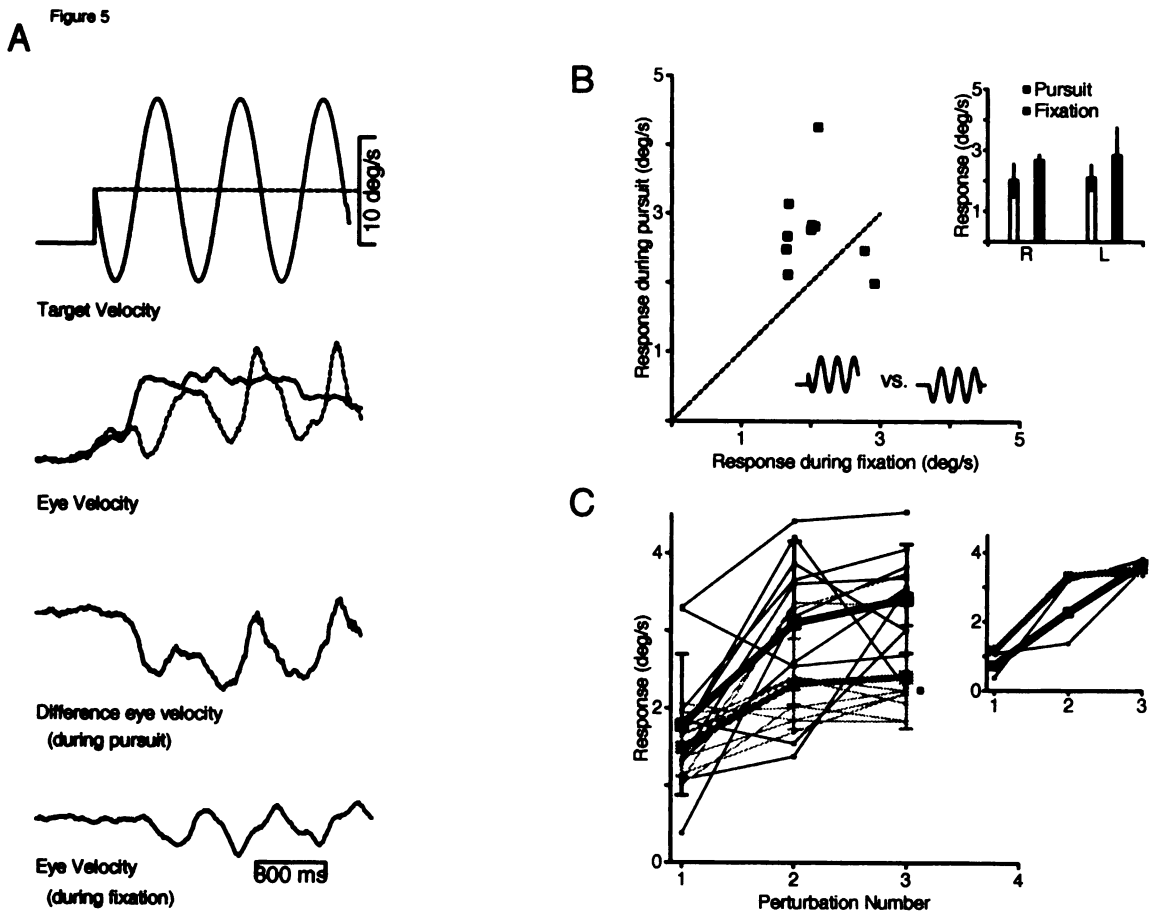
A
10 deg/s
Target Velocity
Eye Velocity
Difference eye velocity
(during pursuit)
Eye Velocity
(during fixation)
800 ms
B
Response during pursuit (deg/s)
Response during fixation (deg/s)
vs.
Pursuit
Fixation
Response (deg/s)
R
L
C
Response (deg/s)
Perturbation Number

Chapter 2: Speed tuning of exraretinal responses in area MST

Abstract

We measured the responses to extraretinal and retinal inputs of single neurons in MST. Extraretinal responses were measured during stabilized pursuit at 7 different velocities (0°/s–30°/s) in two directions. Almost all neurons were clearly speed-tuned and exhibited a variety of responses to increasing eye velocity. Most frequently, however, firing rates simply increased monotonically with eye velocity. Retinal responses were measured by presenting large patches of coherently moving dots in the neuron's receptive field at 9 different velocities (0°/s–128°/s). Again, a variety of tuning curves were observed, but most frequently firing rates simply increased monotonically with stimulus speed.

Introduction

Interpreting the visual world requires not only processing visual signals but also understanding them in the context of movements. Smooth pursuit eye movements, which act to eliminate image velocity on the retina (for review, see Keller and Heinen 1991; Lisberger et al. 1987), can dramatically change the pattern of visual inputs to the brain. For example, consider an observer watching a target of interest move across a patterned background. Once the subject begins to accurately pursue the target, the movement of the eyes will mostly eliminate target motion on the retina. However, this same movement of the eyes will also add motion signals to the stationary patterned background surrounding the target. From the point of view of the retina and early visual areas, the moving target will appear stationary while the stationary background appears to move. The motion signals from the background can be quite complex, particularly if the movement of the eyes is added to movement of the observer through space: in this case, pursuit can further distort the complex optic flow fields caused by self motion (Royden et al. 1992; Royden et al. 1994; Shenoy et al. 2002).

Behavioral evidence suggests that the brain can successfully interpret visual information in the context of eye movements. The simplest behavioral evidence is the observation that subjects continue to pursue at the right velocity even after motion from a target has been eliminated. The pursuit system, which is engaged by visual motion, persists at the appropriate speed instead of responding as if the target were stationary. A neural estimate of ongoing eye velocity could indicate to the pursuit system that the absence of motion on the retina is not due to a stationary target. Behavioral experiments

provide further evidence that the pursuit system relies on an estimate eye velocity even when image velocity is mostly absent. In both humans and monkeys, responses to small perturbations of target motion depend on ongoing eye velocity (Churchland and Lisberger 2002; Schwartz and Lisberger 1994): responses are large when perturbations are presented during pursuit, and much smaller when perturbations are presented during fixation. This finding has suggested that the pursuit system is modulated by an online gain control, the strength of which is determined, at least in part, by eye ongoing velocity. Response amplitudes to stimulation in the pursuit region of the frontal eye fields are likewise dependent on ongoing eye pursuit (Tanaka and Lisberger 2002), suggesting that eye velocity signals are used to set pursuit gain at the level of the cortex, rather than in subcortical pursuit areas. The origin of these eye velocity signals is not known.

Responses of some neurons in cortical area MST suggest they might provide the neural estimate of eye velocity suggested by behavioral observations. These neurons are active during pursuit eye movements, even under conditions used to eliminate any visual inputs (Newsome et al. 1988). Because the responses are driven by inputs that are not retinal in origin, they were named extraretinal responses. The extraretinal responses observed in cortical area MST could provide an eye velocity signal to subserve both the persistence of accurate pursuit responses when image velocity is eliminated and the variable responses to perturbations seen at different eye velocities. If so, the extraretinal responses should exhibit clear speed and direction tuning. A number of papers have examined direction tuning of pursuit responses. In the original paper describing extraretinal responses (Newsome et al. 1988), the authors observed that responses

frequently depended on pursuit direction. Later on, Squatrito and Maioli (1997) and Erickson and Their (1991) also observed that extraretinal responses are frequently directional, although extraretinal responses were not explicitly separated from visual responses in either study. A few studies have measured responses of MST neurons to different pursuit speeds (Shenoy et al. 2002) in the context of other experiments, but the speed tuning of extraretinal responses has never been explored using a stimulus configuration designed to separate extraretinal from visual signals. In addition, although the existence of extraretinal responses has been known for some time, the resolution with which they reflect eye velocity has never been calculated.

In the current paper, we report that responses of MST neurons during pursuit are speed tuned, even in conditions that eliminate visual motion inputs. In addition, we measure the resolution of the neural response and compare it to the resolution of the eye velocity signal suggested by behavioral experiments. Lastly, we explore the relationship between speed tuning of the visual response and speed tuning of the extraretinal response.

Methods

Eye movement and neural recordings were obtained from two adult male rhesus monkeys (*Macaca mulatta*) that were trained to fixate and pursue visual targets for fluid reward. Monkeys were implanted with head restraints and scleral search coils as described elsewhere (Churchland and Lisberger 2000), (Judge et al. 1980). After initial training, monkeys were implanted with stainless steel head holders and stainless steel or

cilux cylinders (Crist instruments, Hagerstown, MD) placed over a 20 mm circular hole cut in the skull to allow access to MST for neural recordings. For each experimental session, the monkey sat in a primate chair affixed with a tube for dispensing fluid rewards. Methods were approved in advance by the Institutional Animal Care and Use Committee at the University of California, San Francisco. All experimental procedures were in accordance with the National Institutes of Health Guide for the Care and Use of Laboratory Animals.

Behavioral Data

Stimulus presentation and eye movement recording and analysis

Visual stimuli were displayed on a 12 inch diagonal analog oscilloscope. The display was positioned 30 cm from the monkey and subtended horizontal and visual angles of 50° and 40°. Visual stimuli consisted of either single spots or patches of moving dots. The aperture size for patches of dots varied from 10°X10° to 30°X30° depending on the preferences of the neuron under study.

Pursuit trials began with the appearance of a fixation point that was between 2° and 10° eccentric from the center along the preferred-null axis. Monkeys were required to maintain fixation for a randomized time between 1000 and 1200 ms. The target then stepped away from the fovea and immediately began to move towards the fovea (Rashbass, 1961) at between 2°/s and 30°/s. Target motion continued for between 1000 and 1200 ms. The monkey was required to maintain an eye position that was within 3° of

target motion throughout the trial or the trial would be terminated and the data not included in analysis.

In some experiments, brief perturbations of target velocity were presented 300 ms after the target began to move. At the time perturbations occurred, pursuit had been successfully initiated so eye velocity was close to target velocity. Perturbations consisted of sinusoidal modulation of target velocity with a frequency of 5 or 10 Hz and an amplitude of 4°/s 8°/s peak-to-peak. Perturbations always caused target speed to first increase and then decrease ("peak-first" orientation) because responses to this phase are easier to interpret than responses to perturbations of the opposite phase (Churchland and Lisberger 2002). Perturbations were presented during ongoing pursuit at seven different target speeds (0, 2, 5, 10, 15, 20 and 30°/s) and in 2 directions (left and right). Perturbations presented during fixation (0°/s) could be either leftwards or rightwards on separate trials since there is no ongoing pursuit velocity when the target is not moving.

In experiments designed to measure speed tuning of the exraretinal response, we used a combination of strategies to reduce visual motion during pursuit maintenance so that we could measure neural responses that were driven by extraretinal, rather than retinal signals. First, responses were recorded in complete darkness. Darkness was assessed both by measuring the ambient illumination in the room (0.0 candelas/m^2) and by dark-adapting experimenters in the room to ensure that no light sources were overlooked. Second, the analog oscilloscope we used was selected because this system can result in less ambient illumination that cathode ray tube displays or projection

systems. Pursuit targets were extremely small and dim (~0.2° across, 1.6 candelas/m^2) so they caused no increase in the ambient illumination in the room. Nonetheless, we feared that the dark-adapted visual system might be sensitive to ambient illumination from the target. Therefore, data collection was routinely stopped for about 30 seconds every ten minutes so that the monkeys could be presented with normal lighting levels to prevent dark adaptation. Lastly, regular pursuit trials were interleaved with trials containing brief (300ms) periods of target stabilization wherein target velocity was driven by eye velocity so that the target could not cause any motion on the retina. Stabilization periods occurred late in the pursuit trial (340 ms after motion onset) when the monkey was already engaged in ongoing pursuit so they typically did not interrupt pursuit considerably. Following the end of the stabilization period, the target continued to move by for a variable amount of time that depended on speed and was randomized within each speed so that the monkey could not predict when the trial would end. Trials not containing a stabilized period were the same duration. Trials with and without a stabilized period were presented in equal numbers to help prevent the monkey from detecting or possibly anticipating the stabilized period and to provide control traces against which stabilized traces could be compared.

The use of stabilization to reduce image motion is potentially problematic if the eye coil is not precisely calibrated because target motion during the stabilized period might be driven by an inaccurate estimate of eye velocity. Three strategies were used to avoid this problem. First, we used very small targets to calibrate the eye coil as accurately as possible and always re-checked the calibration when a new neuron was encountered.

Second, we compared eye velocity responses during periods where the target was stabilized to the same period from control trials (for example, the black and red traces in figure 1). Large differences in responses to the two types of trials would indicate that the stabilizing the target was interrupting the monkey's pursuit, perhaps because target velocity was driven by an inaccurate estimate of eye velocity. Although eye velocity at the end of the stabilized period was sometimes slightly slower than eye velocity in control trials at the same time, this difference was never more than a degree or two per second for the neurons that were included for analysis.

Lastly, we explored how small amounts of image velocity affected eye velocity during the stabilized period to could determine whether a mis-calibration or other problems with the stabilization could be detected. To this end, we measured responses to trials where target velocity during the stabilized period equaled the monkey's eye velocity plus or minus a small amount of additional velocity (0.5°/s, 1°/s or 2°/s; figure 1A). The green, purple and cyan traces in figure 1B suggest that small amounts of image velocity can have a clear effect on eye velocity during the stabilized period. That as little as 0.5°/s of image velocity had a clear effect on pursuit responses gave us confidence that we would be able to detect and correct instances of mis-calibration simply by comparing eye velocity responses to trials that did or did not contain a stabilized period.

Eye velocity recording and analysis

Signals related to horizontal eye velocity and eye position were digitized at a sampling rate of 1000 Hz for each channel. The eye position signal was low-pass filtered with a cutoff at 300 Hz and voltages proportional to eye velocity were obtained by differentiating the eye position signals with an analog circuit. Data analysis was performed after the experiment. For pursuit trials used to measure speed tuning of extraretinal responses, traces that contained saccades in the 300 ms stabilization interval (or the equivalent time period in control trials) were identified. Trials containing saccades in this interval were excluded from subsequent analysis. At least 10 trials for each speed were collected for all the neurons analyzed.

To display the pursuit responses for figure 3, responses were aligned to the onset of pursuit initiation. We determined the onset of pursuit initiation for each trial using the intersection of constraints method (Carl and Gellman 1987).

For pursuit trials containing perturbations of target velocity, trials that contained saccades that took place near or during the peak or trough of the response to the perturbation were excluded from further analysis. To determine the tightness of the link between ongoing eye velocity and the response to perturbations, the peak and trough of the perturbation response were measured in each trial at each speed to determine response amplitude. Response amplitudes were then grouped according to the ongoing pursuit speed during which they were presented providing 7 distributions, one for each speed. One trial was then removed from each of the 7 distributions, yielding 7 excluded responses. The remaining responses were fit with a normal probability density function.

We then determined which of the 7 distributions each of the excluded points was maximally likely to have been drawn from. Stated more simply, we asked how well we could guess the ongoing pursuit velocity by looking at the size of the response to a perturbation. For each excluded response, the distribution most likely to have produced the response either corresponded to the actual ongoing pursuit velocity during which the response was generated (a correct assignment) or a different ongoing pursuit velocity (an incorrect assignment). At least10 trials were tested at each of the seven speeds, so the analysis was repeated 10 times, excluding a different trial each time. In preliminary analyses, we compared ideal observer performance when distributions were fit with a normal probability density function with performance when a poisson probability density function was used. The two distributions caused very similar results except that performance using the poisson probability density function was consistently about 2% better than when the normal probability density function was used.

To provide a control trace for comparison, the amplitudes for each trial were randomly assigned to each of the 7 speeds tested. The same procedure described above was used, providing an estimate of the percentage correct that would be expected by chance.

Neural Data

Extracellular action potentials were recorded from single units in area MST. Recordings from two monkeys were made. Recordings were made using sharp, 1-3 MΩ tungsten microelectrodes (Frederick Haer Co, Bowdoinham, ME). The electrode location

was determined by a guide tube inserted in a plastic grid (Crist Instruments) which was positioned daily in a cylinder over the superior temporal sulcus each day. The voltage recorded by the electrode was amplified conventionally (Dagan, Minneapolis, MN) bandpass filtered from 100Hz to 5 or 10Khz and viewed on an analog oscilloscope.

Identification of sites

Neurons were recorded from throughout area MST in two monkeys. Both monkeys had cylinders centered at approximately 15 mm lateral and 2 mm posterior. Cylinders were oriented so that electrodes were introduced perpendicular to the cortical surface. The advantage of this configuration is that penetrations typically include area MST, the lumen of the superior temporal sulcus and the middle temporal area (MT) making it straightforward to distinguish MST from MT. Neurons were identified as being part of MST if they were dorsal to the lumen and had large receptive fields. Receptive fields frequently included the fovea and large parts of the ipsilateral field. Neurons with smaller receptive fields were sometimes included if they were close to neurons that were clearly MST neurons or if they were dorsal to the lumen of the superior temporal sulcus. Both monkeys are still being used in other experiments so histology is not available.

Neuronal recording and analysis of extraretinal response

After isolating a neuron, we first estimated its preferred pursuit direction by presenting pursuit trials in each of 8 directions. Neurons were selected for study if they

showed above baseline responses to pursuit in the dark in at least one of 8 directions. Firing rates in response to trials in the same direction were averaged resulting in 8 2-dimensional vectors consisting of direction and firing rate. To determine the neuron's preferred pursuit direction, the eight vectors were summed and the resulting direction was taken as the neuron's preferred direction. The opposite direction was taken as the null direction. We observed preferred directions that spanned 360°, but noted a bias towards ipsiversive pursuit that is in good agreement with data reported elsewhere (Shenoy et al. 2002; Squatrito and Maioli 1997). Pursuit trials designed to test speed tuning were presented in preferred and null directions at speeds ranging from -30°/s to 30°/s. We collected data from at least 10 stabilized and 10 control trials at each of 6 speeds in 2 directions. In addition, 10 stabilized and 10 control trials were taken in response to a stationary target. For many cells, we also collected data from stabilized trials at 20°/s in 8 directions. This allowed us to confirm that the direction in which the speed trials were presented was indeed the neuron's best direction. Fortunately, we never encountered a cell where our initial estimate of preferred direction was very far off.

Some responses in MST are modulated by eye position rather than eye velocity (Bremmer et al. 1997; de Oliveira et al. 1997; Thiele et al. 1997). To test whether neurons we encountered had responses that were modulated by eye position, responses from each neuron were recorded during a center-out saccade task. Neurons that exhibited directional responses during the sustained period after the saccade were not studied. To further rule out the possibility that eye position was modulating responses, pursuit trials were configured so that the during the 300 ms stabilization period (or the equivalent non-

stabilized period in control trials) spanned approximately the same orbital positions for each speed. This was accomplished by starting target motion at progressively more eccentric positions for faster target speeds so that the 300 ms interval during pursuit maintenance always took place when the eyes were as close as possible to the center of the orbit.

Before analyzing speed-tuning properties, we first assessed whether firing rates varied significantly as a function of speed. Responses were subjected to a one-way ANOVA (using speed as the main factor) and a criterion of $p = 0.01$. Four neurons were excluded from further analysis because their responses failed to exhibit significant speed tuning. To quantify the best extraretinal speed of the neurons, responses were fit with a smoothing cubic spline function (Shikin and Plis 1995). Functions that are more traditionally used for fitting speed-tuning data, such as skewed Gaussians (Priebe and Lisberger 2002), were inappropriate for this dataset since for many neurons, firing rate simply increased progressively with eye velocity. The knots of the spline were the speeds where we tested each neuron's response (from –30°/s to 30°/s). The smoothness of the spline was set so that the speed tuning properties from the fitted curves agreed well with visual inspection and the same smoothness was used for all cells. Our methods of determining significance of speed tuning and ascertaining preferred speed have been similarly used to analyze visual responses in area MT (Liu and Newsome 2003).

Neuronal recording and analysis of visual response

To determine the speed tuning for the purely visual response of the neuron, patches of moving dots were presented to the monkey during fixation. Each trial began with the onset of a fixation point, followed 600 ms later by the onset of a stationary patch. Two hundred ms later, dots in the patch began to move coherently and continued to move for 500 ms. The patch was then extinguished and the fixation light remained on for 200 ms. When a neuron was first isolated, a series of tests were conducted to determine the optimal size, receptive field placement and direction of motion for the patch. Because most neurons had large receptive fields that at least included the contralateral hemisphere, a large 30°X30° patch that occupied most of the contralateral field was most frequently used. The patch was sometimes placed in the ipsilateral portion of the visual field if receptive field mapping indicated that visual stimuli were more effective when placed in the ipsilateral hemifield. The large 30°X30° patch contained 500 dots (~0.2°/dot) that moved in each of 8 directions to determine the neuron's best speed. Subsequent trials were then presented in both the direction that was most effective in driving the cell and (for some neurons) the opposite direction. Responses to the last 400 ms of motion were analyzed. Trials where the monkey failed to stay within a 2.5° fixation window were aborted and not included in subsequent analysis.

Between 4 and 10 responses were measured at each speed: speeds ranged from 2°/s to 128°/s. We used the same procedures described above to test whether each neuron exhibited significant speed tuning, except that the significance of each neuron's speed tuning was assessed twice: once including all the speeds tested, and a second time excluding those speeds that were not used to test pursuit responses because they were too

high (the pursuit gain in response to 64°/s or 128°/s motion is low). Neurons that reached significance at $p<0.05$ were further studied to determine their preferred speed. Again, responses were fit with a smoothing cubic spline function with the same smoothness used to assess the best speed of pursuit responses. Best speed was assessed twice, once using all the speeds and once excluding speeds higher than the ones used for pursuit. Best speed was always determined from responses to motion in the neuron's preferred direction, whether the preferred direction was the same or opposite to the preferred direction for pursuit.

Estimate of population response and resolution over time

To determine how extraretinal responses evolved over time, we measured responses in 20 ms windows over the duration of the trial. Twenty ms was selected as the window size because it was brief enough to provide good temporal resolution of the response but long enough to reduce noise. The average response to each neuron's preferred speed was computed and normalized at each timepoint. Then, these responses were averaged across neurons. To determine the response of the pursuit system over time for comparison, we averaged eye velocity responses in the same way: first averaging across trials and then across neurons.

To estimate the resolution of the extraretinal signal, we quantified how well an ideal observer could determine actual eye velocity by examining the neural responses recorded during each eye velocity. For this analysis, we examined the firing rates from

each of the bins described above. Once again, one response from each speed was eliminated. For each speed, the histogram of spike counts was fit with both a normal and a poisson probability density function. We then took the spike count from each excluded trial to and asked from which of the 7 distributions the spike count was most likely to have been drawn. This distribution either corresponded to the eye velocity actually used to generate the spike count (a correct assignment) or a different eye velocity (an incorrect assignment). Ten trials were tested at each of the seven speeds, so the analysis was repeated 10 times, excluding a different trial each time. Thus each time point allowed us to determine the most likely distribution for 70 trials. The percentage of those trials that were assigned to the correct speed is reported for each time point. Again, only the percentage correct generated by the normal probability density function is shown because the two were almost identical except that the percentage correct generated by the poisson probability density function was consistently 2% better.

Control traces were computed as above, by shuffling the data at each time point and repeating the analysis.

We then asked whether the resolution might be improved by averaging responses across the population. For each trial, we averaged the responses of all the neurons, resulting in 10 responses for each of 7 speeds. We then repeated the ideal observer analysis as before.

Results

Two sources of visual inputs are present during pursuit (figure 2). The first source is motion from the background. Unless animals are pursuing in complete darkness, moving the eyes in one direction causes movement of the background in the opposite direction (figure 2A, grey dashed trace). Motion of the background in a brightly lit room has been shown to drive neurons in the superior temporal sulcus (Sakata et al. 1983). Pilot studies in our laboratory suggested that motion of the background even in a very dimly lit room can likewise drive responses in some neurons that are quite quiet during pursuit in complete darkness. Examples of the responses from such neurons in dim light (figure 2B and C, solid trace) and in darkness (figure 2B and C, dashed trace) suggest that a neuron could be mis-classified as responding to extraretinal inputs when in fact it is driven exclusively by visual inputs from the background. To ensure that motion from the background did not provide an input to the neurons tested here, we attempted to eliminate all sources of ambient light from the room (see methods). This way, no background is present to generate visual motion in the opposite direction from pursuit.

The second source of visual motion is motion from the target. Because eye velocity during pursuit does not match target velocity perfectly, the target itself can cause motion on the retina (Goldreich et al. 1992). The grey solid trace in figure 2B shows image velocity from the target. Many MST neurons are driven best by large, full field stimuli (Tanaka et al. 1986) that are moving quickly (Kawano et al. 1994), so we were unsure whether many neurons we encountered would respond robustly to relatively slow motion from a single, very small spot. Nevertheless, we did not want to rule out the possibility that some neurons might be driven by visual motion from the target. For this

reason, we presented the monkey with some trials that included brief periods (300 ms) of velocity stabilization: periods where target velocity was driven by eye velocity to eliminate target motion on the retina.

We recorded responses during pursuit from 85 neurons, of which 79 showed significant speed tuning during conditions designed to eliminate visual motion inputs. Six additional neurons failed to show significant speed tuning (methods) and were excluded from further analysis. Eye velocities and responses from two example neurons are shown in figure 3A and C. Figure 3A and C show average (n=10) eye velocities elicited by target motion from 0 to 30°/s in preferred and null directions (responses to 2°/s are excluded from this figure so that traces may be distinguished from one another). As in these examples, a comparison of eye velocity responses to stabilized and unstabilized responses normally did not reveal dissimilarities (compare grey and black traces in figure 3A and C). In the rare instances where large differences were encountered, the cell was eliminated from further analysis. Analysis of pursuit around the time that stabilization began (indicated by the vertical dashed lines which are displaced 100 ms from onset of stabilization to allow for visuomotor processing delays) further suggests that stabilization did not interrupt ongoing pursuit.

Inspection of the accompanying rasters (which correspond to responses on trials containing a stabilized period and are aligned to the onset of pursuit) in figures 3A and C shows that for both examples, firing rates depended on eye velocity. The two cells presented here are similar in a number of ways. First, they are typical in that they both

fired more for faster than for slower speeds. Second, this increase is strongly directional: even for the fasted speed tested, both cells responded almost exclusively in the neuron's preferred direction. Third, the examples are similar in the time course of their responses to pursuit: in both cases, firing rates increased most dramatically about 100 ms following the initiation of pursuit (indicated by the dotted lines on the rasters). Fourth, in neither case do the firing rates appear to change very much during the stabilized period. A final similarity becomes apparent when the average response during the stabilized period (and the average response during the same 300 ms interval for control trials) is plotted as a function of eye speed (black and grey traces in figure 3B and 3D). In both examples, the black and grey traces are similar, though not identical. Differences between the black and grey traces might reflect different inputs to the neurons during stabilized and unstabilized pursuit, or could be due to natural fluctuations in firing rate.

The example neurons in figure 3 also differ in a number of ways. First, a comparison of the rasters before pursuit is initiated indicates that the neuron in figure 3A has a clear baseline firing rate while the neuron in figure 3C responds only during pursuit. A second difference is that the firing of the neuron in figure 3B plateaus as eye velocity increases, while the response of the neuron in figure 3D increases continually with eye velocity up to the maximum that we tested. Both these speed profiles were observed frequently in the neurons we tested.

For both example neurons, the peak of the speed tuning curve (indicated by a star) is similar for stabilized and control responses. When we compared the best speed

computed from stabilized responses with the best speed computed from control responses for the population (figure 4a), we found that they were frequently very similar ($r=0.623$, $p<.01$). However, a number of neurons had best speeds during stabilized trials that were quite different from the best speed during control trials. In some cases, the differences arose because the firing rates for both conditions were quite variable; nevertheless, the scatter apparent in figure 4a emphasizes that visual inputs from the target can affect responses in MST.

Further inspection of figure 4a reveals that for both stabilized and control trials, the distribution of preferred speeds was highly skewed. Almost a third of the neurons we observed (24/79) preferred 30°/s pursuit, the fastest speed tested, for both stabilized and control trials.

We next tested whether the neurons' best speeds depended on whether responses in the null direction were taken into account. Theoretical and psychophysical studies suggest that perception of visual motion in a particular direction may depend not only on responses of neurons preferring that direction, but also on responses of neurons preferring the opposite direction (Heeger et al. 1999; Levinson and Sekuler 1975a, b). To approximate this opponent computation using a limited number of neurons, the responses to motion in a neuron's null direction are subtracted from responses in a neuron's preferred direction (Churchland and Lisberger 2001b). In the example neurons in figure 3, very little firing is evident in during pursuit in the null direction of the neurons. For both these examples, the best speed computed from the opponent response (preferred

– null) would differ little from the best speed computed from responses in the preferred direction only. We less frequently observed neurons with considerable firing in the null direction. The tuning curve for an example neuron is shown in figure 4b. The black trace indicates responses to pursuit in both directions, as in figure 3. The grey trace indicates the difference between preferred and null responses at each speed. The best speed of the opponent responses (grey star) in this case, is lower than the best speed taken from responses in the preferred direction only (black star). To determine whether the population estimate of eye motion might differ depending on whether a preferred-only or opponent computation was used, we computed the opponent response for each neuron and re-computed the best speed. The absence of much firing in the null direction that is evident in figure 3 was typical of the neurons we tested. Figure 4c plots the best opponent speed as a function of the best non-opponent speed for the population of cells recorded from both monkeys. The circled point corresponds to the example in 4b and is an outlier. Few of the neurons we observed had sufficient tuning in the null direction to change the preferred speed very much so most of the points lie along the line x=y.

Temporal evolution of extraretinal responses

We next asked how the extraretinal response evolved as pursuit was initiated. Eye velocity is close to 0 when target motion begins and only starts to approximate target velocity about 200 ms later. The rasters in figures 3A and 3C suggest that extraretinal responses might likewise increase gradually. We tested this, acknowledging that in our

stimulus configuration, the stabilized period is the only time during the trial where we can be certain that firing rates reflect only extraretinal, rather than visual inputs.

The black trace in figure 5A shows the average eye velocity response to 30°/s motion alongside the average firing rate in response to the same trials (30°/s was the neuron's best speed). Examination of the red and black traces reveals that he neural response is perhaps slightly delayed relative to the eye velocity response. Figure 5C (red trace) shows the average timecourse for the firing rates of all 79 neurons in the population. The timecourse of the average eye velocity signal is shown in the same figure (black trace). The population neural response appears to lead the eye velocity response slightly at first, but later appears to lag it by about 60 ms. Both the neural response and the eye velocity response appear to have reached a plateau by the time the stabilized period begins (indicated by the dashed lines), and neither response changes dramatically over the 300 ms stabilized period.

To begin to address how accurately the extraretinal response could provide the monkey with an estimate of his eye velocity, we computed, as a function of time, how well an ideal observer would be able to correctly determine eye velocity by looking at each neural response. Figure 5B shows the performance of an ideal observer for a single neuron (red) alongside a control trace indicating chance performance for comparison (blue).

To provide a comparison of the resolution of the neural response, we computed two behavioral estimates of resolution. To test the unlikely possibility that the extraretinal signal had the resolution of eye velocity itself, we computed the performance of an ideal observer whose goal is to determine which of the seven target velocities gave rise to a particular eye velocity. The black curve in figure 5B shows the ideal-observer performance from eye velocities obtained during recording of a single neuron. Note that the axes for the neuron and the behavior now represent the same quantity, performance of an ideal observer, but are different scales. Figure 5D shows discriminability of the neurons and of eye velocity averaged across the population. As in the example, neural performance appears to lag the behavioral performance, and is about 3 times worse. Over the stabilized period, ideal observer performance for the neural signal ranged from 23.9% to 25.9% and averaged 25.0%. Over the same time period, ideal observer performance for the eye velocity signal ranged from 68.9% to 81.8% and averaged 76.1%. Despite differences in magnitude, the two nonetheless have approximately the same shape.

To compare the resolution of eye velocity and extraretinal responses of individual neurons, we plotted values for each taken from the stabilized period in figure 6. The resolution of the neural response never exceeded the resolution of the eye velocity response. There is a weak negative correlation between the two variables ($r=-0.206$) which failed to reach statistical significance. The absence of a positive correlation between resolution of the eye velocity signal and resolution of the neural response suggests that daily variability in eye velocity is not matched by variability at the single neuron level.

To ask whether our population of neurons could collectively reflect eye velocity with greater resolution than single neurons, we recomputed ideal observer performance for the population. In the previous analysis, we computed ideal observer performance separately for each neuron and then averaged the result. In the current analysis, we averaged the normalized firing rate across neurons for each trial, creating a single distribution of responses for each speed. We then performed ideal observer analysis as before. Performance over he stabilized interval ranged from 22.5% to 53.1% and averaged 40.1%. This was a considerable improvement over performance observed in single neurons, but is again considerably lower than the resolution we observed for eye velocity itself.

The extraretinal signal might lack the resolution of eye velocity itself, but still be sufficiently accurate to provide the pursuit system with the estimate of eye velocity that has been suggested by the behavioral data about online gain (Churchland and Lisberger 2002; Schwartz and Lisberger 1994). We tested whether the extraretinal signal has sufficient resolution to subserve the behavioral observation that perturbation responses depends on ongoing pursuit speed (figure 7A). To make this comparison, we first measured the behavioral response to perturbations taking place during different ongoing pursuit speeds in both monkeys (figure 7A and 7B). This confirmed previous observations that the response is larger when ongoing pursuit speed is faster (Churchland and Lisberger 2002; Schwartz and Lisberger 1994). We then performed an ideal observer analysis as above: we asked whether an ideal observer could use the amplitude of a

perturbation response to determine the ongoing pursuit speed during which the perturbation was presented. Because perturbations were presented only once per trial, this method did not allow us to estimate how the eye velocity signal evolved over time. Presenting perturbations during pursuit initiation is impractical because the large amounts of image velocity make responses too variable (Churchland and Lisberger 2001a). A range of perturbation sizes and frequencies were tested eliciting ideal observer performance ranging from 32% correct to 49% correct (table 1). Performance was somewhat variable but did not appear to depend predictably on the perturbation parameters tested.

To compare the estimate of resolution suggested by the behavior with the estimate of resolution suggested by the neurons, we averaged ideal observer performance over the 300 ms stabilization period for each neuron. We then took a typical perturbation size, 5Hz $\pm$8°/s, and averaged together responses from both monkeys in both directions. The average ideal observer performance of the behavior (figure 7c, black bar) was slightly larger than the neural ideal observer performance for single neurons (figure 7c, white bar), and slightly smaller than neural ideal observer performance for the population (figure 7c, grey bar). The resolution of the extraretinal signal suggested by this second behavioral measure was much closer to what we actually observed in the neurons than the resolution suggested by eye velocity itself, where the average ideal observer performance over the same time period was 76%.

Relationship between speed tuning of visual and extra-retinal signals

To explore the speed tuning of purely visual responses in MST, we recorded responses of the same cells to visual motion presented during fixation. Examples of the target motion and visual responses from two neurons are shows in figure 8. The rasters for two example neurons are shown in figure 8a and 8c. In both cases, an "on" response is present at about 80 ms after motion onset (which is indicated by grey bars). This is followed by a sustained response that continues through the duration of each trial. Reponses up to 30°/s are shown to allow comparison with pursuit responses, although we actually measured responses up to 128°/s,

Each black point in figure 8b and d represents the averaged response taken from the period 150 ms after motion onset (so that the motion onset transient is excluded from the average) until the motion ended. Responses shown here are normalized to 1 to allow comparison with extraretinal responses, which are shown in grey. Each black point represents the averaged responses of the same cell to exraretinal motion, analyzed in the way described previously. Normalizing responses was necessary because we rarely observed that visual and extraretinal responses were of similar magnitude.

Data were fit with smoothing cubic splines to determine the best visual speed. Figure 9A plots the best extraretinal speed as a function of the best visual speed for each neuron. We wished to compare visual responses to the same speeds used to measure pursuit responses so, for this plot, visual responses to speeds faster than 30°/s were not

included when the significance of the speed tuning and the preferred speed were determined. As a result, the visual responses of more than half of the neurons failed to exhibit significant speed tuning (45 out of 79 were excluded). This was not unexpected since many neurons in area MST have been shown to prefer faster speeds (Kawano et al. 1994). The remaining 32 neurons showed uncorrelated best speeds for extraretinal and visual inputs ($r=0.072$, $p=0.5$). The scatter of points on the plot does not indicate that neurons were similarly driven best by the fastest pursuit speed tested and the fasted visual speed tested. When we included responses to faster speeds (64°/s and 128°/s), more neurons exhibited significant visual speed tuning (only 25 out of 79 were excluded). However, the inclusion of 20 more neurons in the analysis did little to change the correlation since the neurons that were added mostly preferred faster speeds than we were unable to test for pursuit. However, plotting the data in this way do refute the possibility that the neurons driven by the fastest pursuit speed were also driven by the fastest visual speed.

Note that the although we had to eliminate a third of the neurons because their responses were not significantly speed tuned, this does not imply that a third of the neurons in MST have visual responses with weak speed-tuning. We recorded only those neurons which, on a pre-test, were clearly responsive during pursuit.

Discussion

The data presented here argue that extraretinal responses in area MST are speed tuned. Most neurons in our population (79/85) that were found to respond in a direction selective way to pursuit also exhibited significant speed tuning. The data were collected during stabilized pursuit in complete darkness and therefore reflect extraretinal, rather than visual inputs. Other studies have provided some evidence that extraretinal responses might depend on speed but speed tuning properties have never been closely examined. Kawano et. Al. (1984) provided data from 4 cells suggesting that extraretinal responses might change with eye velocity. More recently, Shenoy et. Al. (2002) examined speed-tuning over a small range of speeds in the context of a different experiment. They, too, found evidence that extraretinal responses might depend on speed. However, ours is the first study that has examined in detail the speed tuning of extraretinal signal using a stimulus configuration designed to eliminate all visual motion inputs.

Extraretinal responses frequently increase with eye velocity

Many of the neurons we observed fired the most during the fastest speed tested. An examination of speed tuning curves sometimes suggested, as in figure 3D, that the change in firing rate as a function of speed increased monotonically over quite a wide range. We are unable to discern how such cells respond at faster pursuit speeds since eliciting reliable pursuit above 30°/s is difficult. It is particularly challenging to elicit very fast pursuit when stabilization is used to eliminate visual motion inputs. Our early attempts to elicit faster pursuit from the monkeys were unsuccessful because even when

we used fast target speeds to elicit pursuit responses above 30°/s, eye velocity slowed down considerably over the course of the stabilization period. Thus not only were eye velocity responses lower than we would have liked, they were quite variable over the course of the stabilized period. However, although we would have liked to observe neural responses to faster pursuit, we are confident that the range of pursuit speed we used, 2°/s-30°/s, includes most of the range over which pursuit normally takes place.

The monotonically increasing responses we frequently observed were rather different from the speed-tuning curves for visual motion that have been observed in area MT (Lagae et al. 1993; Maunsell and Van Essen 1983; Perrone and Thiele 2001). In area MT, neurons tend to be bandpass tuned for a particular speed and rarely show speed-tuned profiles that increase monotonically. One difference between the bandpass coding strategy observed for visual motion in MT and the monotonically increasing coding strategy we observed in MST for pursuit is that in the latter, each firing rate is associated with a single speed. When responses are bandpass tuned for a particular speed, a given firing rate would be observed in response to speeds that were either higher or lower than the preferred speed. A population of such responses is required to ascertain the actual stimulus speed. When responses are monotonically increasing, on the other hand, the actual stimulus speed can be garnered from the response of a single neuron.

The speed-tuning of the extraretinal signal in MST differs from the speed-tuning of the visual response in area MT in a second way: we observed that the best extraretinal speed of MST neurons did not typically depend on whether it was calculated from

opponent responses or from responses in the preferred direction only. By contrast, in area MT, many neurons lose their directionality at fast speeds (Churchland and Lisberger 2001b) so speed tuning computed from opponent signals can differ from speed tuning computed from the preferred direction only. The differences between speed tuning for visual responses in MT and speed tuning for pursuit responses in MST may arise from the distinct origins of the two types of responses. Speed tuning for visual responses in MT is thought to arise from direction-tuned V1 inputs (Perrone and Thiele 2002; Priebe et al. 2002). The origin of the extraretinal responses, while not yet known, is more likely to be feedback from structures later in the pursuit pathway.

Visual and extraretinal speed tuning appear unrelated

We observed that extraretinal responses in MST were similar to visual responses in MST in that both were frequently larger with faster speeds. However, the speed tuning of visual and extraretinal responses was nonetheless uncorrelated. Our finding that many MST neurons prefer fast visual speeds is in agreement with other studies in area MST (Kawano et al. 1994) . The speed tuning of the visual response in area MST is, like the pursuit responses, different from the speed tuning of visual responses in area MT. The reason for the preponderance of neurons preferring fast speeds in area MST is not known.

Temporal evolution of pursuit response

Presenting averaged responses as a function of time, as we have done here (figure5A and B), allows a comparison of the relative onset times for pursuit and the extraretinal response. Early in the trial, extraretinal responses may lead eye velocity slightly while shortly thereafter, extraretinal responses lag eye velocity. The small, dim pursuit targets used in our study were poor stimuli for driving visual responses in area MST, but we still we cannot rule out the possibility that the responses of some neurons during pursuit initiation were visual.

Two other studies have addressed the relative timing of extraretinal firing and eye movements. In the first of these studies, most MST responses were reported to lag pursuit initiation by at least 50 ms (Newsome et al. 1988). Our observation that the averaged exraretinal response lagged eye velocity during most of pursuit initiation is in agreement with this (figure 5c). The Newsome et al (1988) study also reported that a small number of MST neurons appeared to begin firing about 100 ms before pursuit initiation. In our population average, we likewise observed a small extraretinal response that preceded the onset of eye velocity. This was variable, however, and was not present in all neurons.

In a second study, the timing of pursuit onset and the onset of extraretinal responses was examined using an "imaginary" target defined by motion in the periphery (Ilg and Thier 2003). This stimulus configuration is advantageous for studying extraretinal responses during pursuit initiation because no image velocity is present in the central retina. The authors report the mean latency of the extraretinal responses which

was about 50 ms shorter than the latency of the eye movements, suggesting that extraretinal responses lead eye velocity. Although, at first, this seems to contradict the observations here and in previous reports (Newsome et al. 1988), it is hard to be certain without knowing the full timecourse of the extraretinal responses. For example, if a small amount of firing, perhaps from a minority of neurons, were present early on, the mean latency would be reported as quite short. This short mean latency could exist even if the extraretinal responses lagged pursuit responses for the remainder of pursuit initiation, as we observed.

Possible functions of the extraretinal signal

One putative function of the extraretinal signal is to allow area MST to represent target velocity (Pack et al. 2001). However, only when speed tuning for visual and extraretinal inputs is similar can target velocity be computed at the level of single neurons. For example, a neuron that responds robustly to image motion at 30°/s before pursuit is initiated and continues responding at about the same rate during 30°/s pursuit maintenance reflects target velocity, which has remained unchanged as eye and image velocity increase and decrease. However, when speed tuning for visual and extraretinal inputs is different, a neuron might respond quite differently to image motion and pursuit even when target velocity is unchanged. Target velocity might still be computed at the level of the population, however, so that areas downstream from MST could receive target velocity inputs.

A second putative function of the extraretinal signal is to provide an estimate of eye velocity that is used to set the visuomotor gain for pursuit. To examine whether the extraretinal signal in MST was suitably accurate for this function, we compared its resolution to that suggested by behavioral experiments probing online gain. Ideal observer analysis of perturbation responses implied the existence of an extraretinal signal with resolution very close to what we observed in the extraretinal signal in area MST. The resolution of the pooled neuronal responses was slightly higher than that implied by the behavior, while the average resolution of single neurons was slightly lower than that implied by the behavior. Additional experiments are needed to establish a causal link between the extraretinal signal in MST and the signal used to set online gain. However, these experiments are an important first step because they suggest that the extraretinal responses in MST carry a signal that is appropriate for establishing the strength of online gain.

The experiments presented here argue that extraretinal responses are ideally suited to provide the eye velocity signal for online gain control: not only do they represent eye velocity with appropriate resolution, they very frequently increase monotonically, as does the visuomotor gain for pursuit (Schwartz and Lisberger 1994). However, the responsiveness to both visual and extraretinal inputs implies that if extraretinal responses were to inform the pursuit system about eye velocity, the population response from MST would need to be read out and decoded. Although representing multiple inputs for a sensorimotor task seems less straightforward that representing eye and image velocity separately, it has been argued that such a scheme might actually be advantageous (Pouget

and Snyder 2000) because it provides a flexible representation that is intermediate between sensory and motor extremes. If neurons with extraretinal tuning were among those that project to the frontal eye fields, the population response from MST could be decoded to extract eye velocity. Although anatomical evidence indicates that MST indeed projects to the pursuit subregion of the frontal eye field (Tian and Lynch 1996), the response properties of projection neurons have not yet been examined. Knowing the properties of projection neurons to downstream sites would help to constrain hypotheses about the function of the speed-tuned extraretinal signal in area MST.

Acknowledgements

The authors are indebted to Leanne Chukoskie for her feedback about earlier versions of the manuscript.

References

Bremmer F, Ilg UJ, Thiele A, Distler C, and Hoffmann KP. Eye position effects in monkey cortex. I. Visual and pursuit-related activity in extrastriate areas MT and MST. *J Neurophysiol* 77: 944-961, 1997.

Carl JR and Gellman RS. Human smooth pursuit: stimulus-dependent responses. *J Neurophysiol* 57: 1446-1463, 1987.

Churchland AK and Lisberger SG. Gain control in human smooth-pursuit eye movements. *J Neurophysiol* 87: 2936-2945, 2002.

Churchland MM and Lisberger SG. Apparent motion produces multiple deficits in visually guided smooth pursuit eye movements of monkeys. *J Neurophysiol* 84: 216-235, 2000.

Churchland MM and Lisberger SG. Experimental and computational analysis of monkey smooth pursuit eye movements. *J Neurophysiol* 86: 741-759, 2001a.

Churchland MM and Lisberger SG. Shifts in the population response in the middle temporal visual area parallel perceptual and motor illusions produced by apparent motion. *J Neurosci* 21: 9387-9402, 2001b.

de Oliveira SC, Thiele A, and Hoffmann KP. Synchronization of neuronal activity during stimulus expectation in a direction discrimination task. *J Neurosci* 17: 9248-9260, 1997.

Goldreich D, Krauzlis RJ, and Lisberger SG. Effect of changing feedback delay on spontaneous oscillations in smooth pursuit eye movements of monkeys. *J Neurophysiol* 67: 625-638, 1992.

Heeger DJ, Boynton GM, Demb JB, Seidemann E, and Newsome WT. Motion opponency in visual cortex. *J Neurosci* 19: 7162-7174, 1999.

Ilg UJ and Thier P. Visual tracking neurons in primate area MST are activated by smooth pursuit eye movements of an "imaginary" target. *J Neurophysiol*, 2003.

Judge SJ, Richmond BJ, and Chu FC. Implantation of magnetic search coils for measurement of eye position: an improved method. *Vision Res* 20: 535-538, 1980.

Kawano K, Shidara M, Watanabe Y, and Yamane S. Neural activity in cortical area MST of alert monkey during ocular following responses. *J Neurophysiol* 71: 2305-2324, 1994.

Keller EL and Heinen SJ. Generation of smooth-pursuit eye movements: neuronal mechanisms and pathways. *Neurosci Res* 11: 79-107, 1991.

Lagae L, Raiguel S, and Orban GA. Speed and direction selectivity of macaque middle temporal neurons. *J Neurophysiol* 69: 19-39, 1993.

Levinson E and Sekuler R. The independence of channels in human vision selective for direction of movement. *J Physiol* 250: 347-366, 1975a.

Levinson E and Sekuler R. Inhibition and disinhibition of direction-specific mechanisms in human vision. *Nature* 254: 692-694, 1975b.

Lisberger SG, Morris EJ, and Tychsen L. Visual motion processing and sensory-motor integration for smooth pursuit eye movements. *Annu Rev Neurosci* 10: 97-129, 1987.

Liu J and Newsome WT. Functional organization of speed tuned neurons in visual area MT. *J Neurophysiol* 89: 246-256, 2003.

Maunsell JH and Van Essen DC. Functional properties of neurons in middle temporal visual area of the macaque monkey. I. Selectivity for stimulus direction, speed, and orientation. *J Neurophysiol* 49: 1127-1147, 1983.

Newsome WT, Wurtz RH, and Komatsu H. Relation of cortical areas MT and MST to pursuit eye movements. II. Differentiation of retinal from extraretinal inputs. *J Neurophysiol* 60: 604-620, 1988.

Pack C, Grossberg S, and Mingolla E. A neural model of smooth pursuit control and motion perception by cortical area MST. *J Cogn Neurosci* 13: 102-120, 2001.

Perrone JA and Thiele A. A model of speed tuning in MT neurons. *Vision Res* 42: 1035-1051, 2002.

Perrone JA and Thiele A. Speed skills: measuring the visual speed analyzing properties of primate MT neurons. *Nat Neurosci* 4: 526-532, 2001.

Pouget A and Snyder LH. Computational approaches to sensorimotor transformations. *Nat Neurosci* 3 Suppl: 1192-1198, 2000.

Priebe NJ, Churchland MM, and Lisberger SG. Constraints on the source of short-term motion adaptation in macaque area MT. I. the role of input and intrinsic mechanisms. *J Neurophysiol* 88: 354-369, 2002.

Priebe NJ and Lisberger SG. Constraints on the source of short-term motion adaptation in macaque area MT. II. tuning of neural circuit mechanisms. *J Neurophysiol* 88: 370-382, 2002.

Royden CS, Banks MS, and Crowell JA. The perception of heading during eye movements. *Nature* 360: 583-585, 1992.

Royden CS, Crowell JA, and Banks MS. Estimating heading during eye movements. *Vision Res* 34: 3197-3214, 1994.

Sakata H, Shibutani H, and Kawano K. Functional properties of visual tracking neurons in posterior parietal association cortex of the monkey. *J Neurophysiol* 49: 1364-1380, 1983.

Schwartz JD and Lisberger SG. Initial tracking conditions modulate the gain of visuo-motor transmission for smooth pursuit eye movements in monkeys. *Vis Neurosci* 11: 411-424, 1994.

Shenoy KV, Crowell JA, and Andersen RA. Pursuit speed compensation in cortical area MSTd. *J Neurophysiol* 88: 2630-2647, 2002.

Shikin EV and Plis AI. *Handbook on splines for the user*. Boca Raton: CRC Press, 1995.

Squatrito S and Maioli MG. Encoding of smooth pursuit direction and eye position by neurons of area MSTd of macaque monkey. *J Neurosci* 17: 3847-3860, 1997.

Tanaka K, Hikosaka K, Saito H, Yukie M, Fukada Y, and Iwai E. Analysis of local and wide-field movements in the superior temporal visual areas of the macaque monkey. *J Neurosci* 6: 134-144, 1986.

Tanaka M and Lisberger SG. Enhancement of multiple components of pursuit eye movement by microstimulation in the arcuate frontal pursuit area in monkeys. *J Neurophysiol* 87: 802-818, 2002.

Thiele A, Bremmer F, Ilg UJ, and Hoffmann KP. Visual responses of neurons from areas V1 and MT in a monkey with late onset strabismus: a case study. *Vision Res* 37: 853-863, 1997.

Tian JR and Lynch JC. Corticocortical input to the smooth and saccadic eye movement subregions of the frontal eye field in Cebus monkeys. *J Neurophysiol* 76: 2754-2771, 1996.

Figure legends

Table 1 Ideal observer performance on distributions of response amplitudes. For each monkey, values on the top row indicate performance of the ideal observer on actual data, while responses in the second rown indicate performance of the ideal observer on shuffled data. Values in each column represent a single stimulus condition as indicated by the bold type atop each column.

Table 1

	5 Hz, 4°/s		10 Hz, 8°/s		5 Hz, 8°/s	
	Right	**Left**	**Right**	**Left**	**Right**	**Left**
yo : data	34.8	48.6	35.3	49	37.9	35.7
yo : shuffled data	12.1	12.9	18.8	11.2	10.6	18.6
mo : data	37.7	34.5	31.8	35.3	30	35.7
mo : shuffled data	23	12.1	10.6	8.8	17.1	15.7

Figure 1 Target and eye velocity traces demonstrating the stabilization process used in this study. A. Target velocity for a target that moves continuously at 5°/s (black trace) or moves at 5°/s except for a 300 ms interval beginning at 540 ms (colored traces). Motion during the 300 ms stabilized interval was either driven by eye velocity (red trace) or by eye velocity with 0.5°/s, 1°/s or 2°/s (cyan, purple and green traces) of image motion added or subtracted. When image motion was added to eye velocity during the stabilized period traces lie above the black control trace; when image motion was subtracted from eye velocity during the stabilized period traces lie above the black control trace. B. Eye velocity responses to the target motion conditions described in A. Dashed lines near the traces indicate standard error of the mean. Dashed black vertical lines indicate the onset and offset of the stabilization period delayed by 100ms to account for delays in visuomotor processing.

Figure 1

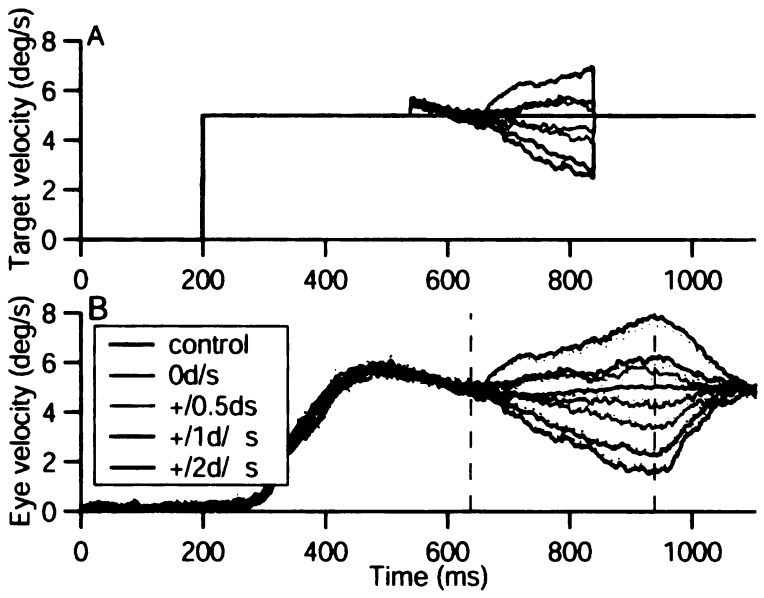
A
Target velocity (deg/s)
8
6
4
2
0
0
200
400
600
800
1000
B
Eye velocity (deg/s)
control
0d/s
+/0.5ds
+/1d/ s
+/2d/ s
Time (ms)

Figure 2 A. Two sources of visual motion inputs during pursuit eye movements across a background. Positive values indicate motion to the right, negative values indicate motion to the left. Black solid trace shows target 5°/s target motion. Grey sold trace shows the image velocity resulting from this target. Black dashed trace shows eye velocity in response to the moving target. Grey dashed trace shows image velocity from the background that results from movement of the eyes. B and C. Responses during pursuit of an example neuron in either very dim light (thick black trace) or darkness (dashed trace). Target motion was the same in both cases but a very dim background was present in the very dim light.

Figure 2

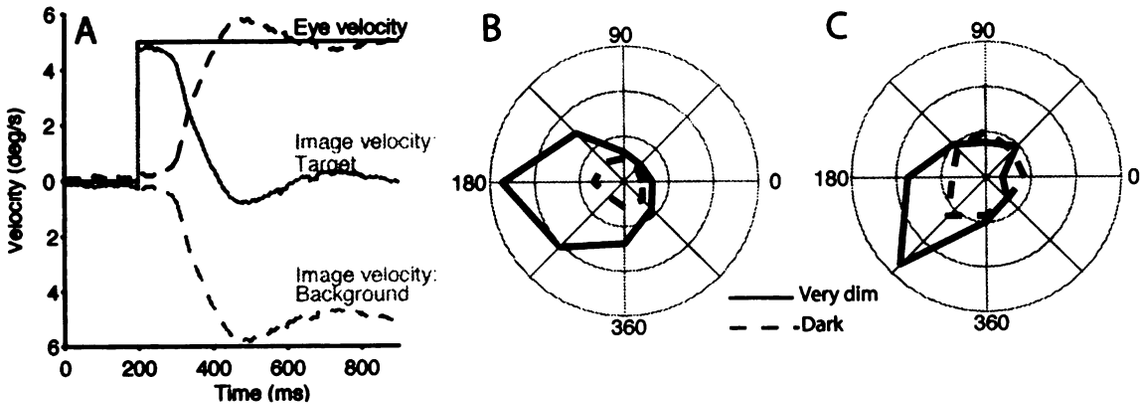
A
Eye velocity
Image velocity: Target
Image velocity: Background
Velocity (deg/s)
6
4
2
0
2
4
6
0
200
400
600
800
Time (ms)
B
90
180
0
360
C
90
180
0
360
Very dim
-Dark

Figure 3 Example eye velocities and neuronal responses to pursuit at different speeds for two neurons. A and C. Left column: Eye velocity traces from stabilized (black) and control (grey) trials at 0, 5 10, 15, 20 and 30°/s. Responses to 2°/s were not included due to space constraints. Dashed black vertical lines indicate the onset and offset of the stabilization period delayed by 100ms. Right column: Rasters aligned to the onset of pursuit indicating firing rates over time for stabilized trials. Dotted lines indicate the onset of pursuit. Dashed black vertical lines indicate the onset and offset of the stabilization period delayed by 100ms. B and D averaged firing rates taken from the stabilized period of trials (or the equivalent 300 ms interval in control trials) at each speed. Black points and curve indicate response taken from stabilized trials, grey points and curve indicate responses taken from control trials. Stars on each trace indicate the neuron's preferred speed as determined by the highest point of the spline fit.

Figure 3

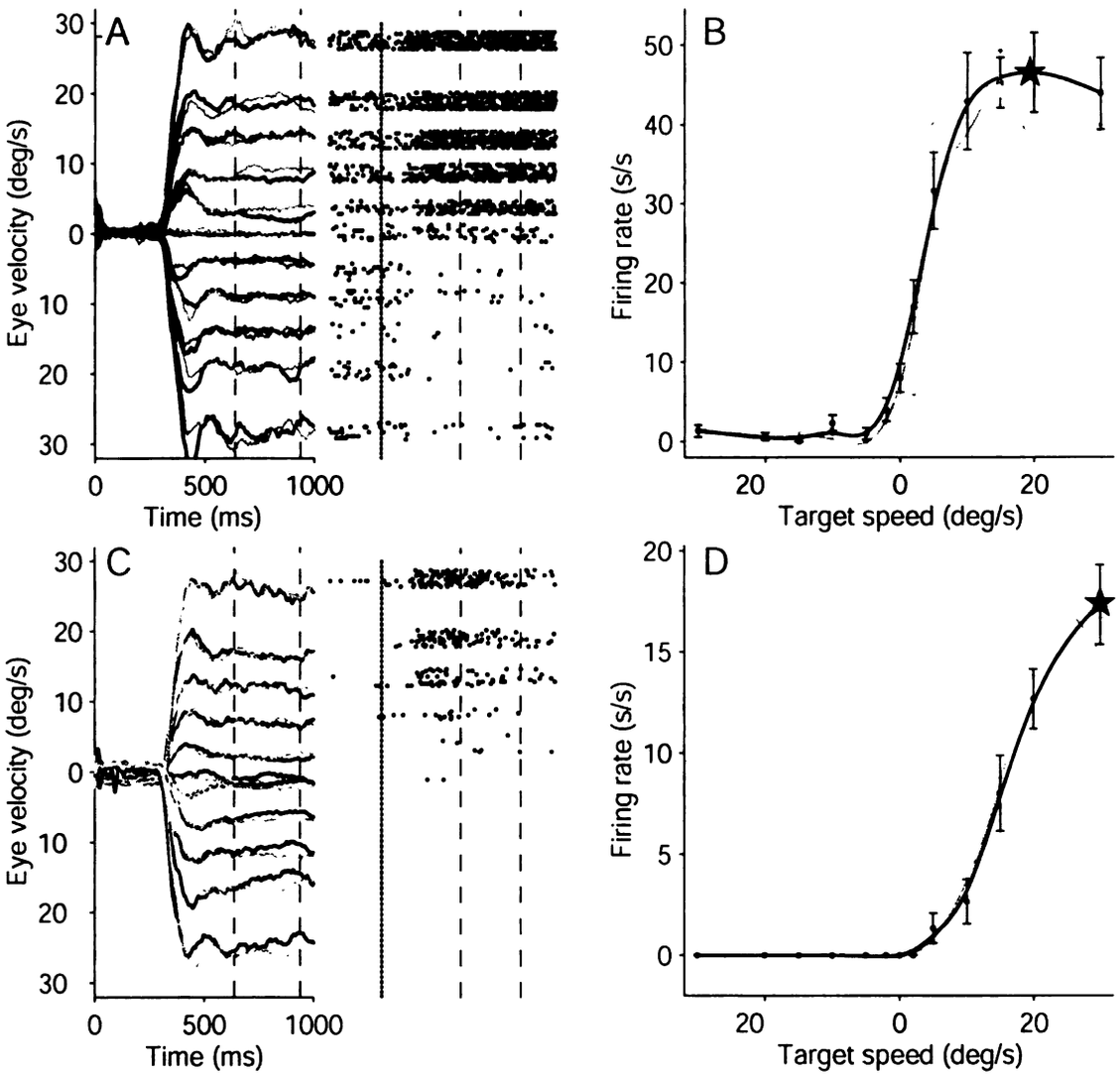
A
B
C
D
Eye velocity (deg/s)
Time (ms)
Firing rate (s/s
Target speed (deg/s)
30
20
10
0
10
20
30
0
500
1000
50
40
30
20
10
0
20
0
20
15
10
5

Figure 4 A. A comparison of the neuron's best speed as determined by responses from control and stabilized trials. Dots and plusses indicate data from each of two monkeys. Circled points correspond to the examples from figure 3. Because so many neurons preferred 30°/s motion for both stabilized and control trials, points were offset slightly to facilitate viewing. B. Example speed tuning computed as the response to the preferred direction only (black) or the opponent response (grey). Stars indicate the neuron's best speed. C. A comparison of the neuron's best speed as determined by responses to the preferred direction of pursuit only, or from the difference between responses in the preferred and null directions. Different symbols indicate each of two monkeys. Circled points correspond to the examples from B.

Figure 4

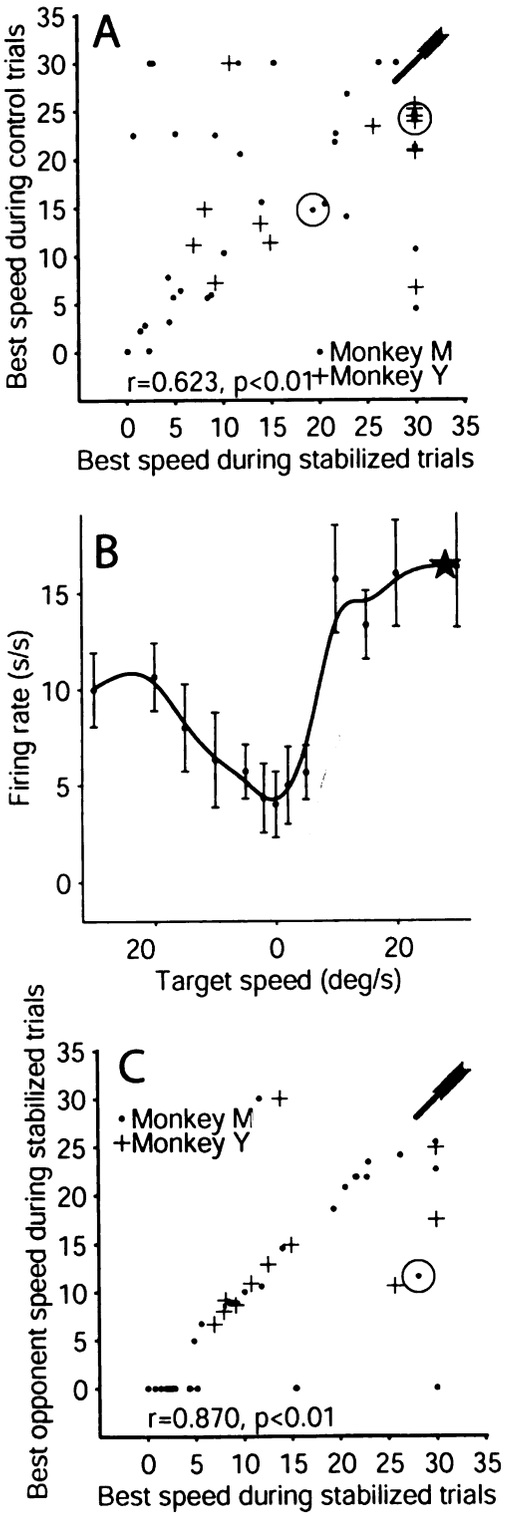
A
Best speed during control trials
Best speed during stabilized trials
• Monkey M
+ Monkey Y
r=0.623, p<0.01
B
Firing rate (s/s)
Target speed (deg/s)
C
Best opponent speed during stabilized trials
Best speed during stabilized trials
• Monkey M
+ Monkey Y
r=0.870, p<0.01

Figure 5 Evolution of responsiveness and discriminability of eye velocity and extraretinal responses over time. A. The magnitude of the neural and behavioral responses as a function of time from an example neuron. Black traces indicate average eye velocity in response at the neuron's best speed; red trace indicates the average firing rate in response. Dotted vertical trace indicates onset of target motion. Dashed black vertical lines indicate the onset and offset of the stabilization period delayed by 100ms. Note that firing rate and eye velocity magnitudes are plotted on a difference scale. B. The same as in A except that the traces correspond to population averages. Error bars indicate standard error of the mean. The eye velocity trace consists of 1000 points so error bars appear as a solid grey trace in the background. The firing rate trace consisted of only 50 points as firing rate was computed in 20 ms bins so error bars appear more discrete. C. Values of D′ for each of 1000 time points for eye velocity (black trace) and neuronal responses (red and blue traces). Discriminability was computed for either the best and worst speeds at each time point (red trace) or for the best and next-best speeds at each time point. Dotted vertical trace indicates onset of target motion. Dashed black vertical lines indicate the onset and offset of the stabilization period delayed by 100ms. Note that firing rate and eye velocity magnitudes are plotted on a difference scale..D. Same as in C except that the traces correspond to population averages. Error bars were computed at each time point and indicate standard error of the mean.

Figure 5

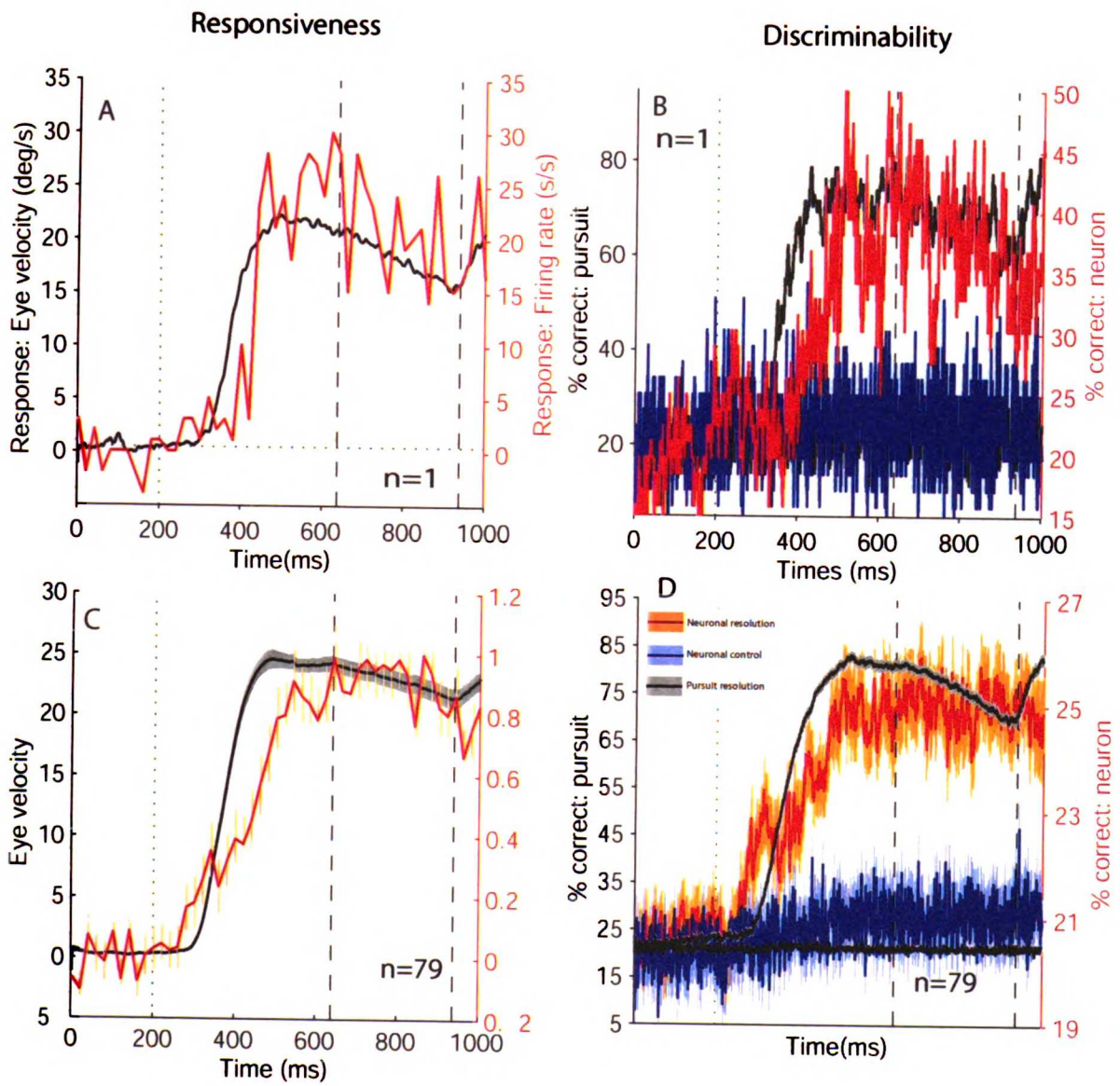
Responsiveness
Discriminability
A
B
C
D
n=1
n=1
n=79
n=79
Response: Eye velocity (deg/s)
Response: Firing rate (s/s)
Time(ms)
% correct: pursuit
% correct: neuron
Times (ms)
Eye velocity
Time (ms)
Neuronal resolution
Neuronal control
Pursuit resolution
% correct: pursuit
% correct: neuron
Time(ms)

Figure 6 A comparison of the resolution of the eye velocity response and the resolution of the neural responses during the stabilized period. Dashed line indicates x=y. Different symbols indicate each of two monkeys.

Figure 6

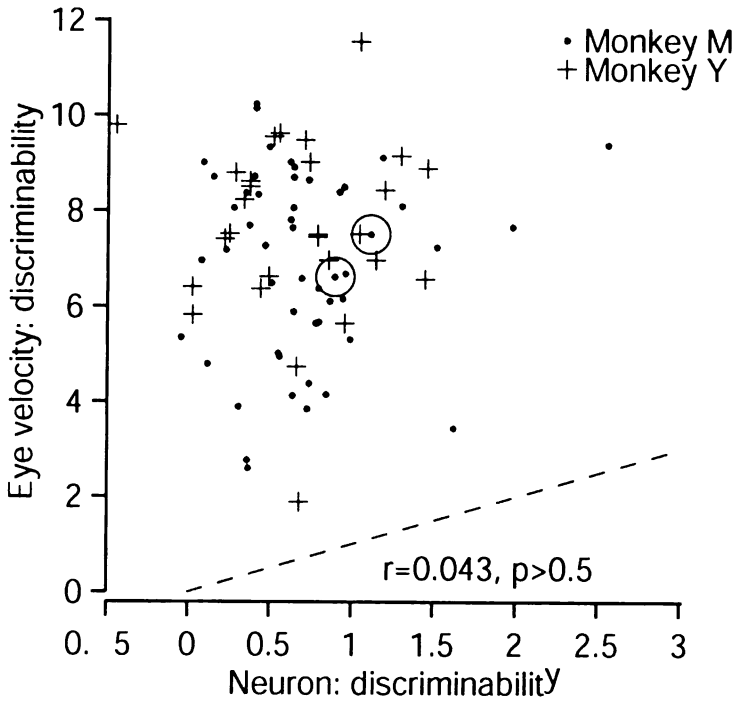
• Monkey M
+ Monkey Y
Eye velocity: discriminability
12
10
8
6
4
2
0
r=0.043, p>0.5
0. 5
0
0.5
1
1.5
2
2.5
3
Neuron: discriminability

Figure 7 A. Target (dashed) and eye (solid) velocity traces demonstrating that the response to a perturbation of target motion depends on the ongoing pursuit velocity during which it is presented. Grey trace: ongoing pursuit at 20°/s; black trace: ongoing pursuit at 5°/s. B. Average response amplitude as a function of ongoing pursuit speed for two monkeys engaged in rightwards (open symbols) or leftwards (closed symbols) pursuit. Perturbations used to generate this plot were +/- 8°/s and were presented at 5Hz. Error bars indicate standard error of the mean. C. Comparison of ideal observer performance for responses to perturbations (black bar), the responses of pooled MST neurons (grey bar) and the responses of single MST neurons (white bar).

Figure 7

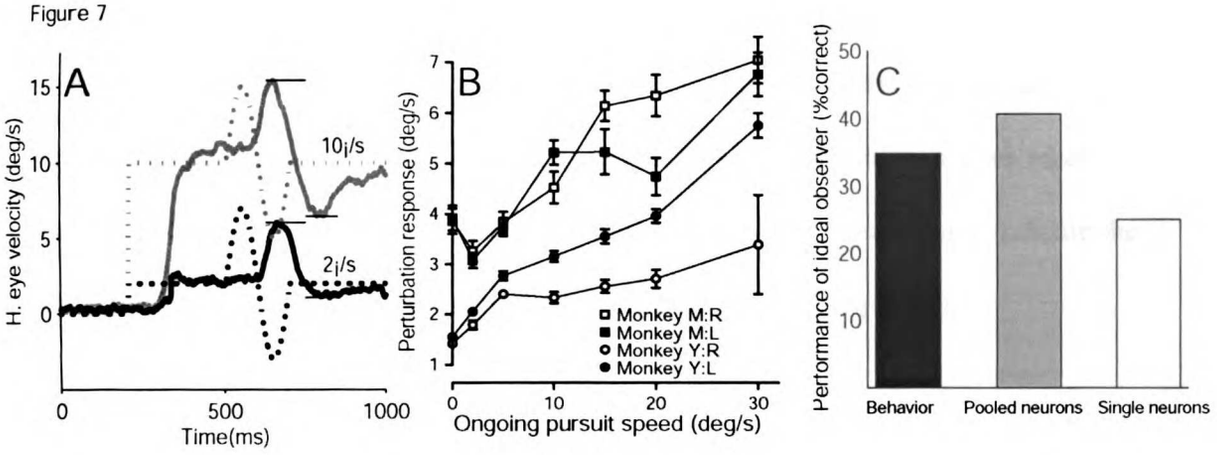
A
H. eye velocity (deg/s)
15
10
5
0
10i/s
2i/s
0
500
1000
Time(ms)
B
Perturbation response (deg/s)
7
6
5
4
3
2
1
Monkey M:R
Monkey M:L
Monkey Y:R
Monkey Y:L
0
10
20
30
Ongoing pursuit speed (deg/s)
C
Performance of ideal observer (%correct)
50
40
30
20
10
Behavior
Pooled neurons
Single neurons

Figure 8 Example target velocities and neuronal responses to motion at different speeds for two neurons. A and C. Left column: Target velocity traces from trials at –32°/s to 32°/s. Right column: Rasters indicating firing rates over time. Grey solid lines indicate the onset of target motion. B and D. Averaged firing rates averaged over a 500 ms period starting 150ms after motion onset at each speed. Black points and curves indicate responses generated from the rasters. Grey points and curves indicate responses taken from the stabilized period of pursuit trials for comparison. Stars on each trace indicate the neuron's preferred speed as determined by the highest point of the spline fit.

Figure 8

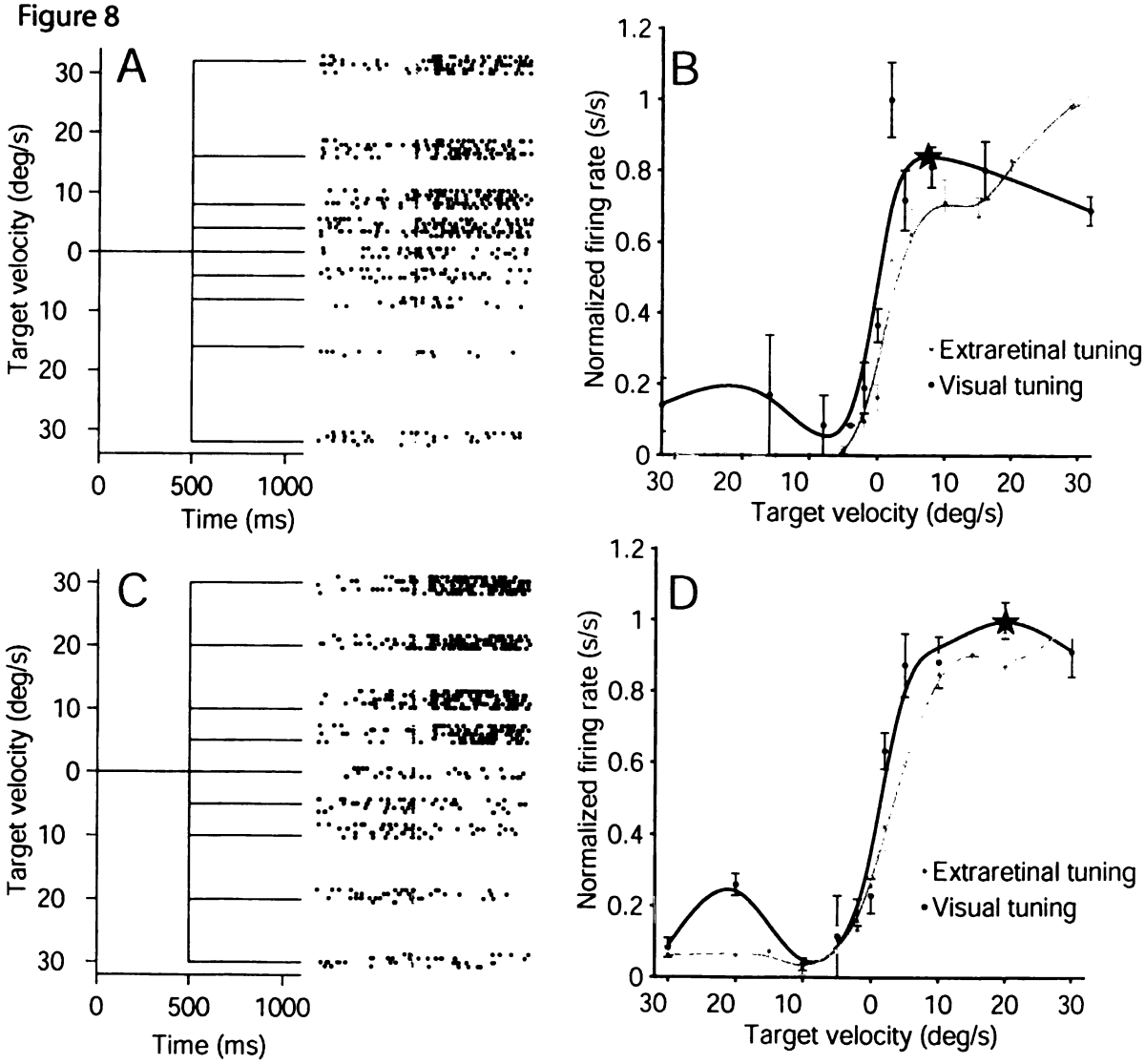
A
Target velocity (deg/s)
30
20
10
0
10
20
30
0
500
1000
Time (ms)
B
Normalized firing rate (s/s)
1.2
1
0.8
0.6
0.4
0.2
0
30
20
10
0
10
20
30
Target velocity (deg/s)
Extraretinal tuning
Visual tuning
C
Target velocity (deg/s)
Time (ms)
D
Normalized firing rate (s/s)
Target velocity (deg/s)
Extraretinal tuning
Visual tuning

Figure 9 A comparison of the best speed of the visual response and the best speed of the pursuit response. A. Best speeds were generated from responses to visual motion excluding speeds higher than those used to examine pursuit. B. Best speeds were generated from responses to visual motion at all speeds tested, including 64°/s and 128°/s. Different symbols indicate each of two monkeys.

Figure 9

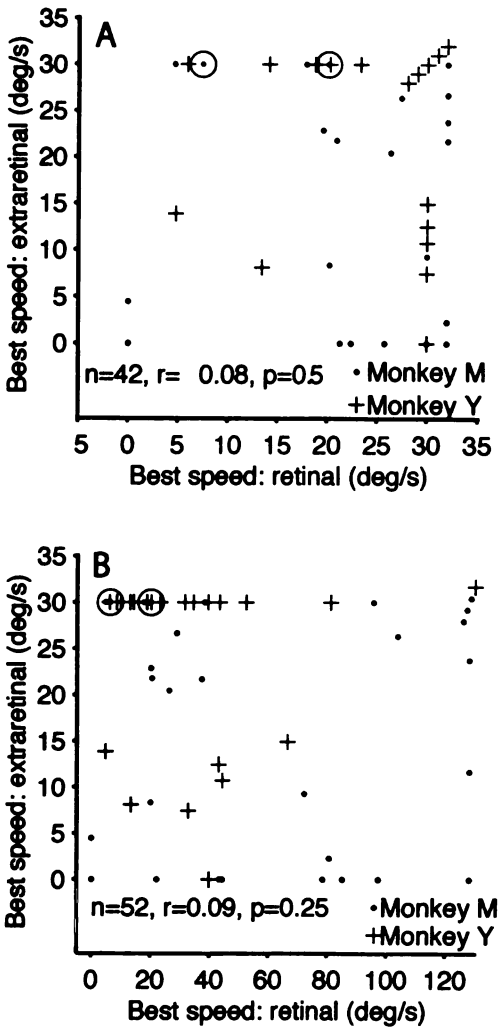
A
Best speed: extraretinal (deg/s)
35
30
25
20
15
10
5
0
n=42, r= 0.08, p=0.5
•Monkey M
+Monkey Y
5 0 5 10 15 20 25 30 35
Best speed: retinal (deg/s)
B
Best speed: extraretinal (deg/s)
35
30
25
20
15
10
5
0
n=52, r=0.09, p=0.25
•Monkey M
+Monkey Y
0 20 40 60 80 100 120
Best speed: retinal (deg/s)

Chapter 3: Effects of pooling on population estimates in MST

Abstract

A number of distinct pooling algorithms were used to test how accurately the eye velocity signal recorded from MST neurons could reflect eye velocity itself. The success of each of the pooling algorithms was tested in two ways. The analysis here provides an upper and lower bound for the accuracy of the neural estimates of eye velocity.

Introduction

One major goal of systems neuroscience is to try and connect the firing of neurons to an animal's behavior. In the previous chapter, we recorded from neurons that fire in proportion to ongoing eye velocity. We hypothesized that one role of this extraretinal signal might be to inform the pursuit system of ongoing eye velocity, enabling it to set online gain for pursuit. To test whether the eye velocity signal in MST has the resolution to subserve this function, we estimated the resolution of the eye velocity signal using ideal observer analysis. However, we found that ideal observer performance of single neurons was, on average, lower than would be expected based on behavioral estimates of the resolution of the eye velocity signal. If the neural estimate of eye velocity is indeed garnered from responses of single neurons over the timescale that we measured, then our estimate may accurately reflect a low-resolution eye velocity signal in MST. However, the neural estimate of eye velocity might be improved if the responses of single neurons were combined to generate a population response.

We explored two strategies to generate population estimates of eye velocity. In the first approach, which will be referred to as the "binary strategy", cells were either included or excluded from the population depending on whether aspects of their responses met certain criteria. Cells with responses that met these criteria were given a weight of 1 and their responses were averaged; cells with responses that failed to meet the criteria were given a weight of 0 so their responses had no effect on the average. For our second strategy, which will be referred to as the "continuous strategy", we did not attempt to select weights for the neurons based on responses properties of the neurons. Instead, weights were arbitrarily generated using linear regression. In the continuous strategy, weights varied continuously so that a neuron wasn't simply included or excluded from the population; rather, neuronal responses had a graded affect on the population estimate.

We used two methods to evaluate the neural estimates generated by each pooling strategies. Our first method, ideal observer analysis, had the advantage of being most easily compared to the behavior. We considered a pooling method to be successful when ideal observer performance of the population response was at least as good as ideal observer performance for the behavior.

Importantly, a neural estimate of eye velocity might generate excellent ideal observer performance even when the estimate bears little resemblance to eye velocity. This is because success of an ideal observer requires only that distributions be distinguishable from one another; they do not have to be in a particular order. For this

reason, we also evaluated neural estimates by computing the mean squared error between the neural estimate of eye velocity and eye velocity itself. The mean squared error will not be comparable to a behavioral measure, but can be compared across different pooling methods to provide and ideal of how closely each population estimate matches eye velocity.

Methods

The general approach taken was to first select weights for each neuron according to a particular strategy, and then to evaluate the accuracy of the population estimate generated by the weights. Accuracy was estimated in two ways: 1) by evaluating the ability of an ideal observer to determine the eye velocity that generated a particular firing rate and 2) computing the mean squared error for the population estimate. The neural responses from 79 neurons used to generate estimates were the normalized responses analyzed in Chapter 2. However, in chapter 2 we elected to use a very short time window (20 ms) to estimate discriminability so that we could evaluate how discriminability evolved over time. Here, we use firing rates averaged over a longer time window (300ms) because shorter time windows made regression analysis too noisy (see below).

Assigning weights

For the binary strategy, a neuron was assigned a weight of 0 if it failed to meet a given criterion, and 1 if it met the criterion. For the continuous strategy, weights were determined using least squares regression so that:

$$R_{ij} \times W_j = S_i$$

Where R was a 79x130 matrix consisting of all the responses (i) from each of 79 neurons (j), W is a 1x79 vector with one weight for each neuron, and S is a 1x130 vector of all the target velocities for each trial. Note that because eye velocity and target velocity were almost identical, we will use the two interchangeably. Generating weights using regression is ill posed if the number of neurons exceeds the number of trials. Our population of neurons was quite large (79) and we tested responses at only 13 speeds: 6 preferred, 6 null and 0°/s. We solved this problem by listing the responses to each speed separately (13 trials X 10 speeds = 130 responses) rather than using the average of the 10 trials at each speed. However, we wanted to be certain that the success of regression was not a necessary consequence of the size of our matrix of firing rates. For this reason, we generated a second matrix wherein each neuron was associated with the same responses as before, but the order of the responses within each neuron was scrambled. When we generated weights using only half the trials from each neuron, mean squared error was computed separately for each monkey so that the number of neurons (51 or 28) would not exceed the number of trials (130/2 = 65 trials).

Estimating population responses

Population estimates were generated by scaling the all responses for each neuron by the weight assigned by the binary or continuous strategy. For example, the population estimate in response to trial i is:

$$\sum_{j=1}^{79} r_{i,j} \times w_j$$

Where each j is a neuron, r is the firing rate, and w is the weight assigned by the binary or continuous strategy. This generated 10 population responses for each speed.

Ideal observer analysis

Ideal observer performance was computed in the same way as described in chapter 2. Our population estimate yielded 10 responses for each speed, creating 7 distributions. For the binary strategy, each trial in the distribution reflects the averaged response of all the neurons accepted into the pool. For the continuous strategy, the 10 trials in each distribution reflect a weighted combination of all neurons in the population. We elected to use data averaged across neurons rather than across trials so that

distributions of pooled neural data would contain the same number of points as distributions of single neurons, or distributions of behavioral responses to perturbations. However, we did perform the same analyses using data averaged across trials rather than across neurons so that each distribution contained as many points as there were neurons in the pool. We observed the same trends using this method although ideal observer performance (which was performed on populations from the binary strategy only) was generally lower and mean squared error higher (data not shown). The less accurate population estimates using this method arose because variability across neurons was greater than variability across trials. Averaging across trials thus did little to reduce variability, while averaging across neurons reduced variability more dramatically.

As in chapter 2, we performed each ideal observer analysis on shuffled data, in addition to actual data, to provide a comparison. Ideal observer performance on shuffled data varied little and was almost always very close to 13%.

Mean squared error of population estimates

Our second method of evaluating population responses was to compare the population estimate of each velocity with eye velocity itself. To do this, we first averaged the 10 population responses that were generated for each speed. The population estimate was then scaled so that the largest response was equal to 30, corresponding to 30°/s, the fastest eye velocity tested. This had almost no effect on population estimates from the continuous strategy since using regression constrained the estimate to be close

to actual eye velocity. However, population estimates from the binary strategy were frequently quite small even when they had the right shape. This is because population estimates for the binary strategy simply reflect averages of sometimes very small pools of normalized responses. To enable a fair comparison between different estimates using the binary strategy and to enable comparison with estimates from the continuous strategy, population estimates were scaled. The mean squared error was then computed between each estimated velocity in the preferred direction and each eye velocity.

Results

We began by re-computing ideal observer performance for each neuron individually. This analysis was performed in the same way as in chapter 2 except that a longer time window (300ms instead of 20ms) was used. When firing rates were averaged over this longer time interval, the average performance of a single neuron was 28.80%. This is a slight improvement over the average performance when a 20 ms time window was used (25.4%). Figure 1 shows the distribution of performances for the 79 neurons tested. Performance varies over quite a large range with the worst neurons achieving 8% correct and the best neuron achieving 57% correct. The variability of responses suggested that a pooling strategy with the right criteria for admittance to the population could increase overall performance considerably.

Binary strategy

For the binary strategy, we asked how we could improve the population estimate by varying the criteria by which cells would be admitted to the pooling population. To establish a baseline against which these estimates could be compared, we first generated a population estimate using all the neurons. We performed ideal observer analysis once on responses that were averaged across neurons instead of on each neuron individually, as we did for figure 1. This is the simplest pooling algorithm: all neurons were included and were equally weighted. For populations of monotonically increasing neurons, this simple pooling strategy can produce estimates that are almost as accurate as those generated by an optimal linear estimator (Guigon 2003; Salinas and Abbott 1994). Our population of neurons was not uniformly monotonically increasing, but this simple method nevertheless generated estimates that were far more accurate than those of single neurons. Ideal observer performance was considerably improved (59.18% for population responses verses 28.80% for single neurons). Ideal observer performance on the behavior was between 30 and 49%, depending on the monkey and stimulus configuration, so even the simplest pooling algorithm generated eye velocity estimates that were the appropriate resolution for the behavior. Nevertheless, we explored more selective pooling methods to determine the upper bound of ideal observer performance and to better understand how it varied according to selection criteria. Further, the mean squared error for the population estimate using all the data was quite large (160.67), and selective pooling criteria might also improve the accuracy of the estimate.

To improve the population estimate, we became selective about which neurons were admitted to the pool used to estimate the population response. Figure 2a and b

shows examples of neurons that were included or excluded from the population when we required that neurons have a preferred speed greater than 20°/s and an F-statistic greater than 25 to be admitted to the pool. Using these strict criteria meant that the 12 neurons accepted into the pool had responses that were similarly shaped to eye velocity itself (figure 2a), while the 67 neurons that were excluded had a variety of tuning curve shapes (7 examples shown in figure 2b). Figures 2c and d show the population estimate (red trace) generated by averaging the included (figure 2c) or excluded (figure 2d) responses. The goal of the population response, actual eye velocity, is plotted for comparison (green dashed trace). For viewing purposes, the population average was scaled so that the estimate at the highest speed was set to 30°/s. Neither population estimate is particularly accurate (mean squared error = 64.87 for selected cells and 189.09 for the remaining cells). The estimate for the included cells (figure 2c) is the wrong shape while the estimate for the excluded cells (figure 2d) is too shallow. Nevertheless, ideal observer performance on the population estimate from the included neurons was much more accurate than the population estimate that included all neurons (87.76% vs. 59.18%). This was the best ideal observer performance we observed. Note that ideal observer performance can be high even when the population estimate is inaccurate as long as the distributions of responses are distinct.

To explore systematically how ideal observer performance changes according to criteria for admittance into the population pool, we varied the strictness of 3 selection criteria. First, we admitted neurons to the pool only when their preferred speeds were above a minimum value. Figure 3a plots ideal observer performance as a function of the

best speed criterion. Performance increased from 60% to 80% as the minimum best speed increased (figure3a, black trace). Naturally, as the criterion become progressively stricter, fewer neurons were admitted to the pool (figure 3a, grey trace). When the most stringent criterion was enforced (black star on figure 3c), only 40 neurons were admitted to the pool. Stricter criteria could not be used because all 40 neurons had preferred speeds of 30°/s. Figure 3b shows eye velocity tuning of the 40 included neurons for the most stringent criteria used (indicated by the star in figure 3a). The similarity of the eye velocity traces explains why averaging these neurons yields improved ideal observer performance relative to an average that included all neurons. When we used the neurons accepted into the pool to generate an estimate of eye velocity, the mean squared error of the estimate was 63.30

Next, we admitted neurons to the pool only when their F-statistics were above a minimum value. Speed-tuned responses will have high F-statistics when the mean responses at each speed are distinct and their variances are low. When we used this criterion, performance varied from 49% to 68% as the minimum best speed increased (figure 3c, black trace). As values of the F-statistic were required to be progressively higher, the number of neurons admitted to the pool shrank (figure 3c, grey trace) while observer performance first increased and then decreased (figure 3c, black trace). When the most stringent criterion was enforced (black star on figure 3c), only 3 neurons were admitted to the pool (figure 3d). These three neurons all had monotonically increasing responses, although requiring a large F-statistic did not necessarily imply that admitted neurons would have a particular shape. This explains why ideal observer performance

was so variable when the F-statistic criterion was used: some included neurons had high F-values but were not monotonically increasing. The distribution of responses at each speed was therefore quite broad, especially when the pool consisted of only a small number of neurons. This weakened ideal observer performance. When we used the neurons accepted into the pool to generate an estimate of eye velocity, the mean squared error of the estimate was 108.73.

Lastly, we admitted neurons to the pool only when their speed selectivity indices exceeded a minimum value. The speed selectivity index was defined for each neuron as

$$1 - (\text{lowest response} / \text{highest response})$$

so that neurons with larger differences between responses to the best and worst stimuli had speed selectivity indices close to 1. Ideal observer performance, which ranged from 43% to 63%, was lower than for the other criteria and was highly variable as the value of the speed selectivity index was increased (figure 3e, black trace). Using the speed selectivity index as a criterion causes some of the same flaws that were apparent when the F-statistic was used because neurons with a variety of tuning-curve shapes had high speed selectivity indices. Further, the speed selectivity index is not affected by variability the way the F-statistic is, so variable neurons which hurt the ideal observer's performance were sometimes accepted into the pool. Performance of an ideal observer was especially reduced when such neurons were accepted into a small pool since the contribution of one noisy neuron could be considerable. Speed-tuning traces for the 18

neurons accepted into the pool when the strictest criterion was used are shown in figure 3f. Ideal observer performance on this population is indicated by the star in figure 3e. Mean squared error of the population estimate was 127.29.

The recording experiments performed to collect these data do not indicate which neurons in MST might actually be contributing the estimation of eye velocity for pursuit. Therefore, it is not possible to know which selection criteria, if any, the brain might use to generate a population estimate of eye velocity and take advantage of the benefits of pooling. However, by varying different selection criteria systematically, we can begin to estimate an upper and lower bound for the accuracy of a population estimate from MST. The data presented here indicate the accuracy of the neural estimates of eye velocity could range from 28.8% (if responses are not pooled) to 87.76% (if the most stringent pooling criteria are used).

Continuous strategy

In the binary strategy, neurons were either included or excluded from the population, that is, they were given a weight of either 0 or 1. In the continuous strategy, all neurons were included, but their weights varied continuously. Further, rather than using observed properties of the neurons to select the weights, we determined the weights using regression so that weights weren't required to reflect properties of the neurons that we considered a priori to be important. Figure 4a shows neurons that were assigned the highest weights. Like the neurons that were selected for the pool using strict criteria in

the first strategy, many of these neurons have responses that are monotonically increasing, like eye velocity itself. Figure 4b shows neurons that were assigned near-zero weights. The responses of these neurons were still included in the population response, but they were weighted much less heavily than neurons in figure 4a. The population estimate for all the neurons is shown in figure 4c. This estimate is very close to eye velocity itself and is much more accurate than any estimate that we generated using the binary strategy. The mean squared error associated with the estimate was only 0.49.

The data points from the new population estimate were used to generate distributions for an ideal observer analysis to allow comparison with the binary strategy and the behavior. We observed good performance, albeit lower than the best performance seen using the binary strategy (regression: 69.39%, best performance in binary strategy: 87.76%). However, the binary strategy that yielded the highest ideal observer performance had a mean squared error that was considerably higher than in the continuous strategy (regression: 0.49, best performance in binary strategy: 64.87).

To illustrate how each neuron contributes to the population estimate, we plotted a series of estimates in figure 4d. Each trace is a population estimate that includes between 1 and 79 neurons. Population estimates were re-computed with the addition of each neuron and every fifth trace is plotted. Traces change in color from light green to red as the number of included neurons increased. The trace generated from only 1 neuron (the light green trace labeled n=1) represents responses from only neuron whose weight had the smallest magnitude. The trace above it (labeled n=6) represents the population

response of the 6 neurons whose weights had the smallest magnitudes, including the neuron from the previous trace. Each trace represents the population response including progressively more neurons. The red trace labeled n=79 was generated using all the data and represents the regression estimate of eye velocity (the same trace as in figure 4c).

The weights of the neurons in the continuous strategy differ from those in the binary strategy in that they were not determined based on a priori ideas about the kinds of neurons that might be best suited to encode eye velocity. Figure 5a and b demonstrate the relationship between the weights used for the continuous strategy and those used for the binary strategy. In figure 5a, a weak but significant relationship ($r=0.27$, $p<0.05$) between the weight in the continuous strategy and the neuron's F statistic is apparent. Similarly, in figure 5b, a weak but significant relationship ($r=0.31$, $p<0.02$) between the weight in the continuous strategy and the neuron's best speed is apparent. However, it is clear that neurons with any given best speed were assigned a variety of different weights.

To determine whether the success of the continuous strategy was inevitable because of the dimensions of the firing rate matrix that was used, we re-estimated eye velocity with a scrambled version of our matrix. The population estimate, which we will refer to as the scrambled estimate, was computed as before and was compared to the original, ordered estimate of eye velocity. The scrambled estimate (figure 6a) is plotted alongside the ordered estimate (figure 6b) for comparison. This is the same trace as in figure 4c, but plotted on a different scale. The mean squared error for the scrambled data is more than 2 orders of magnitude larger (scrambled: 103.0 vs actual data: 0.49).

Surprisingly, however, the shape of the scrambled estimate is approximately correct. We then re-computed the scrambled and actual estimates using only half of the data: 5 trials from each speed instead of 10. Again, both the scrambled estimates (red, traces, figure 6c and e) were approximately the same shape as the ordered estimates (red traces, figure 6d and 6f) although the mean squared errors were much higher (labeled *fit:mse* on each plot). Next, we used the weights generated using 5 trials from each speed, and computed a population estimate for the remaining 5 trials at each speed. For this estimate, the trials used to compute the population estimate were not the same trials that were used to generate the weights. When the matrices were comprised of ordered data, the population estimates were still quite accurate (grey traces, figures 6d and 6f). Importantly, however, when the matrices were comprised of scrambled data, the scrambled estimates were totally inaccurate and mean squared errors were enormous (grey traces, figure 6f and 6e). Only when the first and second half of the data vary around the same mean will the weights generated by half of the data be appropriate for the remaining half of the data. The very poor estimates that were generated using the remaining half of the scrambled matrix provide reassurance that the success of the continuous strategy was not inevitable because of the size of the firing rate matrix that was used

Discussion

We set out to determine whether a pooled neural response could provide an eye velocity signal with sufficient resolution to support our behavioral observations. In

chapter 2, our analysis of the eye velocity response to perturbations suggested that the eye velocity signal must be quite accurate: ideal observer performance of the behavior was between 30 and 49% depending on the monkey and stimulus configuration. By contrast, average performance of single neurons was only 28.80%. Different pooling strategies for MST neurons generated ideal observer performance between 59 and 88%, suggesting that pooling can easily improve the resolution of the eye velocity signal. Even when we used the simplest pooling method, weighting all the neurons equally and excluding none of them, ideal observer performance was higher than we observed in the behavior. Unfortunately, the behavior does not therefore constrain which pooling strategies are likely to be plausible. On a more positive note, the success of so many pooling strategies argues that if any of a number of pooling mechanisms were implemented in MST, the neural estimate of eye velocity could easily have sufficient resolution to provide the pursuit system with an estimate of eye velocity.

We found sufficiently high ideal observer performance even when the simplest pooling algorithm was used: including all the neurons and weighting them equally. However, this simple approach was only successful when firing rates were averaged over a 300 ms time window. When a 20 ms time window was used, ideal observer performance was only 42%, a little too low to account for our behavioral observations. If future behavioral experiments can pinpoint the time window over which eye velocity is used to set the visuomotor gain for pursuit, our analysis could be restricted to a specific time window, perhaps making it more clear which pooling methods were appropriate. However, we were unsure how to select the length of the time window over which

responses were averaged. Our initial behavioral observations in chapter 1 suggested that when eye velocity was changed even for only 180 ms, clear changes in visuomotor gain followed (chapter 1). Further, we found that when eye velocity was changed for only 50 ms, no changes in visuomotor gain were evident. Therefore, 20 ms intervals seemed too brief. A second reason we were reluctant to use 20 ms was that trial-to-trial variability tended to be quite large. We were less confident in the regression analysis when variability was so high because the weights generated using half the data were frequently quite inappropriate for the remaining half of the data. We used the similarity of estimates from the first and remaining halves of the data as assurance that the successful estimates of regression were non-trivial. As a result, we were hesitant to use timescales that generated non-similar estimates.

Two strategies were used to pool single neurons to generate population estimates of eye velocity, and two methods were used to evaluate the success of those population estimates. The different pooling strategies generated eye velocity estimates with mean squared errors ranging from 0.49 to 160.67 and ideal observer performance ranging from 59.18% to 87.76%. We observed the lowest mean squared error (0.49) using the continuous strategy and the best ideal observer performance (87.76%) using the binary strategy with strict criteria. In the continuous strategy, we used least squares regression to find the weights that best mapped firing rates to target velocity. Therefore it is not surprising that we observed the smallest mean squared errors in this strategy. Further, because least squares regression does not optimize the distance between distributions of

responses, it is perhaps not surprising that ideal observer performance was lower here than on the best binary strategy. The success of the continuous method in generating accurate population estimates does not necessarily imply that MST actually uses regression to determine the optimal strength of connections between each of its neurons and their targets. However, its success does emphasize that the selection of weights need not reflect lofty computational principles in order to be accurate.

We observed accurate ideal observer performance when the only neurons admitted to the pool were those with F-statistics above 25 and preferred speeds above 20°/s. Neurons that had a high F-statistic from an ANOVA both responded distinctly at the different speeds and had sufficiently low variance that responses at one speed were reliably different from responses at another. Therefore it is not surprising that pools which included such neurons resulted in response distributions with high ideal observer performance. Including only neurons with high preferred speeds similarly improved ideal observer performance but for a different reason. Consider performing an ideal observer analysis on a population estimate including neurons with a range of different preferred speeds. The distribution of responses to 2°/s would include high firing rates from neurons that preferred slower speeds close to 2°/s and reduced firing rates from neurons that preferred 30°/s. Similarly, the distribution of responses to 30°/s would include high firing rates from neurons with fast preferred speeds, and reduced firing rates from neurons that preferred slower speeds. Therefore, the two distributions of population responses to 2°/s and 30°/s would look quite similar even though few individual neurons responded similarly at the two speeds. This same issue has been addressed in other

studies estimating population responses to the direction, rather than speed of motion. To avoid this problem, population responses are generally estimated after aligning the responses so that all the neurons have the same preferred direction (Britten et al. 1992). This technique makes the reasonable assumption that any neuron recorded during an experiment probably has a counterpart elsewhere with the same response properties but a different preferred direction. The same technique is not sensible when measuring speed rather than direction, however, because speed doesn't vary circularly as direction does. When we accepted only those neurons with high preferred speeds into our population, we somewhat circumvented the problem of having neurons with different preferred speeds in the same distribution.

For both strategies, many of the neurons that were selected or heavily weighted were neurons that preferred fast speeds and thus had responses that increased monotonically over a wide range of speeds. Single neuron data from one neural area do not address whether fast-preferring neurons actually contribute preferentially to eye velocity computations. Nevertheless, we are willing to consider this possibility for 2 reasons. First, the neurons we included that had high preferred speeds frequently had responses that increased monotonically with speed. As will be discussed in chapter 4, these neurons might represent speed in an ideal way for communicating with downstream areas. Unlike bandpass responses, which need to be decoded, each firing rate in a monotonically increasing response corresponds to a unique speed. Second, if one role of the extraretinal signal is to inform the pursuit system of ongoing eye velocity to set the visuomotor gain for pursuit, neurons with high preferred speeds are particularly well-

suited. Not only are their responses straightforward to decode, but their monotonically increasing responses match the visuomotor gain which appears to scale monotonically with pursuit speed (Churchland and Lisberger 2002; Schwartz and Lisberger 1994).

Because the neurons in our experiment were measured individually, we were not able to estimate the degree to which firing between neurons is correlated. Studies in MT have suggested that correlations are weak and range from 0.12 to 0.19 depending on the similarity of the neurons' preferred directions. Even such weak correlations limit the degree to which pooling responses can reduce noise (Shadlen et al. 1996). However, improvements due to averaging in MT persist until about 50 to100 neurons are included with a correlation value of 0.18. The largest pool size we used was 79 neurons, with preferred speeds that varied across the population. If interneuronal correlations in MST are as high as 0.18 even for neurons with different preferred speeds, population estimates in the brain might be slightly noisier than population estimates here.

Other methods for selecting and weighting neurons are not reported here. For example, the center-of-mass or vector average method for generating a population estimate proved unsuited to MST responses. This population estimate has been used to estimate both direction and speed in area MT (Churchland and Lisberger 2001), and direction of movement in primary motor cortex (Georgopoulos et al. 1986). However, the center-of-mass estimate is inappropriate for MST responses for 2 reasons. First, a center-of-mass estimation will only be successful when neurons in the population are equally likely to prefer any speed. In MST, the distribution of preferred speeds is highly

skewed towards faster speeds. As a result, population estimates tend to be too high. Secondly, even when a population has evenly distributed preferred speeds, a center-of-mass estimate will be skewed slightly at the upper and lower edges of the responses (Salinas and Abbott 1994).

References

Britten KH, Shadlen MN, Newsome WT, and Movshon JA. The analysis of visual motion: a comparison of neuronal and psychophysical performance. *J Neurosci* 12: 4745-4765, 1992.

Churchland AK and Lisberger SG. Gain control in human smooth-pursuit eye movements. *J Neurophysiol* 87: 2936-2945, 2002.

Churchland MM and Lisberger SG. Shifts in the population response in the middle temporal visual area parallel perceptual and motor illusions produced by apparent motion. *J Neurosci* 21: 9387-9402, 2001.

Georgopoulos AP, Schwartz AB, and Kettner RE. Neuronal population coding of movement direction. *Science* 233: 1416-1419, 1986.

Guigon E. Computing with populations of monotonically tuned neurons. *Neural Comput* 15: 2115-2127, 2003.

Salinas E and Abbott LF. Vector reconstruction from firing rates. *J Comput Neurosci* 1: 89-107, 1994.

Schwartz JD and Lisberger SG. Initial tracking conditions modulate the gain of visuo-motor transmission for smooth pursuit eye movements in monkeys. *Vis Neurosci* 11: 411-424, 1994.

Shadlen MN, Britten KH, Newsome WT, and Movshon JA. A **computational analysis of the relationship between** neuronal and behavioral responses to visual **motion.** ***J Neurosci*** 16: 1486-1510, 1996.

Zohary E, Shadlen MN, and Newsome WT. Correlated neuronal **discharge rate and its implications for psychophysical** performance. *Nature* 370: 140-143, **1994.**

Figure legends

Figure 1. Distribution of performance of an ideal observer for 79 MST neurons. Thick black lines indicates the population mean.

Figure 1

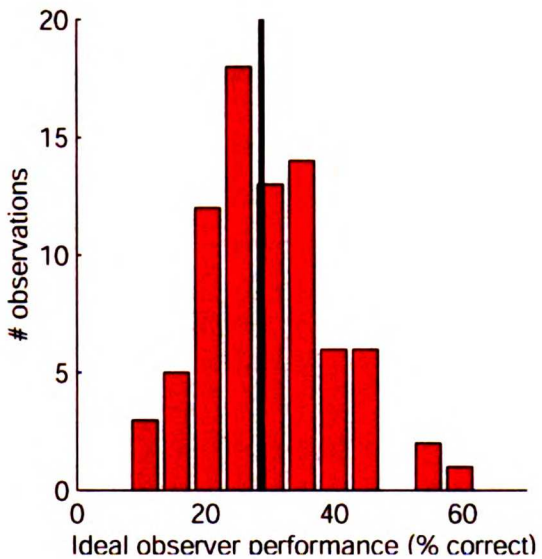
20
15
10
5
0
observations
0
20
40
60
Ideal observer performance (% correct)

Figure 2. A. Firing rate as a function of speed for the 12 neurons with preferred speeds and F-values appropriate for admittance to the population pool. B. Firing rate as a function of speed for 7 example neurons with preferred speeds and F-values inappropriate for admittance to the population pool. C and D. Red trace: Population estimate of eye velocity for neurons that were included (C) or excluded (D) from the population. Green dashed trace: Eye or target velocity.

figure 2

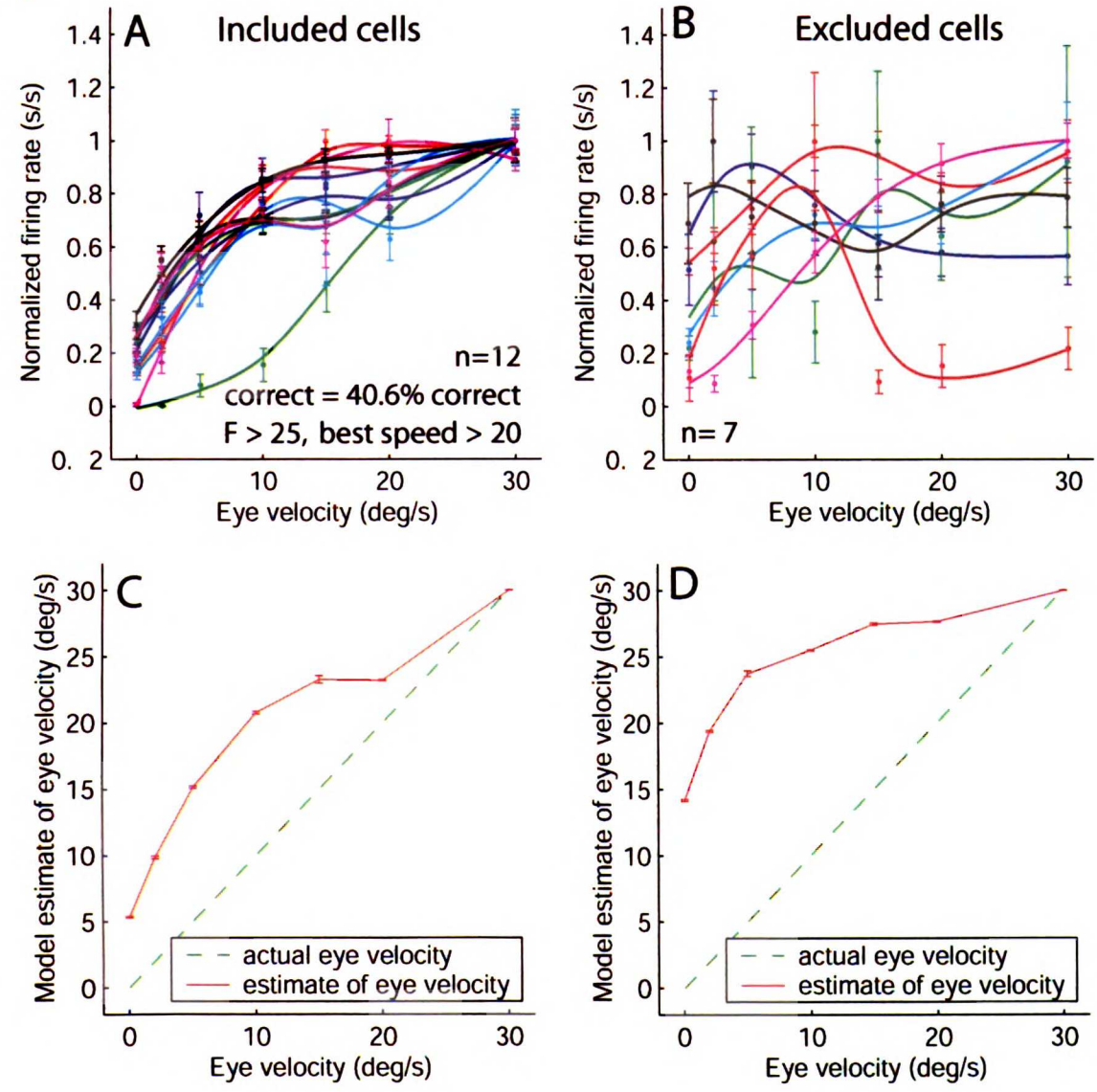
A
Included cells
Normalized firing rate (s/s)
Eye velocity (deg/s)
n=12
correct = 40.6% correct
F > 25, best speed > 20
B
Excluded cells
n= 7
C
D
Model estimate of eye velocity (deg/s)
actual eye velocity
estimate of eye velocity

Figure 3. A. Black trace: ideal observer performance as a function of the minimum preferred speed required for admittance to the population pool. Grey trace: number of neurons admitted at each criterion level. B. Speed tuning traces from neurons included at the strictest criteria used, as indicated by the black star in A. C and D: same as A and B except that criterion for admittance to the population pool was value of the F statistic from an ANOVA. E and F: same as A and B except that criterion for admittance to the population pool was the value of the speed selectivity index.

figure 3

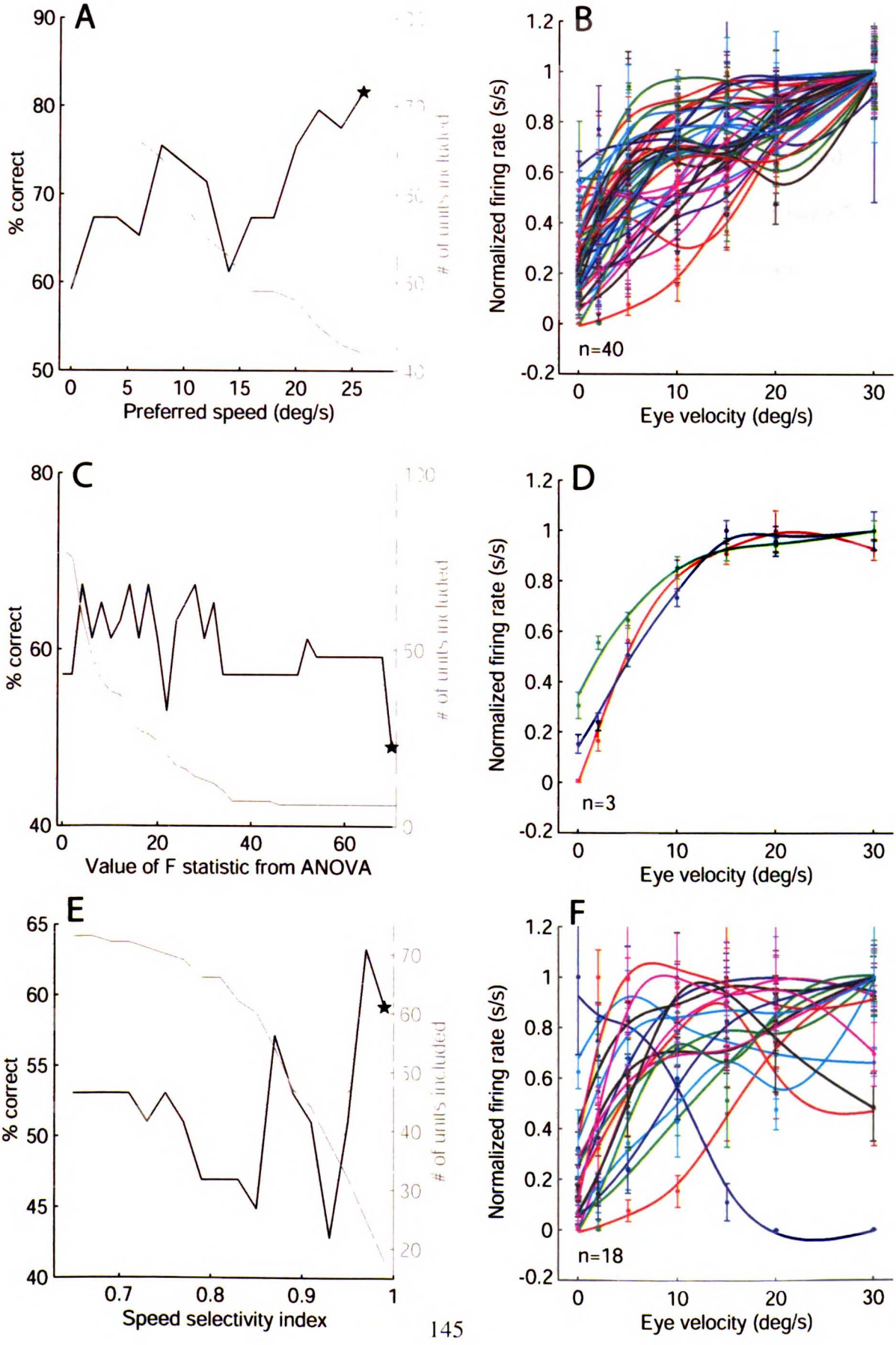
A
% correct
# of units included
Preferred speed (deg/s)
B
Normalized firing rate (s/s)
n=40
Eye velocity (deg/s)
C
% correct
# of units included
Value of F statistic from ANOVA
D
Normalized firing rate (s/s)
n=3
Eye velocity (deg/s)
E
% correct
# of units included
Speed selectivity index
F
Normalized firing rate (s/s)
n=18
Eye velocity (deg/s)

Figure 4. A and B. Examples of speed tuning traces from neurons that were assigned high weights (A) or near-zero weights (B). C. Red trace: Population estimate of eye velocity. Green dashed trace: Eye/target velocity. D. Population estimates including progressively more neurons. Yellow trace labeled n=1: population estimate computed using only the neurons assigned the lowest weight by regression. Each trace includes 5 more neurons than the previous trace. Traces become redder as more neurons are included. Green dashed trace: Eye or target velocity.

Figure 4

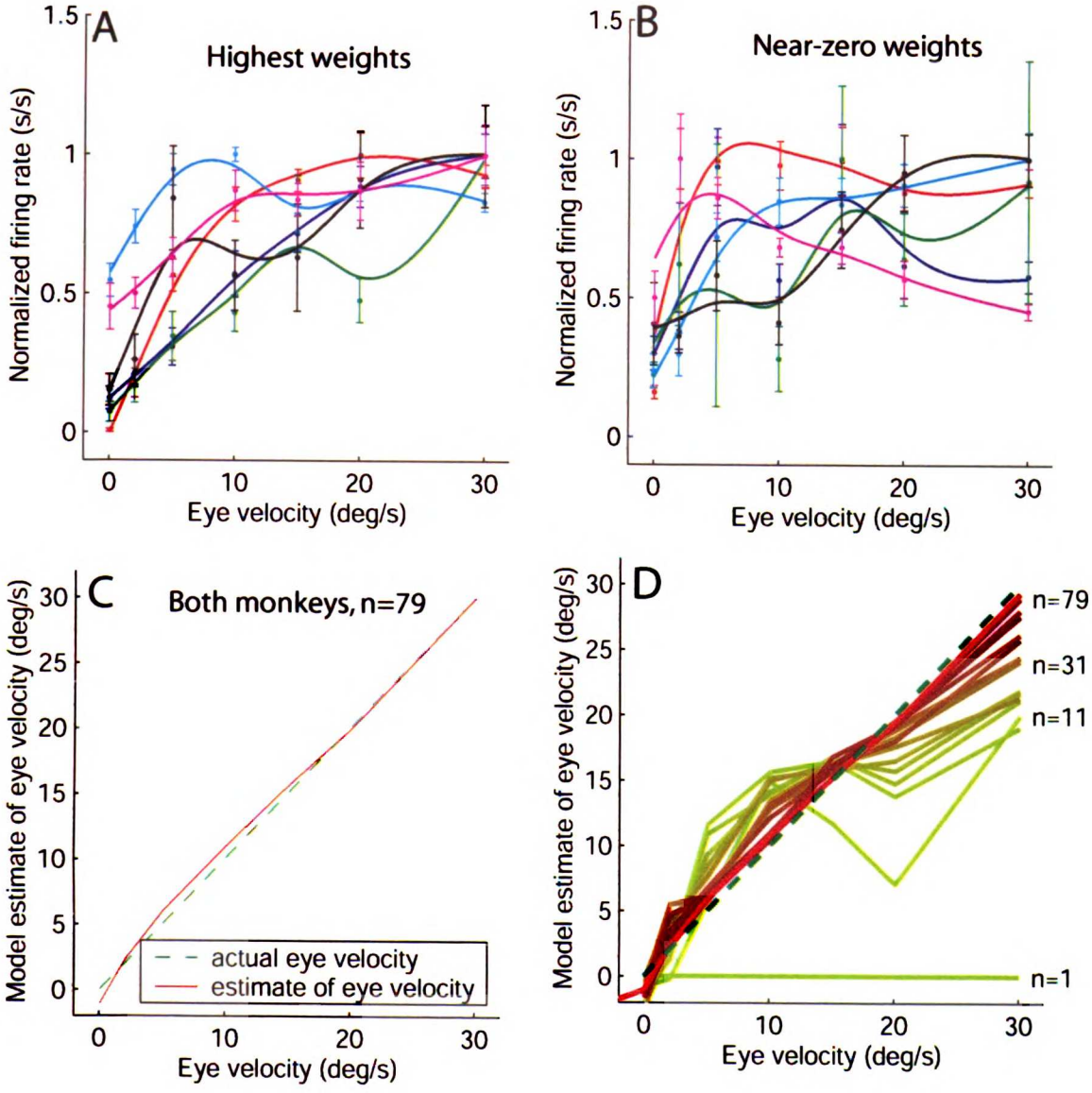
A
Highest weights
Normalized firing rate (s/s)
Eye velocity (deg/s)
B
Near-zero weights
Normalized firing rate (s/s)
Eye velocity (deg/s)
C
Both monkeys, n=79
Model estimate of eye velocity (deg/s)
actual eye velocity
estimate of eye velocity
Eye velocity (deg/s)
D
Model estimate of eye velocity (deg/s)
n=79
n=31
n=11
n=1
Eye velocity (deg/s)

Figure 5. A. Relationship between weight assigned to a neurons by the regression analysis and the F-statistic generated using an ANOVA for that neuron. B. Relationship between weight assigned to a neuron by the regression analysis and the preferred speed of the neuron.

figure 5

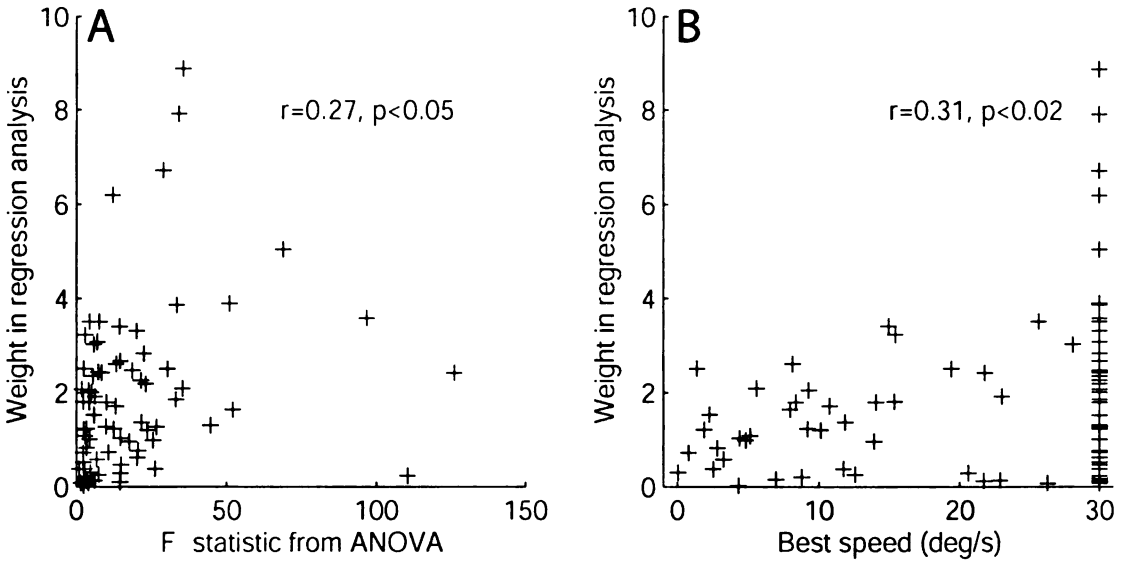
A
B
r=0.27, p<0.05
r=0.31, p<0.02
Weight in regression analysis
F statistic from ANOVA
Best speed (deg/s)
0
2
4
6
8
10
0
50
100
150
10
20
30

Figure 6. A. Red trace: population estimate using regression on a scrambled version of the data matrix. Green dashed trace: eye or target velocity. B. Red trace: population estimate using regression on the actual data matrix. Green dashed trace: Eye or target velocity. C. Red trace: population estimate using regression on half the10 trials taken at each speed in a scrambled version of the matrix with 51 neurons from monkey Mo. Grey trace: population estimate from the remaining 5 trials using the weights generated from the first half of the data. Green dashed trace: Eye or target velocity. D. Red trace: population estimate using regression on half the10 trials taken at each speed in the ordered data matrix with 51 neurons from monkey Mo. Grey trace: population estimate from the remaining 5 trials using the weights generated from the first half of the data. Green dashed trace: Eye or target velocity. E. Red trace: population estimate using regression on half the10 trials taken at each speed in a scrambled version of the matrix with 28 neurons from monkey Yo. Grey trace: population estimate from the remaining 5 trials using the weights generated from the first half of the data. Green dashed trace: Eye or target velocity. F. Red trace: population estimate using regression on half the10 trials taken at each speed in the ordered data matrix with 28 neurons from monkey Yo. Grey trace: population estimate from the remaining 5 trials using the weights generated from the first half of the data. Green dashed trace: Eye or target velocity.

Figure 6

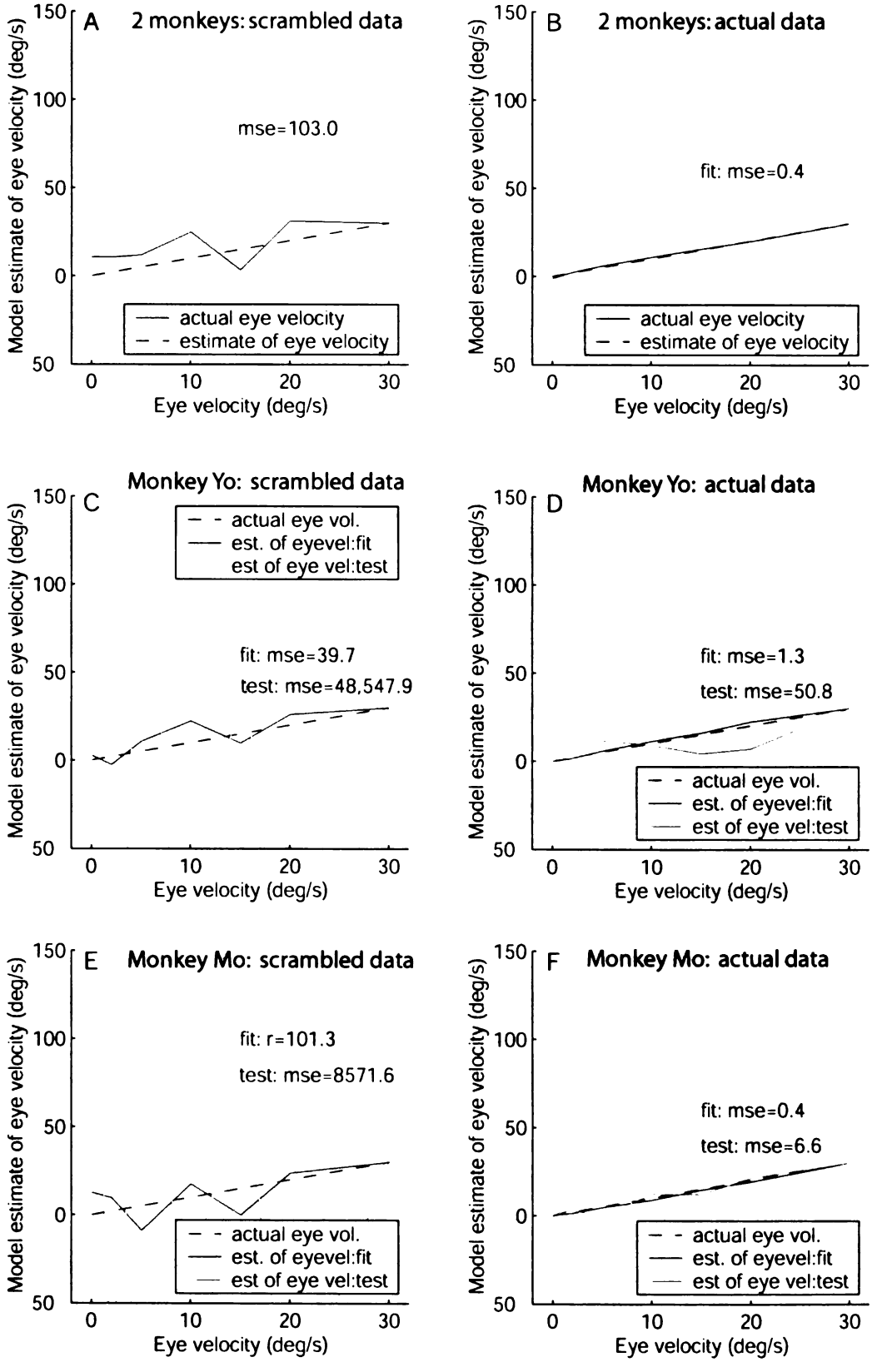
A
2 monkeys: scrambled data
mse=103.0
B
2 monkeys: actual data
fit: mse=0.4
C
Monkey Yo: scrambled data
fit: mse=39.7
test: mse=48,547.9
D
Monkey Yo: actual data
fit: mse=1.3
test: mse=50.8
E
Monkey Mo: scrambled data
fit: r=101.3
test: mse=8571.6
F
Monkey Mo: actual data
fit: mse=0.4
test: mse=6.6
actual eye velocity
estimate of eye velocity
actual eye vol.
est. of eyevel:fit
est of eye vel:test
Model estimate of eye velocity (deg/s)
Eye velocity (deg/s)
150
100
50
0
50
0
10
20
30

Chapter 4: MST neurons that decode responses from area MT

Abstract

Responses from MT and MST neurons were recorded during presentation of apparent motion stimuli with progressively longer temporal separations (Δt) between stimulus presentations. Responses of single MT neurons decreased progressively as Δt became longer; only the population response was able to account for behavioral observations during smooth pursuit eye movements. Responses of single neurons in area MST, on the other hand, reflected both the population output of area MT and accounted for the behavioral observations during pursuit. This suggests that one role of MST is to decode responses from area MT.

Introduction

Although research has uncovered much about the response properties in different visual cortical areas devoted to motion processing, one difficult problem has been in understanding the computations that take place between the areas. For example, the middle temporal area (MT) is known to project to the medial superior temporal area (MST), and both areas have been reported to contain a large number of neurons that respond well to motion in the visual field (Maunsell and Van Essen 1983; Saito et al. 1986; Tanaka et al. 1986). Both areas are known to contribute to the generation of smooth eye movements, and both contain neurons that are sensitive to the speed of moving stimuli. Although the existence of some MST neurons responding to complex motion patterns has suggested that it processes motion information from MT, the nature of that processing is not well understood.

One comparison between responses in MT and MST suggests a particular relationship between neurons in the two areas. It has been known for quite some time that many neurons in area MST prefer fast stimulus speeds (Kawano et al. 1994). In fact, responses of many MST neurons increase monotonically with stimulus speeds over quite a broad range (Churchland and Lisberger submitted). One possibility is that responses in MST reflect the decoded population response in area MT. In MT, most neurons respond to progressively faster speeds in what we described as a bandpass response pattern: although the speed of the image motion input is monotonically increasing, the neuron's response first increases and then decreases. A number of studies have suggested that a collection of such bandpass responses can be decoded so that the population response increases monotonically in parallel with the image motion inputs (Priebe et al. 2001). Unlike MT, in MST many individual neurons have firing rates that increase monotonically in parallel with image motion. These responses don't increase forever, but many of them are monotonically increasing up to 128°/s (Churchland and Lisberger submitted), certainly including most of the speeds that are normally encountered in the visual world and matching the point at which psychophysical thresholds become elevated (De Bruyn and Orban 1988). In other words, the responses in MST, at least over a range, resemble what the decoded output from MT might look like.

The fact that many responses in MST increase monotonically with stimulus speed is not, by itself, strong evidence that MST neurons decode responses from MT. Certainly,

there might be other explanations for why MST responses are monotonically increasing over such a wide range. MST might simply be optimized to process faster speeds than MT. To test the possibility that some MST responses reflect the decoded response from area MT, we identified a stimulus condition where the population output from area MT is likely distinct from the responses of individual MT neurons. The stimuli we used were apparent motion stimuli which create the impression of smooth motion using sequential presentations of the same stimulus at different positions. We predicted that neurons with high preferred speeds, which will be monotonically increasing over the largest range of speeds, will have responses to smooth motion that match both the population output from area MT and the behavior.

Results

In apparent motion stimuli, when the temporal separation (Δt) between subsequent stimulus presentations is short, motion can look fairly smooth, while lengthening the Δt causes the motion to appear progressively more degraded. Patches of apparent motion stimuli can be used as targets for smooth pursuit eye movements (figure 1a) even when values of Δt are long, but these stimuli have a paradoxical effect on the initiation of smooth pursuit (Churchland and Lisberger 2000). As progressively longer values of Δt degrade the motion stimulus, eye acceleration during pursuit initiation actually increases. Figure 1b plots the relationship between eye acceleration and Δt as it has been reported previously (Churchland and Lisberger 2000, 2001). When the motion stimulus is considerably degraded with a Δt between about 20 and 44 ms, eye acceleration is actually faster than when the motion appears smooth at a Δt of 4 ms

(figure 1b, solid trace, open circles). Before describing responses to MST neurons to apparent motion, we will briefly review how MT neurons respond to apparent motion, as has been previously published (Churchland and Lisberger 2001).

Eye acceleration during initiation of smooth pursuit is believed to reflect processing in visual motion areas before visual feedback has time to affect responses (Lisberger and Westbrook 1985). Because motion sensitive neurons in area MT are likely to provide visual motion inputs for pursuit (Komatsu and Wurtz 1989, 1988; Newsome and Pare 1988), responses of MT neurons were measured from 73 single, isolated neurons in area MT during the presentation of apparent motion stimuli. Surprisingly, responses of single neurons in area MT do not account for the paradoxical increase in eye acceleration observed in pursuit. Instead, responses of MT neurons simply become progressively lower when Δt becomes long. Responses from an example MT neuron are shown in figure 2a and b. This neuron was typical of area MT in that it exhibited speed-tuned responses (figure 2a) with the peak indicated by a star. The neuron was presented with a series of apparent motion stimuli with Δts ranging from 4 to 44 or 64 ms. These Δts were used for motion at 16°/s (figure 2b, black trace) and 32°/s (figure 2b, grey trace). The black or grey star on each trace indicates the peak of the smoothing spline function used to fit the data. In both cases, the peak of the curve is at the shortest Δt tested because responses tended to simply shrink when Δt became long.

When the population response of area MT is computed using a standard vector average (methods), the population output, like the responses of single neurons, simply

decreases as Δt becomes longer (figure 2c, grey and black solid traces). This population response does not reflect eye acceleration, which first increases and then decreases (figure 2c, black and grey dashed traces) for both 16°/s and 32°/s motion. On the other hand, when the population response is estimated as an opponent vector average (figure 3d, grey and black solid traces), the population response reflects the observed changes in eye acceleration nicely. The opponent vector average normalizes the response at each value of Δt by the difference between preferred and null responses at that value. The reason for the population shift using the opponent vector average arises from a difference in responses to apparent motion in neurons with slow and fast preferred speeds. Neurons with fast preferred speeds tend to be more resistant to apparent motion so that their responses remain unchanged for longer. Thus at long values of Δt, neurons preferring slower speeds have firing rates that are very reduced, while neurons preferring faster speeds have firing rates that are more moderately reduced. The vector average of the population therefore shifts slightly towards faster speeds.

When responses in MT are decoded using the opponent vector average, the population response, which matches pursuit eye acceleration, differs considerably from the responses of individual neurons, which simply decrease as Δt gets longer. The lynchpin of the opponent vector average computation is that population responses at each value of Δt are normalized by the sum of opponent responses for the population. If responses of MST neurons with monotonically increasing responses to stimulus speed reflect the population output of area MT, as we have suggested, then responses of

single neurons should match both pursuit eye acceleration and the population output of MT neurons that we have modeled.

We recorded 73 single, isolated neurons in area MST during the presentation of apparent motion stimuli. Examples of 3 neurons are shown in figure 3. Figure 3a shows the speed tuning for a typical MST neuron. In response to smooth motion (figure 3a), the neuron's firing rate increases monotonically with smooth motion all the way up to 128°/s. When presented with apparent motion stimuli (figure 3b), responses of this neuron are similar to both the population output of area MT and pursuit eye acceleration: as the separation between flashes increased, responses to both 16°/s motion (black trace) and 32°/s motion (grey trace) increased dramatically. The neuron responded most robustly at 32°/s motion when it was presented with a Δt of 44 ms. At this Δt, the neuron's response was about equal to it's response during 128°/s smooth motion (compare peak of figures 3a and b). To emphasize the similarity between this single neuron and the behavior, we indicated (dashed black and grey lines) the Δts corresponding to the peaks of the behavioral and the population output of MT, for 16°/s and 32°/s motion. The peak of the MST response during 32°/s motion is, like the behavior, to the left of the peak for motion at 16°/s. This suggests that neurons are sensitive not only to the temporal separation between flashes (Δt) but also the spatial separation between flashes (Δx).

MST neurons without monotonically increasing responses to smooth motion frequently exhibited rather different responses to apparent motion stimuli. The neuron

in figure 3c, like many MT neurons, exhibited bandpass tuning in response to smooth motion. The neuron's response to apparent motion is likewise quite similar to apparent motion responses in area MT (figure 3d). As the separation between flashes increased, responses to both 16°/s motion (black trace) and 32°/s (grey trace) motion increased only slightly at quite short flash separations before decreasing dramatically.

A third example neuron from MST was more rarely encountered but provides evidence that increasing the flash separation in apparent motion stimuli is, from the point of view of the cell, akin to increasing the speed rather than changing the firing rate in some nonspecific way. The neuron shown in figure 3e and f changed its preferred direction as a function of visual motion speed so that the difference between preferred and null responses is negative at slower speeds and positive at faster speeds (figure 3e): the direction eliciting good responses at high speeds, the right, was arbitrarily chosen as the neuron's best direction. In response to apparent motion at short flash separations (figure 3f), the opponent response was negative, indicating that leftwards motion was a better stimulus than rightwards motion. However as Δt became longer, the opponent response became large and positive, indicating that rightwards was the preferred direction, even though for smooth motion at 16 or 32°/s, rightwards was the null direction.

For this neuron, the peak of the apparent motion response (grey or black star) was at a slightly longer Δt than the peak of the behavior or population response from MT

(dashed black or grey line). The peaks were in the right place relative to one another (16°/s longer than 32°/s), but both were slightly too long.

To determine which changes in firing were significant, we compared distributions of responses at the shortest Δt with distributions of responses at longer Δts. For each neuron, we determined whether any of the increases in firing were significant to $p<0.05$ on a one-tailed t-test. We found that for neurons recorded in area MT during 16°/s motion, 6.9% had responses for at the shortest Δt that were significantly smaller than responses at another Δt. For MT neurons recorded in area MT during 32°/s motion, 5.5% had responses for at the shortest Δt that were significantly smaller than responses at another Δt. By contrast, neurons in MST had responses for the shortest Δt that were significantly smaller than responses at another Δt 37% and 38% of the time for 16 and 32°/s motion. Interestingly, as figure 3 suggests, neurons that had significant increases in firing were more likely to prefer fast speeds. For example, MST neurons without significant increases in firing at 32°/s had an average preferred speed of 57.1°/s, while MST neurons with significant increases in firing rate had an average preferred speed of 106.8°/s, almost twice as fast! For motion at both 16°/s and 32°/s, neurons that increased their firing rates in response to apparent motion had preferred speeds that were significantly faster than those neurons that did not increase their firing rates in response to apparent motion (16°/s: $p<0.01$; 32°/s: $p<0.01$).

To demonstrate how the population response changes as a function of Δt, we averaged responses across neurons at each value of Δt. Because our previous analysis

suggested that neurons preferring fast speeds might have different responses than those preferring slower speeds, we averaged responses of neurons preferring fast separately from neurons preferring slower speeds. The averaged response of MST neurons preferring speeds less than 50°/s is shown in figure 4a for 16°/s (thick black trace) and 32°/s (thick grey trace). The averaged response decreases steadily for both speeds at Δts longer than 16ms. Averaged responses for MT neurons with preferred speeds less than 50°/s were similarly averaged and likewise decrease steadily for both 16°/s (thin black trace) and 32°/s (thin grey trace). The averaged response of neurons with preferred speeds that were faster than 50°/s, however, was quite different. Amazingly, simply averaging single neuron responses to motion at both 16°/s (figure 4b, thick black trace) and 32°/s (figure 4b, thick grey trace) produced a population response that increased over a range of Δt values comparable to that seen in the population output of MT and in pursuit eye acceleration. This simple average matches further subtleties of the eye acceleration data and population response. In both the population response and eye acceleration, the peak for 16°/s (indicated by the black dashed vertical line in figure 4b) is at a longer Δt than that for 32°/s (indicated by the grey dashed vertical line in figure 4b). In the simple average of MST responses, the peak for 16°/s is similarly at a longer Δt than that for 32°/s.

We have plotted averaged responses of MT neurons with fast preferred speeds for comparison although only a small number of MT neurons had preferred speeds greater than 50°/s (n=6). Responses of MT neurons preferring fast speeds were resistant to apparent motion for longer than those preferring slower speeds (compare

thin traces in figure 4a and b) but showed only a very small increase compared to the one observed in area MST.

The population response in MT parallels the pursuit response to apparent motion best when opponent responses were used (Churchland and Lisberger 2001). In MST, however, we observed a more modest difference between population estimates calculated from opponent responses verses preferred only responses. Population averages computed using only responses in the preferred direction are shown in figure 4c and d. The shapes of the averaged response for neurons preferring low and high speeds did not depend strongly on whether the opponent or preferred-only response was used. The only difference was that the increased response for long Δts was more modest when only preferred responses were averaged.

To demonstrate in more detail the relationship between preferred speed and response to apparent motion in MST neurons, we explored how the preferred speed of individual neurons varied with the Δt that elicited the greatest response from the neuron. The best speed and the "best Δt" were taken as the peak of the curve used to fit speed tuning or apparent motion responses, as indicated by the black and grey stars in figure 3. For responses at both 16°/s (figure 4a) and 32°/s (figure 4b) the best Δt was positively correlated with the preferred speed (16°/s: $r=0.58$, $p<0.001$, 32°/s: $r=0.74$, $p<0.001$). Although the correlation is highly significant for both speeds, considerable scatter is apparent. Neurons with slow preferred speeds almost always responded best at the shortest value of Δt, but neurons with fast preferred speeds were less consistent

and sometimes also responded well at the shortest Δt tested. When we took the best speed and best Δt from responses in the preferred direction only, the same relationship was observed (16°/s: $r=0.54$, $p<0.001$, 32°/s: $r=0.69$, $p<0.001$, data not shown).

Figure 5a and b suggest that for the population, responses to apparent motion presented at 16°/s are similar to, though slightly noisier than, apparent motion responses presented at 32°/s. To compare responses of individual neurons, we plotted the best Δt for 16°/s motion against the best Δt for 32°/s motion in figure 5c. Two trends are evident in the data. First, peak responses at one speed are correlated with peak responses at the other. Second, the best Δt for 32°/s motion was frequently shorter than the best Δt for 16°/s, so almost all points lie above the dotted line indicating $x=y$. Note that for a given Δt, motion at 32°/s will have a larger spatial separation that motion at 16°/s. Had the neurons been sensitive only to the temporal separation and not the spatial separation between stimulus presentations, the points in figure 5c would lie along the dotted line. On the other hand, had the neurons been exclusively sensitive to the spatial separation, the peak Δt for 16°/s would have been twice that of 32°/s for each neuron, and the points in figure 5c would lie along the dashed line indicating $x=2y$. This line is perhaps a closer fit to the data, but the amount of scatter suggests that neurons are sensitive to a combination of the spatial and temporal separations between subsequent stimulus presentations.

Discussion

We have used apparent motion stimuli as a tool to test the hypothesis that MST neurons preferring fast speeds reflect the decoded population response from MT. Apparent motion stimuli are ideally suited to this endeavor because they are likely to have an effect on the population of neurons in MT that is distinct from the effect on individual neurons. If MST neurons have fast preferred speeds only to extend the range of speeds available to the visual system, MST responses to apparent motion should be no different than those observed in area MT. On the other hand, if MST neurons truly decode the population response from MT, their responses to apparent motion should parallel the population output of MT at the level of individual neurons. This is indeed what we observed.

Our data is consistent with the hypothesis that the population response in area MT is generated using an opponent vector average algorithm because other population estimates in MT, such as the standard vector average, failed to parallel the behavioral observations from pursuit. The reason for this is that MT neurons lose their directionality not only via reduced firing rates in the preferred direction, but also by increased firing rates in the null direction. As a result, the population response only resembles eye acceleration when the responses at each temporal separation are normalized by the summed opponent response. In MST, generating a population response that parallels eye acceleration is much simpler. Because the responses of individual neurons match pursuit quite closely, we were able to generate an accurate

population response simply by averaging the responses of single neurons preferring fast speeds. Even without assigning weights according to preferred speed, computing the opponent signal, or normalizing the population response as we did for area MT, we were able to generate a population response that was a close match to the shape of the behavior for both 16°/s and 32°/s.

We observed that, on average, responses from MST neurons preferring slower speeds resemble individual neurons in MT, while the average response from neurons preferring faster speeds is a close match to the population response in MT. We initially hypothesized that the speed tuning in response to smooth motion of fast-preferring neurons in MST is similar to the population response from MT. Therefore, it is particularly exciting that the neurons preferring fast speeds were the most likely to have apparent motion responses that resembled the population response from area MT. Neurons preferring lower speeds lacked monotonically increasing responses that resembled the population output from MT and accordingly, their responses to apparent motion likewise failed to resemble the population output from area MT.

Interestingly, the data in figure 6 suggest that the degree to which neurons increase their responses to apparent motion varies continuously as a function of the degree to which they are monotonically increasing. For example, neurons with preferred speeds near 50°/s, which increase monotonically only over a short range, exhibited peak responses to apparent motion at shorter Δts than neurons with preferred speeds near 128°/s. This continuous shift in the degree to which responses to apparent motion

increase perhaps indicates that responses from MT are decoded in varying degrees by different MST neurons. Further, we observed some variability in the best Δt that was observed for neurons with a given preferred speed. This was especially true for motion presented at 16°/s: some neurons preferring fast motion had long best Δts, while others peaked at shorter values of Δt. This suggests that the degree to which a neuron exhibits monotonically increasing responses over a range of speeds is not the only predictor of whether it reflects the population response from area MT.

We were surprised to find a small population of MT neurons that had significant increases during apparent motion stimuli. These represented only between 5 and 7% of the total population were likely to have slightly larger preferred speeds than the general population. The existence of these neurons suggests that responses may be decoded to differing degrees in different areas. The percentage of neurons that have increasing responses to apparent motion may steadily grow as signals travel from MT to MST and beyond. Area 7a, which is a projection target of area MST (Boussaoud et al. 1990) has also been reported to have a high percentage of neurons with monotonically increasing responses , might contain an even larger percentage of neurons that increase in response to apparent motion.

One particularly exciting aspect of these results is that they present a rather different picture of how motion signals are represented in MST. Some of the stimuli that best drive typical MST neurons, such as combinations of spiral motion and expansion, suggest that motion signals from area MT are transformed to generate sensitivity to

very complex stimuli in MST. Our data certainly do not refute this possibility, but they suggest an additional role of MST neurons: neurons with high preferred speeds might decode the population response from MT and represent translational speed in a very straightforward fashion.

Methods

Eye movement and neural recordings were obtained from four adult male rhesus monkeys (*Macaca mulatta*) that were trained to fixate and pursue visual targets for fluid reward. Monkeys were implanted with head restraints and scleral search coils as described elsewhere (Churchland and Lisberger 2000), (Judge et al. 1980). After initial training, monkeys were implanted with stainless steel head holders and stainless steel or cilux cylinders (Crist instruments, Hagerstown, MD) placed over a 20 mm circular hole cut in the skull to allow access to MST for neural recordings. For each experimental session, the monkey sat in a primate chair affixed with a tube for dispensing fluid rewards. Methods were approved in advance by the Institutional Animal Care and Use Committee at the University of California, San Francisco. All experimental procedures were in accordance with the National Institutes of Health Guide for the Care and Use of Laboratory Animals.

Stimulus presentation and eye movement recording

Visual stimuli were displayed on a 12 inch diagonal analog oscilloscope. The display was positioned 30 cm from the monkey and subtended horizontal and visual

angles of 50° and 40°. Visual stimuli consisted of patches of moving dots. The aperture size for patches of dots was either 8°X 8° for neurons in area MT or 30°X30° for neurons in area MST. Patches contained either 24 or 500 randomly placed dots that moved coherently. Each dot in the patch was ~0.2° across and had a luminance of 1.6 cd/m^2. The control signals for the oscilloscopes were provided by the digital to analog converters of a digital signal processing board that ran in a Pentium computer. Each dot in the stimulus was flashed sequentially at different locations, with a spatial and temporal separation between locations that varied according to stimulus parameters. We refer to the spatial and temporal separations as Δx and Δt, with the apparent speed defined as $\Delta x/\Delta t$. When Δx and Δt were small (<20ms) motion appeared smooth. As Δx and Δt became longer, the motion appeared progressively more degraded. All dots within the patch were updated at virtually the same time; i.e. presentation of dots during a flash was essentially synchronous (with no dots being presented until the next flash). The specifications of the display oscilloscopes indicate that the phosphor decayed to 10% of its maximal level in 10μs to 1 ms.

Visual stimuli were presented in "trials," each of which contained motion at a particular speed and Δt. Trials began with the onset of a fixation point, followed 600 ms later by the onset of a stationary patch. 200 ms later, dots in the patch began to move coherently and continued to move for 500 ms. The patch was then extinguished and the fixation light remained on for 200 ms. When the monkeys successfully maintained fixation within a 4-5° window throughout the trial, they were rewarded with a drop of juice or water that was approximately 0.1 mL. Actual fixation accuracy was typically much better that 4-5°with the exception that fast stimuli presented near the

fovea sometimes evoked a small response that the monkey was unable to entirely suppress. Each experiment contained trials of different speeds and Δt that were presented in random order.

Neural recordings

Extracellular action potentials were recorded from single units in area MT and MST. Recordings from two monkeys were made in each area. Some of the data recorded in MT has been reported previously (Churchland and Lisberger 2001). Recordings were made using sharp, 1-3 MΩ tungsten microelectrodes (Frederick Haer Co, Bowdoinham, ME). The electrode location was determined by a guide tube inserted in a plastic grid (Crist Instruments) which was positioned daily in a cylinder over the superior temporal sulcus each day. The voltage recorded by the electrode was amplified conventionally (Dagan, Minneapolis, MN) bandpass filtered from 100Hz to 5 or 10Khz and viewed on an analog oscilloscope.

All 4 monkeys had cylinders centered at approximately 15 mm lateral and 2 mm posterior. Cylinders were oriented so that electrodes were introduced perpendicular to the cortical surface. The advantage of this configuration is that penetrations typically include area MST, the lumen of the superior temporal sulcus and the middle temporal area (MT) making it straightforward to distinguish MST from MT. Typically, the two areas were distinguished based on the well-described response properties in each area (Maunsell and Van Essen 1983; Saito et al. 1986; Tanaka et al. 1986), and the location

of surrounding areas V4 and 7a. All four monkeys are still being used in other experiments so histology is not available.

In the two monkeys where MT responses were recorded, neurons were identified as belonging to MT if they had a very high probability of being strongly directional, had receptive field sizes that were appropriate for their eccentricity and were located beneath the lumen of the superior temporal sulcus.

In the two monkeys where MST responses were recorded, neurons were identified as being part of MST if they had large receptive fields with sizes greater than would be expected based on eccentricity in MT(Tanaka et al. 1986) and were dorsal to the lumen. Receptive fields frequently included the fovea and large parts of the ipsilateral field. Neurons with smaller receptive fields were sometimes included if they were close to neurons that were clearly MST neurons or if they were dorsal to the lumen of the superior temporal sulcus. We wished to be conservative in only selecting neurons that we were certain were part of area MST so neurons that were more ventrally located were excluded if we could not completely rule out the possibility that they were part of are MT. For this reason, recordings made in area MST are likely to include mostly neurons from the dorsal subregion (MSTd) rather than the lateral subregion (MSTl)(Komatsu and Wurtz 1988; Tanaka et al. 1986).

After isolating a neuron, we first estimated its preferred direction by using a set of eight trials, each of which presented motion at a different speed. Dot motion was

presented within an 8° window if the receptive field size and location were known and was within a large window otherwise. Motion in the eight directions was usually presented at 30°/s if the preferred speed was not known. However, if the neuron failed to exhibit directional responses at 30°/s, faster and slower speeds were tried. Responses to the last 400 ms of motion in each direction were analyzed and the neuron's best direction was determined. The preferred speed was then estimated by presenting a series of trials in the neuron's preferred direction at speeds ranging from 0.5°/s to 128°/s. Once the preferred speed was determined, the neuron's receptive field was mapped either by using a list of trials that presented patches of dots in the preferred speed and direction and different locations, or by manually moving a patch to find receptive field edges. An 8°X8° patch was commonly used although this proved a poor stimulus for some MST neurons and larger patches were used. In MT, receptive field sizes ranged from 2.7° to 8.9°. Receptive field sizes were of the same order as the 8° square patch stimulus used to measure responses to apparent motion. In MST, receptive field sizes were larger so the 8°x8° patch proved a poor stimulus for many cells. For this reason, a large 30°x30° patch was used to measure apparent motion responses. To study the apparent motion responses of each neuron, we presented a series of trials with motion at different speeds at Δts. For neurons in MST, apparent motion was presented at 16°/s and 32°/s at Δt = 4,12, 24, 32, 44 and 64 ms. For neurons in area MT, apparent motion was presented at 16°/s (Δt = 4,12, 16,20,24, 32, 44 and 64 ms) and 32°/s (Δt = 4,12, 24, 32,and 44ms). Trials were also included to re-assess the speed tuning of the neuron under study. Responses were also collected during presentation of smooth motion (Δt = 4ms) ranging from 8°/s to 128°/s. All trial

types were presented in both the preferred direction of the neuron and the opposite (null) direction. Responses were collected until the accumulated histograms showed a reasonable signal to noise ratio. This typically required about 10 repetitions of each trial type, or about 15-30 minutes.

To compare single neuron responses to different stimulus conditions, we calculated the mean and standard error of the spike rate over a 600 ms interval that began with the onset of the stimulus and ended 100 ms after the offset of the stimulus. The mean spike rate during this period was calculated separately for responses in the preferred and null direction of each neuron. We favored comparisons of the opponent responses at different Δts because changes in opponent firing during apparent motion are not due to nonspecific effects, such as transient on-responses to each presentation of the stimulus, as has been observed in MT (Newsome et al. 1986).

Preferred speed was computed by taking the peak value from a cubic smoothing spline. For neurons in area MT, this estimate of preferred speed was typically similar to the estimate of preferred speed taken from the peak of a skewed Gaussian. However, we were unable to fit speed tuning responses in area MST using a skewed Gaussian because too many neurons had responses that were monotonically increasing. The same smoothness parameter was used for data from both areas.

To estimate population responses for area MT, two vector average computations were used: standard and opponent. The standard vector average is

$$\frac{\sum_i s_i R_i^{pref} + (-s_i) R_i^{null}}{\varepsilon + \sum_i (R_i^{pref} + R_i^{null})}$$

Where R is the response of the neuron in the preferred of null direction, s is the preferred speed of the neuron and ε is a free parameter used to ensure that the denominator does not become too close to zero at long values of Δt. The opponent vector average is

$$\frac{\sum_i s_i (R_i^{pref} - R_i^{null})}{\varepsilon + \sum_i (R_i^{pref} - R_i^{null})}$$

Acknowledgements

Mark Churchland was a collaborator on the work in this chapter and collected the data from area MT.

References

Boussaoud D, Ungerleider LG, and Desimone R. Pathways for motion analysis: cortical connections of the medial superior temporal and fundus of the superior temporal visual areas in the macaque. *J Comp Neurol* 296: 462-495, 1990.

Churchland A and Lisberger S. Speed tuning of exraretinal responses in area MST. submitted.

Churchland MM and Lisberger SG. Apparent motion produces multiple deficits in visually guided smooth pursuit eye movements of monkeys. *J Neurophysiol* 84: 216-235, 2000.

Churchland MM and Lisberger SG. Shifts in the population response in the middle temporal visual area parallel perceptual and motor illusions produced by apparent motion. *J Neurosci* 21: 9387-9402, 2001.

De Bruyn B and Orban GA. Human velocity and direction discrimination measured with random dot patterns. *Vision Res* 28: 1323-1335, 1988.

Judge SJ, Richmond BJ, and Chu FC. Implantation of magnetic search coils for measurement of eye position: an improved method. *Vision Res* 20: 535-538, 1980.

Kawano K, Shidara M, Watanabe Y, and Yamane S. Neural activity in cortical area MST of alert monkey during ocular following responses. *J Neurophysiol* 71: 2305-2324, 1994.

Komatsu H and Wurtz RH. Modulation of pursuit eye movements by stimulation of cortical areas MT and MST. *J Neurophysiol* 62: 31-47, 1989.

Komatsu H and Wurtz RH. Relation of cortical areas MT and MST to pursuit eye movements. I. Localization and visual properties of neurons. *J Neurophysiol* 60: 580-603, 1988.

Lisberger SG and Westbrook LE. Properties of visual inputs that initiate horizontal smooth pursuit eye movements in monkeys. *J Neurosci* 5: 1662-1673, 1985.

Maunsell JH and Van Essen DC. Functional properties of neurons in middle temporal visual area of the macaque monkey. I. Selectivity for stimulus direction, speed, and orientation. *J Neurophysiol* 49: 1127-1147, 1983.

Newsome WT, Mikami A, and Wurtz RH. Motion selectivity in macaque visual cortex. III. Psychophysics and physiology of apparent motion. *J Neurophysiol* 55: 1340-1351, 1986.

Newsome WT and Pare EB. A selective impairment of motion perception following lesions of the middle temporal visual area (MT). *J Neurosci* 8: 2201-2211, 1988.

Priebe NJ, Churchland MM, and Lisberger SG. Reconstruction of target speed for the guidance of pursuit eye movements. *J Neurosci* 21: 3196-3206, 2001.

Saito H, Yukie M, Tanaka K, Hikosaka K, Fukada Y, and Iwai E. Integration of direction signals of image motion in the superior temporal sulcus of the macaque monkey. *J Neurosci* 6: 145-157, 1986.

Tanaka K, Hikosaka K, Saito H, Yukie M, Fukada Y, and Iwai E. Analysis of local and wide-field movements in the superior temporal visual areas of the macaque monkey. *J Neurosci* 6: 134-144, 1986.

Figure legends

Figure 1. A. Schematic depicting the configuration of pursuit trials used to measure behavioral responses to apparent motion. Trials began with the appearance of a fixation point which was later extinguished as a patch of apparent motion appeared eccentrically and began to move towards the fovea. B. Normalized eye acceleration (open circles) and change in latency (open triangles) as a function of flash separation (Δt).

Figure 1

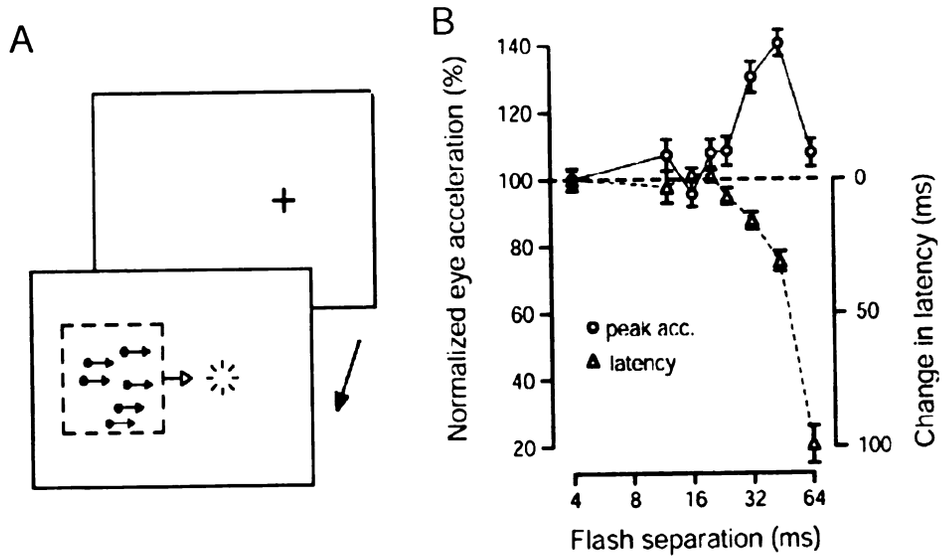
A
B
Normalized eye acceleration (%)
140
120
100
80
60
40
20
peak acc.
latency
0
50
100
Change in latency (ms)
4
8
16
32
64
Flash separation (ms)

Figure 2. Individual and population responses to apparent motion from in area MT. A. Speed tuning in response to smooth motion. The peak of the spline function fit to the data is indicated by a star. B. Firing rates in response to apparent motion at different values of Δt presented at 16°/s (grey trace) or 32°/s (black trace). The peak of the spline function used to fit the data is indicated by a star of the same color as the trace. C. Solid traces with filled symbols: normalized population response for 16°/s (grey trace) or 32°/s (black trace) as estimated by the standard vector average (methods). Dashed traces with open symbols: normalized eye acceleration in response to pursuit during apparent motion stimuli moving at 16°/s (grey trace) or 32°/s (black trace). The value of the first point of each trace is always set to 1. D. Solid traces with filled symbols: normalized population response for 16°/s (grey trace) or 32°/s (black trace) as estimated by the opponent vector average (methods). Dashed traces with open symbols: same as in C.

Figure 2

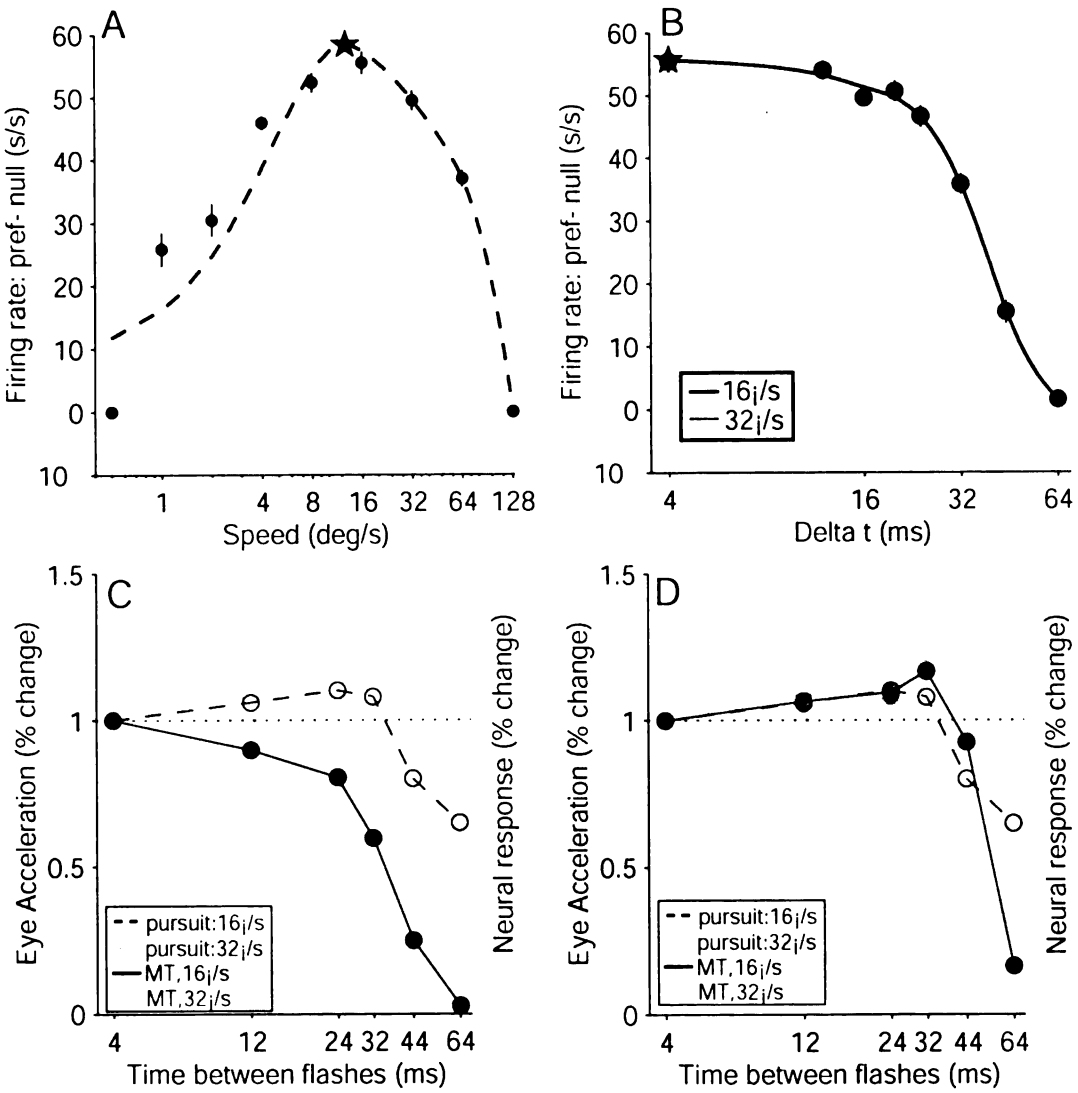
A
Firing rate: pref- null (s/s)
60
50
40
30
20
10
0
10
1
4
8
16
32
64
128
Speed (deg/s)
B
Firing rate: pref- null (s/s)
16j/s
32j/s
4
16
32
64
Delta t (ms)
C
Eye Acceleration (% change)
Neural response (% change)
1.5
1
0.5
0
pursuit:16j/s
pursuit:32j/s
MT,16j/s
MT,32j/s
4
12
24 32 44 64
Time between flashes (ms)
D
Eye Acceleration (% change)
Neural response (% change)
pursuit:16j/s
pursuit:32j/s
MT,16j/s
MT,32j/s
Time between flashes (ms)

Figure 3. Example responses to apparent motion from area MST neurons. A,C & E. Left panel: Speed tuning in response to smooth motion. The peak of the spline function fit to the data is indicated by a star. B,D,&F: firing rates in response to apparent motion at different values of Δt presented at 16°/s (grey trace) or 32°/s (black trace). The peak of the spline function used to fit the data at each speed is indicated by a star of the same color as the trace. Black and grey dashed lines indicate the peaks of the population response from MT at 16°/s and 32°/s for comparison.

Figure 3

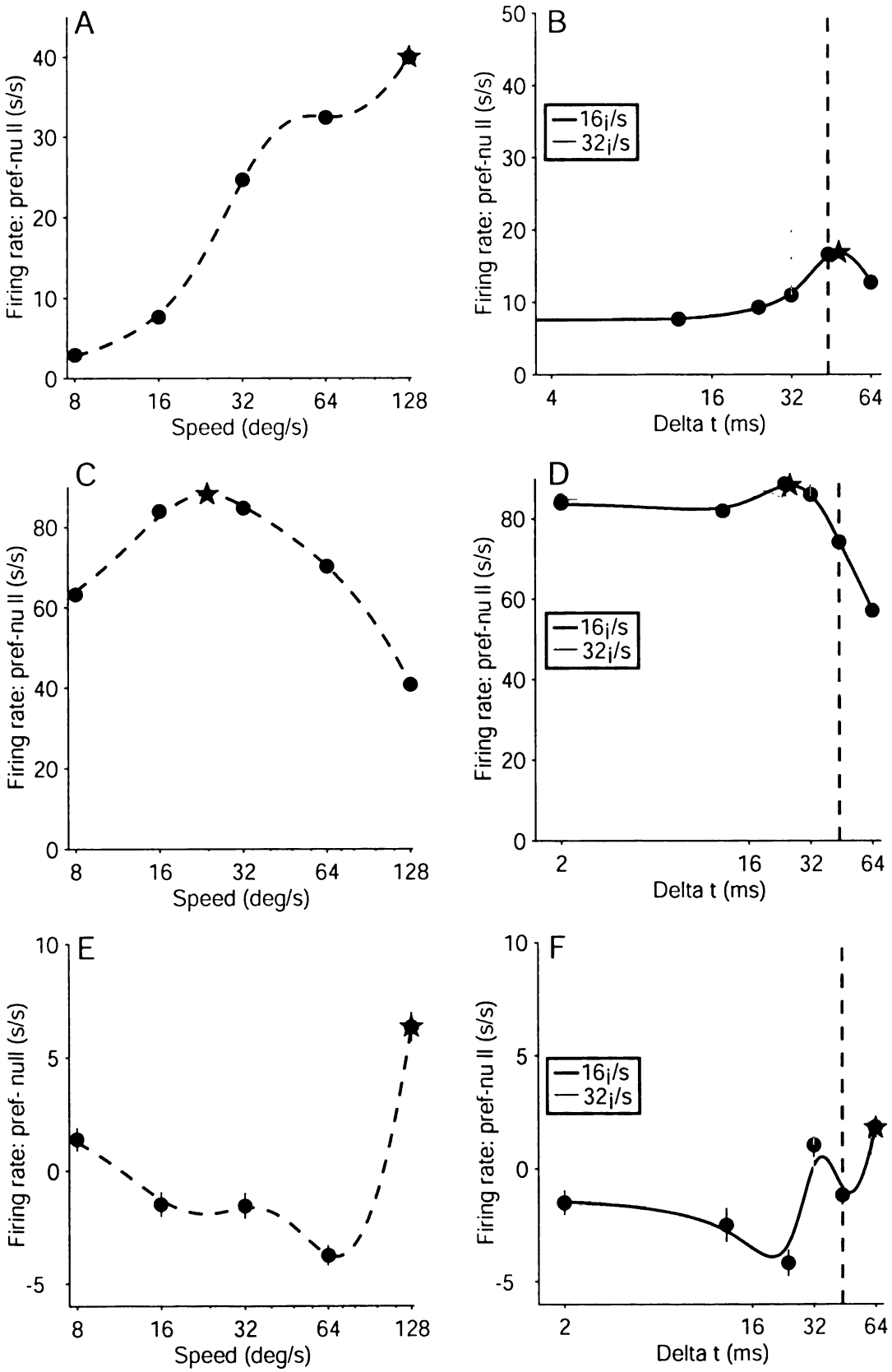
A
Firing rate: pref-nu II (s/s)
Speed (deg/s)
B
Firing rate: pref-nu II (s/s)
16i/s
32i/s
Delta t (ms)
C
Firing rate: pref-nu II (s/s)
Speed (deg/s)
D
Firing rate: pref-nu II (s/s)
16i/s
32i/s
Delta t (ms)
E
Firing rate: pref- null (s/s)
Speed (deg/s)
F
Firing rate: pref-nu II (s/s)
16i/s
32i/s
Delta t (ms)

Figure 4. Population averages from MT and MST neurons. A. % change in firing rate of averaged apparent motion responses for neurons with preferred speeds slower than 50°/s for apparent motion stimuli moving at 16°/s (grey trace) or 32°/s (black trace). The value of the first point of each trace is always set to 1. Thick traces indicate averaged MST data while thin traces indicate averaged MT data. % change was calculated from the opponent response. Black and grey dashed lines indicate the peaks of the population response from MT and of eye acceleration at 16°/s and 32°/s. B. Same as in A except that averages reflect neurons with preferred speeds faster than 50°/s. C and D. Same as A and B except that % change was calculated from the preferred direction only.

Figure 4

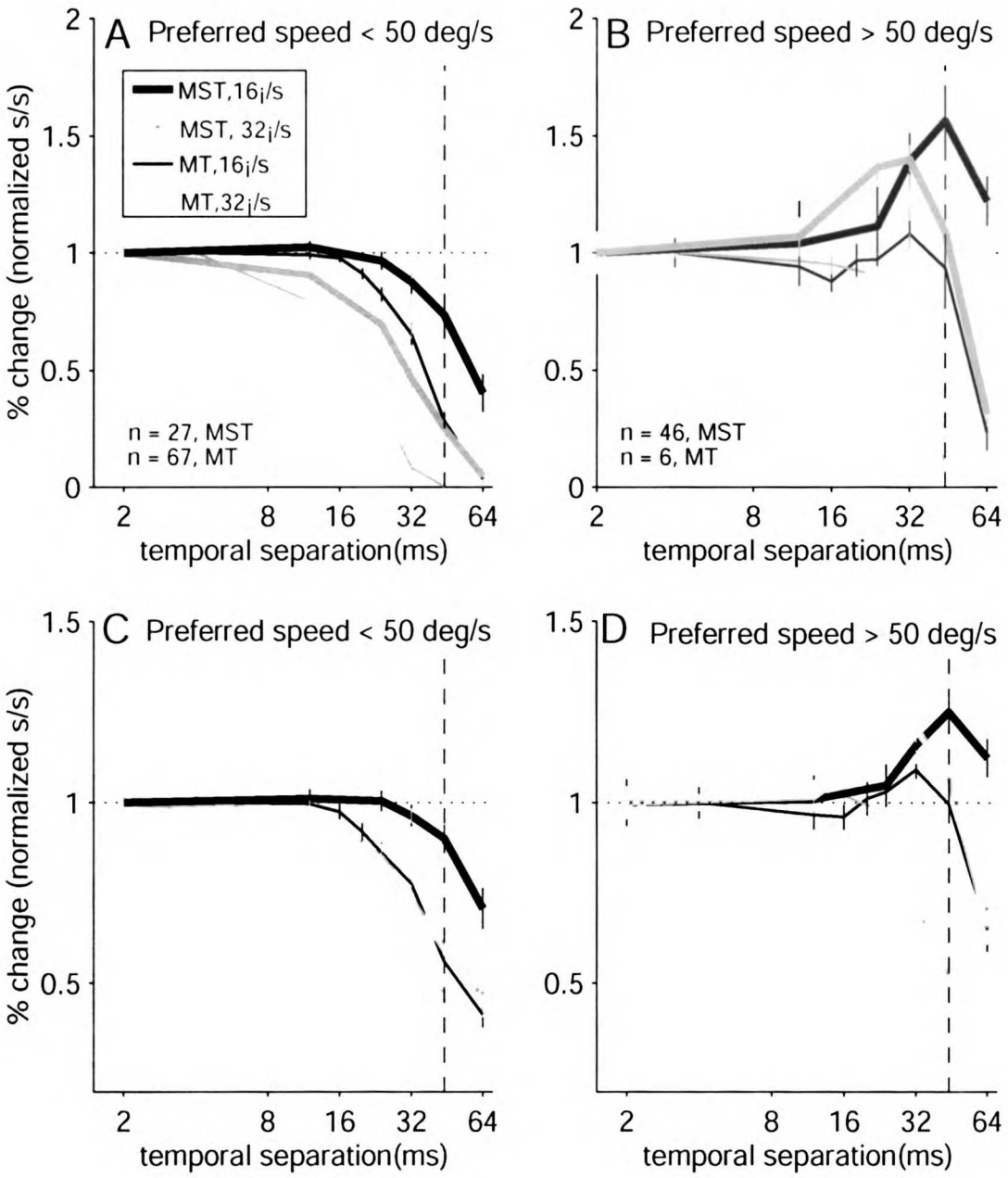
A Preferred speed < 50 deg/s
B Preferred speed > 50 deg/s
C Preferred speed < 50 deg/s
D Preferred speed > 50 deg/s
MST,16i/s
MST, 32i/s
MT,16i/s
MT,32i/s
n = 27, MST
n = 67, MT
n = 46, MST
n = 6, MT
% change (normalized s/s)
temporal separation(ms)
2
8
16
32
64
0
0.5
1
1.5

Figure 5. A and B. Relationship between peak apparent motion response and preferred speed for 73 MST neurons. Values for preferred speed and preferred Δt were taken from the peak of the spline fits to the data. Solid line indicates the best linear fit to the data. A. Responses from apparent motion stimuli moving at 16°/s. B. Responses from apparent motion stimuli moving at 32°/s. C. Relationship between the peak Δt for 16 and 32°/s motion. Dotted line corresponds to x=y, dashed line corresponds to x=2y.

Figure 5

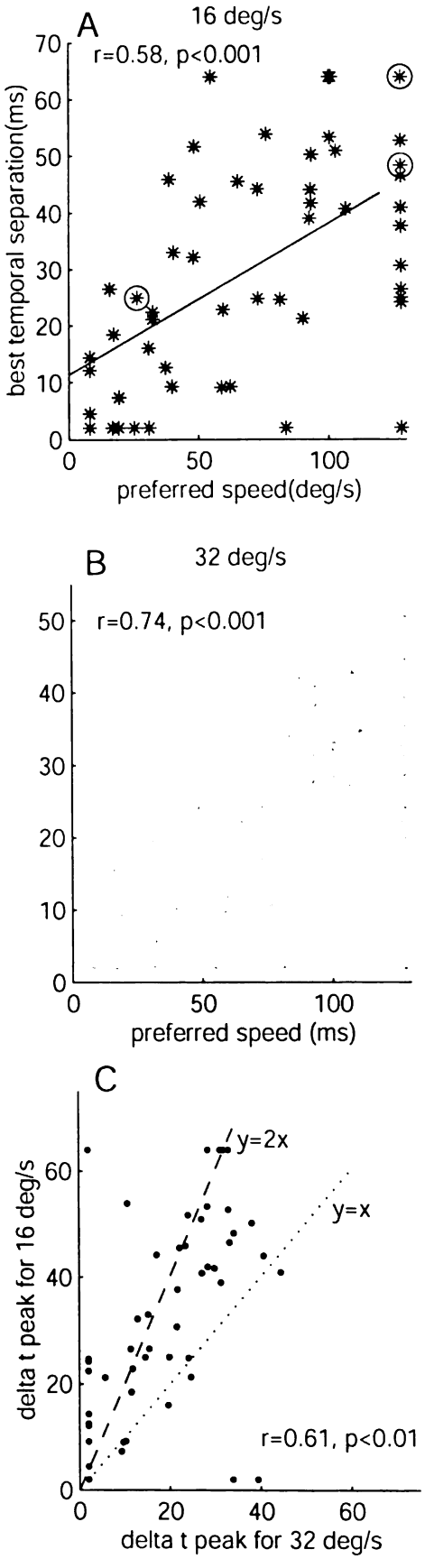
A
16 deg/s
r=0.58, p<0.001
best temporal separation(ms)
preferred speed(deg/s)
B
32 deg/s
r=0.74, p<0.001
preferred speed (ms)
C
y=2x
y=x
r=0.61, p<0.01
delta t peak for 16 deg/s
delta t peak for 32 deg/s

Chapter 5: Opposed preferred directions during pursuit and visual motion for antidromically activated MST neurons

Abstract

Antidromic stimulation was used to identify MST neurons that project to the FEF_{SEM}. The small population of identified neurons was distinct from the population in general in that the majority of neurons had opposite preferred directions for pursuit and visual motion. By contrast, in the general population, neurons were equally likely to prefer the same or opposite directions of visual motion and pursuit.

Introduction

One general approach to understanding how the brain generates behavior is to use physiological techniques to try and discern the function of cytoarchitecturally distinct neural areas. One shortcoming with this approach is that it presumes that the neurons within an area all contribute to the same behavior. In fact, neurons in a given cortical area frequently project to a number of different targets, suggesting they may play a role in many different behaviors. In area MST, projection targets include the dorsal lateral pontine nuclei (DLPN) (Boussaoud et al. 1992; Glickstein et al. 1980), saccadic and smooth eye movement subregions of the frontal eye field (FEF_{SEM} and $FEF_{saccade}$), (Tian and Lynch 1996), the dorsal terminal nucleus of the accessory optic system (NOT-DTN) (Hoffmann et al. 2002), the superior temporal polysensory area, the lateral intraparietal area (LIP) and the ventral intraparietal area (VIP), and area TEO (Boussaoud et al. 1990).

To understand how area MST contributes to the generation of smooth pursuit eye movements, a number of groups have recorded from MST neurons during pursuit

(Bremmer et al. 1997; Chukoskie and Movshon submitted; Churchland and Lisberger submitted; Squatrito and Maioli 1997). Many neurons in MST project to regions known to play a role in pursuit, such as the FEF_{SEM} (Gottlieb et al. 1993; Gottlieb et al. 1994; Tanaka and Fukushima 1998) and the DLPN (May et al. 1988; Suzuki and Keller 1984; Suzuki et al. 1985), so a given MST neuron could indeed contribute to smooth pursuit. However, the neuron might instead be important for programming saccacdes if it projects to LIP, VIP or the $FEF_{saccade}$, or for generating the optokinetic response if it projects to the NOT-DTN. In fact, because the saccadic system needs to be informed about ongoing pursuit velocity in order to generate movements of the appropriate size and direction (Schlag et al. 1990), even the existence of extraretinal tuning in a neuron might not indicate that it drives pursuit. Determining how a given neuron in MST contributes to pursuit is difficult if its projection target is not known.

How might the MST neurons that drive pursuit differ from the MST population in general? Several lines of evidence have suggested that the signals in MST that are important for pursuit have a strong directional bias. First, lesions in area MST cause the most severe pursuit deficits during pursuit towards the site of the lesion (Dursteler et al. 1987). Second, microstimulation in MST increases ongoing pursuit only during pursuit towards the side of stimulation (Komatsu and Wurtz 1989). Third, stimulation in the FEF_{SEM}, a known projection target of MST, causes smooth eye movements that are primarily ipsiversive (Gottlieb et al. 1993; Gottlieb et al. 1994). Taken together, these observations suggest that neurons driven by ipsiversive stimuli are those most likely to play a role in driving pursuit. Komatsu and Wurtz (1989) argued that the ipsiversive

acceleration seen during stimulation is due to modification of purely visual signals. If this is the case, MST neurons preferring *ipsiversive visual motion* might play the biggest role in pursuit and be the most likely to project to downstream pursuit areas. On the other hand, the deficits seen after MST lesions tend to be most apparent during pursuit maintenance rather than pursuit initiation, suggesting that lesions in MST that impair pursuit do so by interfering with extraretinal signals. If this is the case, MST neurons preferring *ipsiversive movements* might play the biggest role in driving pursuit and be the most likely to project to downstream pursuit areas.

We hoped to test whether MST neurons that project to downstream pursuit areas show ipsiversive biases for pursuit or visual motion stimuli. To do this, we stimulated in the FEF_{SEM} while recording in MST. This allowed us identify, through antidromic stimulation, only those MST neurons that project to an area known to be important for pursuit. Because the projection from MST to the FEF_{SEM}, is small (Tian and Lynch 1996), locating such neurons proved difficult. A small amount of preliminary data regarding the nature of the projection from MST to the FEF_{SEM} is provided.

Methods

Subjects

Two adult rhesus monkeys were used in these experiments. Most of the data is from monkey Yo, whose neural data are also included in chapters 2, 3, and 4. A small amount of data is from Monkey Dw, whose neural data is included in chapter 4.

Behavioral testing:

We report neural responses to visual motion during fixation and pursuit. In both cases, visual stimuli were displayed on a 12 inch diagonal analog oscilloscope. The display was positioned 30 cm from the monkey and subtended horizontal and vertical visual angles of 50° and 40°. Visual stimuli consisted of either single spots or patches of moving dots. The aperture size for patches of dots varied from 10°X10° to 30°X30° depending on the receptive field size of the neuron under study.

Visual motion trials began with the onset of a fixation point, followed 600 ms later by the onset of a stationary patch. 200 ms later, dots in the patch began to move coherently and continued to move for 500 ms. The patch was then extinguished and the fixation light remained on for 200 ms.

Pursuit trials began with the appearance of a fixation point that was between 2° and 10° eccentric from the center along the preferred-null axis. Monkeys were required to maintain fixation for a randomized time between 1000 and 1200 ms. The target then stepped away from the fovea and immediately began to move back towards the fovea (Rashbass, 1961) at between 2°/s and 30°/s. Target motion continued for between 900 and 1200 ms. Target motion was most often presented at 20°'s, but slower target motion was used when motion at 20°/s failed to elicit a response. When the monkey did not maintain an eye position that was within 3° of the target throughout the trial, the trial was

terminated and the data not included in analysis. Pursuit trials were performed in complete darkness to eliminate visual motion inputs from the background during pursuit.

Neural testing

Monkeys were fitted with cylinders over the superior temporal sulcus (as described in chapter 2) and the FEF_{SEM}. Both cylinders were placed over the right hemisphere so rightwards stimulus motion and rightwards pursuit are always ipsiversive. Cylinders over the FEF_{SEM} were placed 24mm anterior and 17mm lateral to stereotaxic zero. Figure 1 is a schematic indicating the configuration of the two cylinders.

The FEF_{SEM} was identified using a combination of recording and physiological techniques. Stimulation consisted of pulse trains at 300 or 500Hz for 80ms at 10 to 80 μA. Elicited responses were frequently ipsiversive, but some were contraversive or omnidirectional. The $FEF_{saccade}$ was identified using the same techniques and was anterior to the FEF_{SEM} as expected (Gottlieb et al. 1994). Neurons were identified as being part of MST using the same criteria descibred in chapter 2.

To search for antidromically activated neurons, we first positioned 3-5 electrodes in the FEF_{SEM} at sites that elicited smooth eye movements. These electrodes were either semichronically implanted and attached to the guide tube with epoxy (Pare and Wurtz 2001), or were introduced daily. A recording electrode was then introduced into the STS cylinder and was advanced until directionally selective neurons were encountered.

Stimulation in the FEF_{SEM} was then repeatedly applied to determine whether any neurons in the hash were activated. Stimulation consisted of a single 0.1-0.2 ms biphasic pulse of 200-1000μA. When stimulation repeatedly caused a spike in MST, we attempted to isolate the neuron. Once the neuron appeared to be well-isolated, as determined by the repeatability of waveforms and the prescence of a refractory period, the collision test was performed to determine whether the activation was orthodromic or antidromic. To perform the collision test, we used the triggered output from the window discriminator as the input to the stimulator. A delay was imposed so that the time between the occurrence of a spike and the onset of stimulation could be varied. We initially used long delays (8-10 ms) to confirm the presence of the activated neuron. Even if the neuron was antidromically activated, this long delay ensured that the stimulation in the FEF_{SEM} did not begin until after the spike that triggered the stimulation had arrived in the FEF_{SEM}. Therefore stimulation still reliably elicited a spike from the activated neuron. Once we could observe the activated neuron reliably, the delay between the occurrence of a spike and the onset of stimulation was shortened to almost 0. When a unit was antidromically activated, stimulation in the FEF_{SEM} began before the spike that triggered the stimulation arrived in the FEF_{SEM}. In this case, stimulation no longer elicited a spike from the activated unit because the stimulus waveform and the spike from the MST neuron collided.

Generally, neurons either clearly passed or clearly failed the collision test. Nevertheless, waveforms were recorded so that offline analysis could be used to confirm

observations made during the experiment. Offline, we computed the probability that stimulation triggered on a spike would cause the neuron to fire. For long delays, this probability was always close to 1. For shorter delays, we concluded that a neuron was antidromically activated as long as the probability was 0.25 or less.

Neurons that passed the collision test were identified as projecting the FEF_{SEM} but neurons that failed the collision test were more difficult to classify. One neuron we encountered was well-isolated and failed the collision test, suggesting that it was orthodromic. However, we encountered 22 additional neurons that failed the collision test for unknown reasons. All 22 neurons were small and poorly isolated, so we were unable to determine whether they failed the collision test because they were orthodromic, or because neurons other than the activated one were driving the stimulation. In this latter scenario, collision would not be expected even if the activated neuron were indeed antidromically activated. We attempted to remedy this problem by first isolating neurons and then testing to see whether they were activated. Unfortunately, we were unsuccessful in ever locating an activated neuron using this technique. This was rather trying.

After identifying an activated neuron and subjecting it to the collision test, we recorded responses of activated neurons during pursuit and visual motion in 8 directions. This data was collected even when neurons failed the collision test. For these neurons, pursuit and visual motion data reflect not only the response of the activated neuron, but also the response of some surrounding neurons. This makes interpreting these data extremely problematic, particularly for analyses of best pursuit direction and best speed

since these stimulus parameters have not been shown to cluster in area MST as best direction has (Britten and Van Wezel 2002). As a result, we present only the data from antidromically activated units that passed the collision test.

Data analysis

For visual motion trials, responses during the period 150 to 500 ms after motion onset were analyzed. The period was selected so that firing rates would reflect the sustained, rather than the transient component of the response. For pursuit trials, responses during the period 300 to 800 ms after target onset were recorded. This period was selected to reflect the response to pursuit maintenance rather than pursuit initiation and to take into account the 100 ms visual motor delay.

To estimate preferred direction and strength of tuning, the response at each direction was taken as a vector where the length corresponded to the amplitude of the response and the angle corresponded to motion direction. The vectors corresponding to all directions were summed. The angle of the resulting vector was taken as the preferred direction of the neuron. The length of the vector, called the direction radius, was taken as a measure of how strongly the cell was tuned. Direction radii can range from 0 (equal firing in all directions) to 2.41 (maximal firing in directions on the same side as the preferred direction and no firing in the opposite direction).

Results

We identified 33 neurons in MST that were activated by stimulation in the FEF_{SEM}. 10 of these neurons passed the collision test. Example waveforms from an activated neuron are in figure 2a. The large amplitude oscillation centered at about 0 ms is the stimulus artifact. To its right, at a constant delay for all overlayed traces is the waveform of the activated unit. The delay between the onset of stimulation and the activated unit is approximately 2 ms, within the range of delays expected for cortico-cortical projections (Ferraina et al. 2002). To determine whether neurons were orthodromically or antidromically activated, all activated neurons were subject to the collision test wherein the firing of the activated unit is used to trigger stimulation. The unit driving stimulation in figure 2a is labeled. A 3 ms delay took place between the firing of the neuron and the onset of stimulation. At this delay, stimulation failed to evoke a waveform in only 3% of trials. For the trace in figure 2b, a delay of 1 ms was used. Examining the region to the right of the stimulus artifact reveals that the waveform from the activated neuron was absent on most trials. At a 1 ms delay, collision was observed 75% of the time for this neuron.

Many of the activated neurons we observed had directional responses to pursuit or visual motion. We collected direction tuning curves for visual and pursuit responses from 30 of the activated neurons. Direction tuning curves for visual (blue) and pursuit (red) responses for 4 example neurons are shown in figure 3 to illustrate the diversity of tuning properties seen in activated neurons. The data shown in figure 3a are for the example

neuron in figure 2. Pursuit responses in this neuron were directionally tuned (red trace) but visual responses were not directionally tuned (blue trace). The value of the directional radius (see methods) is labeled in blue for visual responses and red for pursuit responses. Appropriately, the directional radius corresponding to the visual response is close to 0 while the directional radius corresponding to the pursuit response is large. The neuron in figure 3b, which also passed the collision test, exhibited clear directional tuning for both visual and pursuit responses. The preferred pursuit direction is rightwards, consistent with the ipsiversive bias for projecting neurons that we hypothesized. Interestingly, the preferred direction for pursuit in this neuron was opposite the preferred visual direction. The neuron in figure 3c, which also passed the collision test, had weaker tuning than the neuron in figure 3b, but was similar in that the preferred visual direction was opposite to the preferred pursuit direction. The neuron in figure 3d was not well-tuned. This neuron did not pass the collision test. Therefore, responses recorded during pursuit and visual trials might include action potentials from neurons not projecting to the FEF_{SEM}. The absence of tuned pursuit and visual motion responses might truly reflect a poorly tuned projection neuron, or might reflect the combined responses of neurons preferring a number of different directions. This neuron, like all those that failed the collision test, was excluded from further analysis.

To determine whether preferred visual or pursuit directions tend to be ipsiversive, we plotted the preferred direction of all projecting neurons. Neurons like the one in figure 3d, for example, would have been excluded even had it passed the collision test because its tuning was too weak. We set a threshold directional radius of 0.4 because

tuning curves with directional radii larger than this were, according to visual inspection, reasonably well-tuned.

Of the 10 activated neurons, 9 had responses during visual motion that met our tuning criterion. In figure 4a, the polar angle of each point indicates the preferred directions of visual motion for 1 neuron. Contrary to our hypothesis, the population does not appear strongly biased towards rightwards motion. The number of neurons with preferred directions in the right (ipsiversive) or left (contraversive) quadrants did not indicate a bias (ipsiversive = 4, contraversive = 5). Further, a Rayleigh test (Batschelet 1981) revealed that the distribution was not significantly different from uniform (n=9, r=0.26, p=0.56). The mean angle and its radius are indicated by the line and diamond in figure 4a.

All 10 activated neurons had responses during pursuit that were sufficiently directional to meet our tuning criterion. In figure 4b, the polar angle of each point indicates the preferred pursuit direction for one neuron. Again, the population does not appear strongly biased towards rightwards motion. The number of neurons with preferred directions in the right (ipsiversive) or left (contraversive) quadrants again did not indicate a bias (ipsiversive = 6, contraversive = 4). A Rayleigh test did not reveal that the distribution was significantly different from uniform (n=10, r=0.23, p=0.63). The mean angle and its radius are indicated by the line and dot in figure 4b.

The data in figures 4a and b show do not reveal whether the preferred visual direction of a neuron is related to its preferred pursuit direction, as was in the case in the example figures 3b and c. To demonstrate how the preferred directions during different stimulus conditions are related, we re-plotted the data from figures 4a and b on figure 5a and connected each neuron's preferred pursuit direction (a dot) to its preferred visual direction (a diamond) with a line. In order to be plotted in figure 5a, neurons were required to have direction radii greater that 0.4 for both stimulus conditions, so one point from figures 4b was excluded. Many lines cross through or near to the origin, indicating opposite preferred directions for pursuit and visual motion.

To examine more directly the relationship between preferred direction during pursuit and visual motion, we subtracted the best pursuit direction from the best visual direction for each neuron in figure 5a. This quantity, which we will refer to as the direction difference, is plotted in figure 5b. Neurons with opposite preferred directions under the two conditions are clustered around 180° while neurons with similar preferred direction cluster around 0°. A Rayleigh test indicated that the distribution of direction differences was significantly different from a uniform distribution ($n=9$, $r=0.7$, $p=<0.008$) The mean angle and its radius are indicated by the black line and circle in figure 5b.

Discussion

We located 33 MST neurons that were activated by stimulation of the FEF_{SEM}. 10 of these passed the collision test and were thus positively identified as antidromic. We

observed that many activated neurons were tuned for the direction of visual motion or for pursuit. While we did not observe a bias in preferred direction during either stimulus condition, we did find that the preferred direction during pursuit tended to be opposite the preferred direction during visual motion.

Ours is the first study we are aware of to examine the population of MST neurons that projects to the FEF_{SEM}. However, a recent study examined the population of MST neurons that was antidromically activated by stimulation in the NOT-DTN (Hoffmann et al. 2002). Interestingly, this study observed a clear ipsiversive bias in preferred direction of stimulus motion for projecting neurons. The directional bias helps to explain the ipsiversive deficits seen during the optokinetic nystagmus, but does not seem to explain the effects seen during pursuit.

We initially hypothesized that the population of neurons projecting to the FEF_{SEM} would similarly exhibit a directional bias. However, no clear directional bias was apparent in either the preferred directions of visual motion or the preferred directions of pursuit. The distributions of visual and pursuit preferred directions were uniform.

The absence of a directional bias for pursuit is particularly surprising since the general population of neurons in MST is reported to have a weak bias towards ipsiversive pursuit (Churchland and Lisberger submitted; Squatrito and Maioli 1997), but see (Komatsu and Wurtz 1988a). However, the observation that the neurons in the FEF_{SEM} have preferred directions that are not biased towards a particular direction of stimulus

motion (Gottlieb et al. 1994) does suggest that it receives inputs from neurons with uniform preferred directions. Preferred directions in the DLPN are similarly unbiased. The clear directional effects seen during stimulation and lesions are puzzling given that recording data do not reveal strong directional biases, and that the population of projecting neurons is similarly unbiased for pursuit direction.

Our observation that projecting neurons tend to have opposite preferred directions for pursuit and visual motion was unexpected. A number of papers have reported the relative preferred directions of pursuit and visual motion for the general population in MST. These papers appear, at first glance, to have made rather disparate observations about relative preferred direction because some groups report that they tend to be opposite (Komatsu and Wurtz 1988b) while others report that they tend to be the same (Chukoskie and Movshon submitted; Squatrito and Maioli 1997). However, a closer investigation reveals that all groups found neurons that had both opposed and aligned pursuit and visual preferred directions; the difference was in the percentage of each. Our data argues that the population of neurons that project to the FEF_{SEM} are a heavily biased subset of a general population that may be slightly biased towards opposed or slightly biased towards aligned preferred directions for pursuit and visual motion.

The tendency for projecting neurons to have opposite preferred directions for pursuit and visual motion does not appear to explain the direction effects observed in lesion and microstimulation studies. However, neurons with opposed preferred directions for pursuit and visual motion may be distinct in a different way. In our stimulus

configuration, neurons with opposite preferred directions for pursuit and visual motion will potentially send ambiguous signals to downstream areas since vigorous firing could result from rightwards pursuit in the dark or from leftwards motion of a visual stimulus during fixation. During normal, lighted viewing conditions, however, rightwards pursuit would, in fact, be coupled with visual motion in the opposite direction. In this configuration, both inputs would be in the optimal direction and could, depending on the interaction between visual and and pursuit inputs, drive the neurons very effectively. The neurons that project to the FEF_{SEM} might therefore be those that fire most vigorously during normal pursuit.

Neurons in area MST have a second target, the DLPN (Boussaoud et al. 1992; Glickstein et al. 1980), which is known to play an important role in the gerenation of smooth pursuit eye movements. Identifying neurons in MST that are antidromically activated by stimulation in the DLPN would provide a more complete picture of the MST neurons playing a role in pursuit. Perhaps the neurons projecting to the DLPN exhibit the directional biases that were absent from neurons projecting to the FEF_{SEM}.

Acknowledgements

Advice and technical support from Martin Paré made these experiments possible.

References

Batschelet E. *Circular statistics in biology*. London ; New York: Academic Press, 1981.

Boussaoud D, Desimone R, and Ungerleider LG. Subcortical connections of visual areas MST and FST in macaques. *Vis Neurosci* 9: 291-302, 1992.

Boussaoud D, Ungerleider LG, and Desimone R. Pathways for motion analysis: cortical connections of the medial superior temporal and fundus of the superior temporal visual areas in the macaque. *J Comp Neurol* 296: 462-495, 1990.

Bremmer F, Ilg UJ, Thiele A, Distler C, and Hoffmann KP. Eye position effects in monkey cortex. I. Visual and pursuit-related activity in extrastriate areas MT and MST. *J Neurophysiol* 77: 944-961, 1997.

Britten KH and Van Wezel RJ. Area MST and heading perception in macaque monkeys. *Cereb Cortex* 12: 692-701, 2002.

Chukoskie L and Movshon JA. Responses of MT and MST neurons during visual motion and pursuit eye movements. submitted.

Churchland A and Lisberger S. Speed tuning of exraretinal responses in area MST. submitted.

Dursteler MR, Wurtz RH, and Newsome WT. Directional pursuit deficits following lesions of the foveal representation within the superior temporal sulcus of the macaque monkey. *J Neurophysiol* 57: 1262-1287, 1987.

Ferraina S, Pare M, and Wurtz RH. Comparison of cortico-cortical and cortico-collicular signals for the generation of saccadic eye movements. *J Neurophysiol* 87: 845-858, 2002.

Glickstein M, Cohen JL, Dixon B, Gibson A, Hollins M, Labossiere E, and Robinson F. Corticopontine visual projections in macaque monkeys. *J Comp Neurol* 190: 209-229, 1980.

Gottlieb JP, Bruce CJ, and MacAvoy MG. Smooth eye movements elicited by microstimulation in the primate frontal eye field. *J Neurophysiol* 69: 786-799, 1993.

Gottlieb JP, MacAvoy MG, and Bruce CJ. Neural responses related to smooth-pursuit eye movements and their correspondence with electrically elicited smooth eye movements in the primate frontal eye field. *J Neurophysiol* 72: 1634-1653, 1994.

Hoffmann KP, Bremmer F, Thiele A, and Distler C. Directional asymmetry of neurons in cortical areas MT and MST projecting to the NOT-DTN in macaques. *J Neurophysiol* 87: 2113-2123, 2002.

Komatsu H and Wurtz RH. Modulation of pursuit eye movements by stimulation of cortical areas MT and MST. *J Neurophysiol* 62: 31-47, 1989.

Komatsu H and Wurtz RH. Relation of cortical areas MT and MST to pursuit eye movements. I. Localization and visual properties of neurons. *J Neurophysiol* 60: 580-603, 1988a.

Komatsu H and Wurtz RH. Relation of cortical areas MT and MST to pursuit eye movements. III. Interaction with full-field visual stimulation. *J Neurophysiol* 60: 621-644, 1988b.

May JG, Keller EL, and Suzuki DA. Smooth-pursuit eye movement deficits with chemical lesions in the dorsolateral pontine nucleus of the monkey. *J Neurophysiol* 59: 952-977, 1988.

Pare M and Wurtz RH. Progression in neuronal processing for saccadic eye movements from parietal cortex area lip to superior colliculus. *J Neurophysiol* 85: 2545-2562, 2001.

Schlag J, Schlag-Rey M, and Dassonville P. Saccades can be aimed at the spatial location of targets flashed during pursuit. *J Neurophysiol* 64: 575-581, 1990.

Squatrito S and Maioli MG. Encoding of smooth pursuit direction and eye position by neurons of area MSTd of macaque monkey. *J Neurosci* 17: 3847-3860, 1997.

Suzuki DA and Keller EL. Visual signals in the dorsolateral pontine nucleus of the alert monkey: their relationship to smooth-pursuit eye movements. *Exp Brain Res* 53: 473-478, 1984.

Suzuki DA, Keller EL, and Yee RD. Smooth-pursuit eye movement related visual and visuo-motor responses in dorsolateral pontine nucleus of alert monkey. *Soc Neurosci Abstr* 11: 473, 1985.

Tanaka M and Fukushima K. Neuronal responses related to smooth pursuit eye movements in the periarcuate cortical area of monkeys. *J Neurophysiol* 80: 28-47, 1998.

Tian JR and Lynch JC. Corticocortical input to the smooth and saccadic eye movement subregions of the frontal eye field in Cebus monkeys. *J Neurophysiol* 76: 2754-2771, 1996.

Figure legends

Figure 1 Schematic illustrating the placement of cylinders of the FEF_{SEM} and the STS and the method used to identify activated neurons in area MST. Stimulating electrodes were placed in the FEF_{SEM} while recording electrodes were placed in MST.

Figure 1

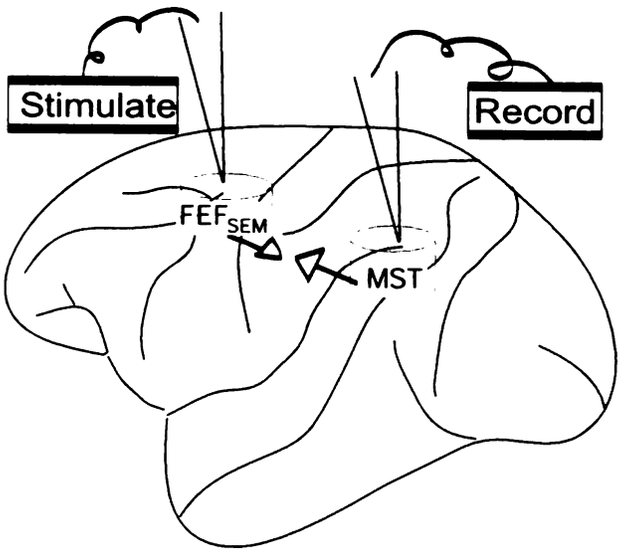

Figure 2 Example waveforms of an activated unit during the collision test. A. Failure to collide when a 3 ms delay is inserted between the firing of the activated unit and the onset of stimulation. B. Mainly successful collisions when a shorter, 1ms delay is inserted between the firing of the activated unit and the onset of stimulation.

Figure 2

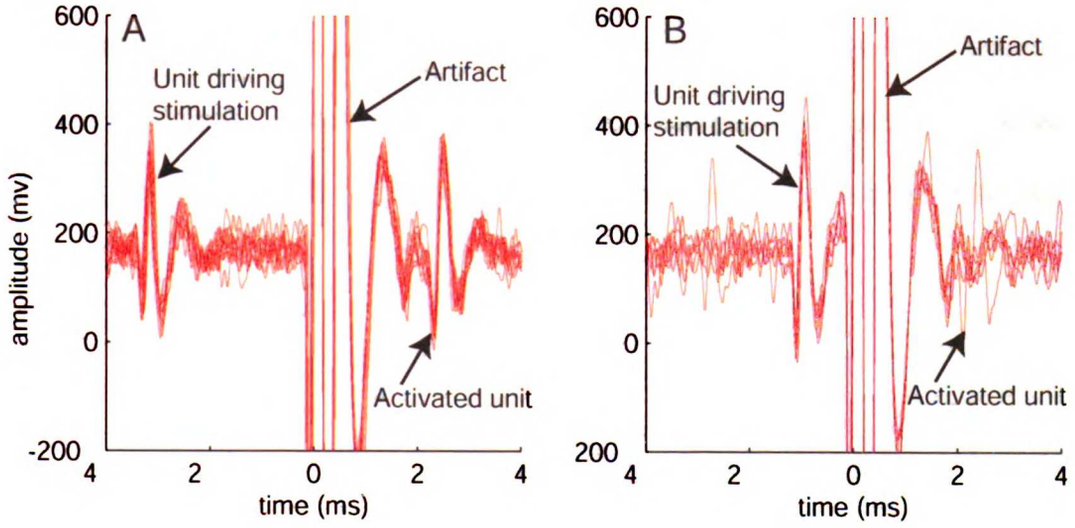
A
B
Unit driving stimulation
Artifact
Activated unit
amplitude (mv)
time (ms)
600
400
200
0
-200
4
2
0
2
4

Figure 3 Example direction tuning curves for pursuit and visual motion taken from 4 activated neurons. Red traces indicate responses to visual motion in 8 directions; blue traces indicate responses to pursuit in the dark in 8 directions. The colored lines indicate the length of the directional radius as a measure of the strength of tuning for visual or pursuit responses. Labels indicate the length of the directional radius for the different stimulus conditions. Traces shown in A, B and C correspond to neurons that passed the collision test. Traces in D correspond to a poorly isolated neuron that failed the collision test.

Figure 3

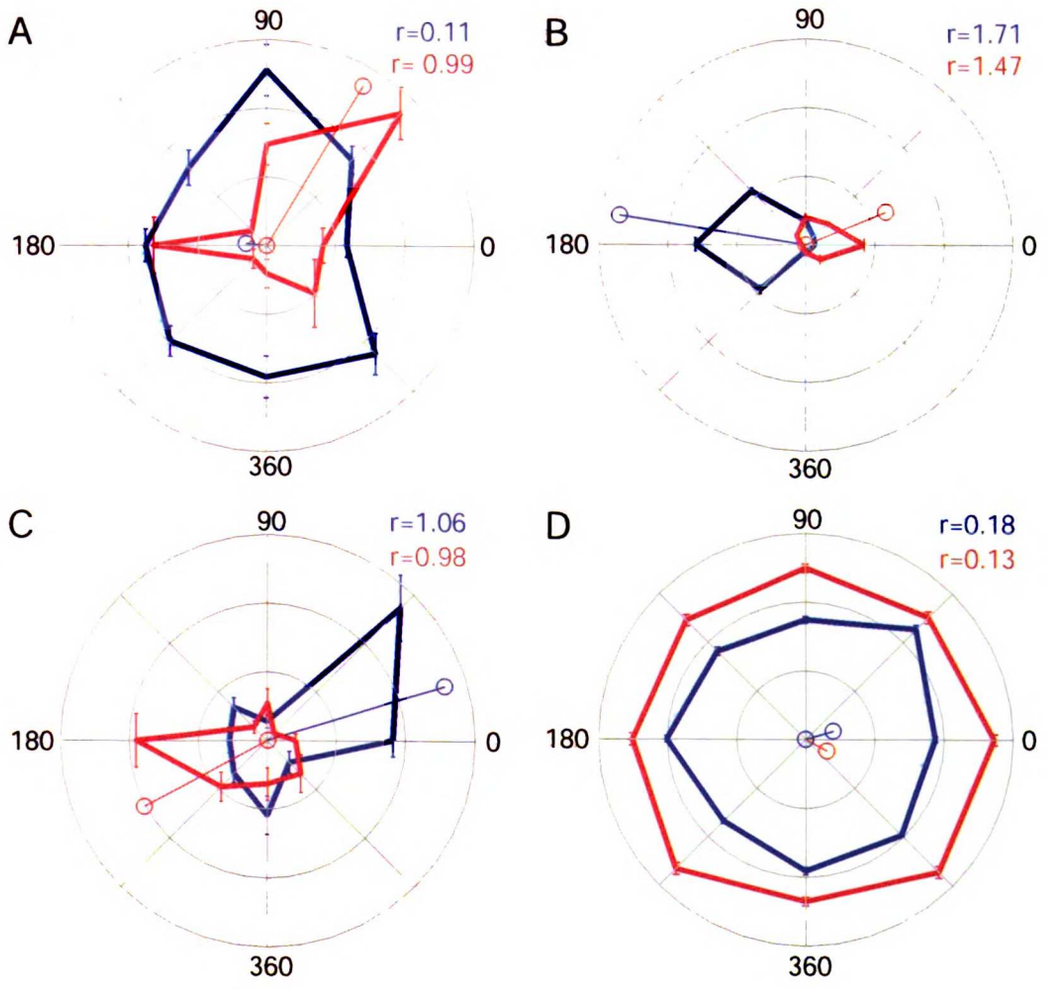
A
90
r=0.11
r= 0.99
180
0
360
B
90
r=1.71
r=1.47
180
0
360
C
90
r=1.06
r=0.98
180
0
360
D
90
r=0.18
r=0.13
180
0
360

Figure 4 A. Preferred direction of visual motion for 9 activated neurons. Polar angle indicates preferred direction, the length of the radius is always 1. The line in the center corresponds to the length and direction of the population average, as determined by a Rayleigh test. The black line represents the same quantity for neurons that failed the collision test. B. Same as A except that the points reflect the preferred pursuit directions of 10 neurons.

Figure 4

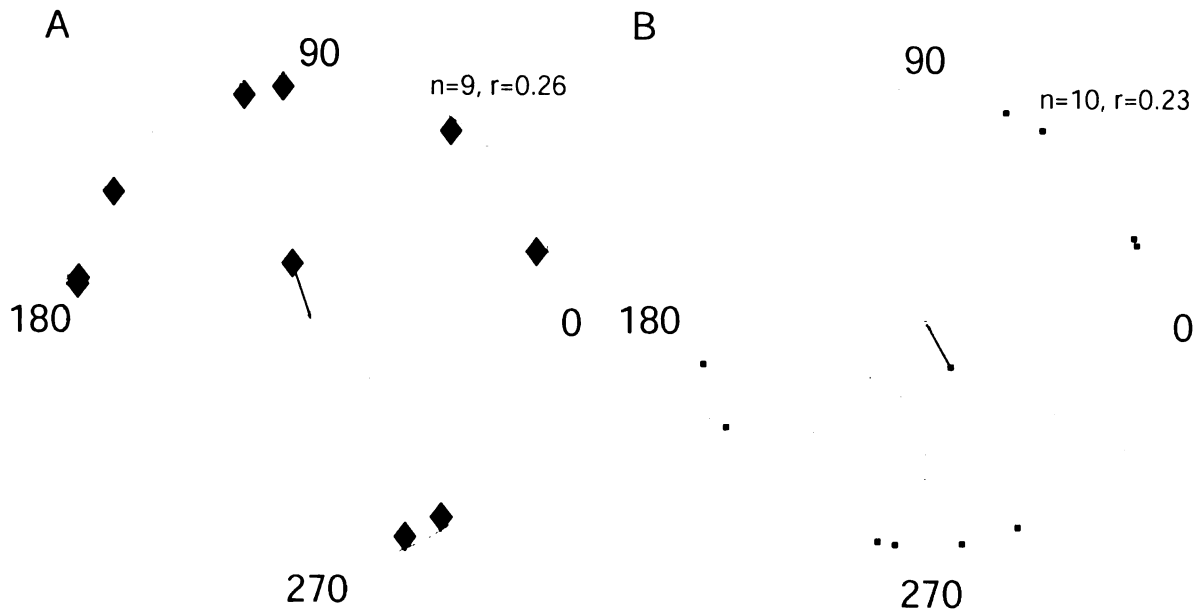

Figure 5 A. Preferred pursuit direction (dots) and preferred visual direction (diamonds) for 9 neurons. Lines connect preferred directions that are for the same neuron. B. Each asterisk represents the difference between preferred pursuit direction and preferred visual direction. Black line indicates the mean angle and length of the population as determined by a Rayleigh test.

Figure 5

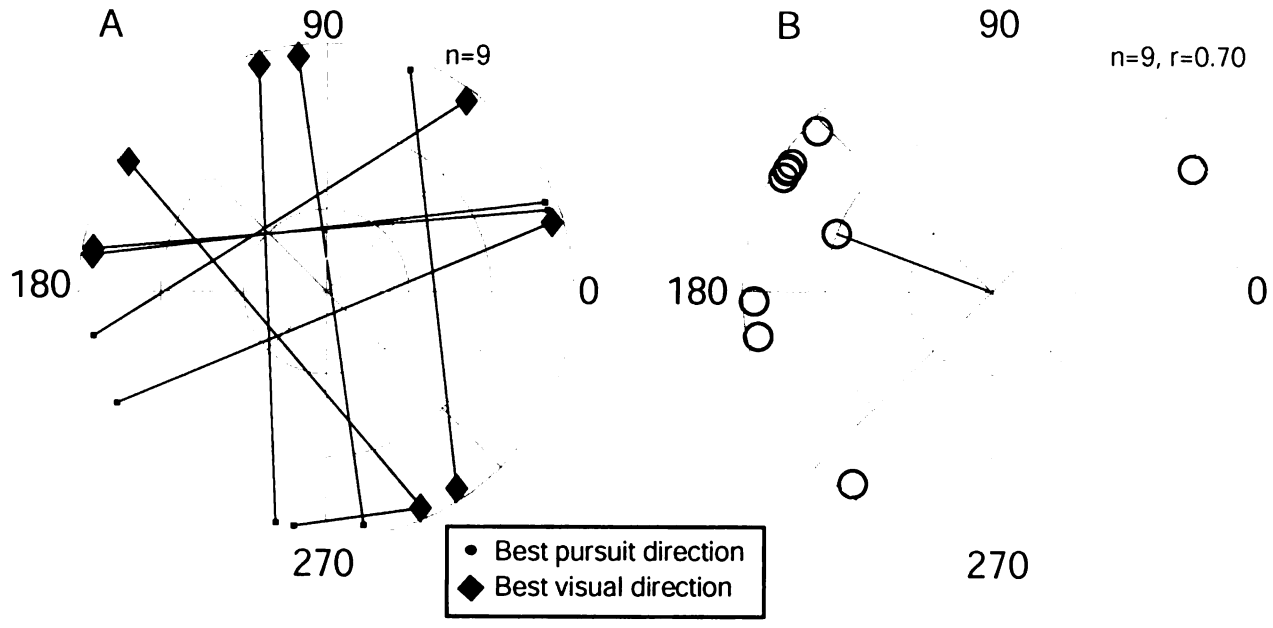
A
90
n=9
180
0
270
Best pursuit direction
Best visual direction
B
90
n=9, r=0.70
180
0
270

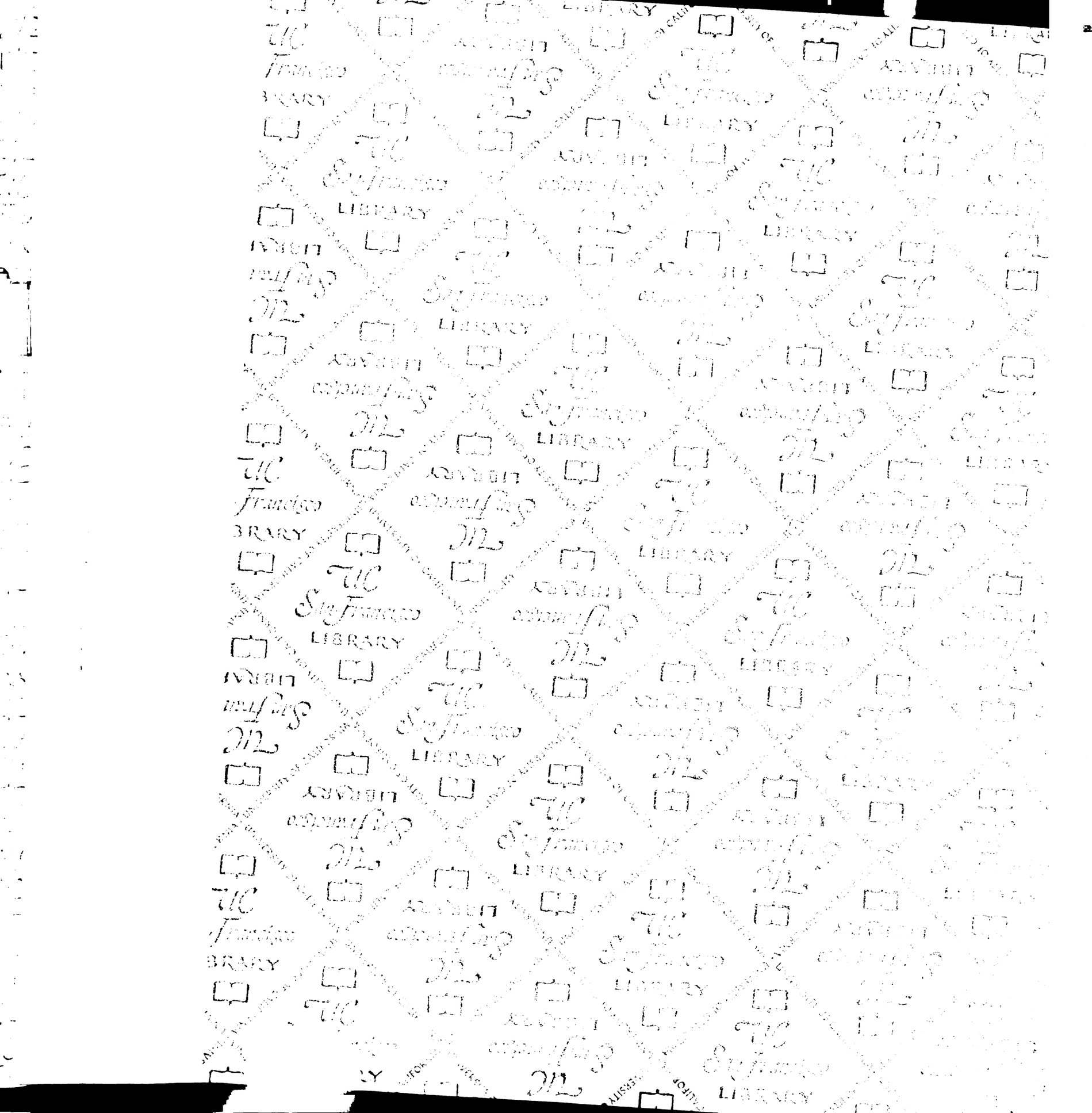
LIBRARY